



**GEOHERMAL STUDIES
OF THE PRECAMBRIAN BASEMENT AND
PHANEROZOIC SEDIMENTARY COVER
IN ESTONIA AND FINLAND**

ARGO JÕELEHT

DISSERTATIONES GEOLOGICAE UNIVERSITATIS TARTUENSIS

DISSERTATIONES GEOLOGICAE UNIVERSITATIS TARTUENSIS

7

**GEOHERMAL STUDIES
OF THE PRECAMBRIAN BASEMENT AND
PHANEROZOIC SEDIMENTARY COVER
IN ESTONIA AND FINLAND**

ARGO JÕELEHT



**TARTU UNIVERSITY
PRESS**

Institute of Geology, Faculty of Biology and Geography, University of Tartu,
Estonia

The Faculty Council of Biology and Geography, University of Tartu, has on the
15th of September 1998 accepted this dissertation to be defended for the degree
of Doctor of Philosophy (in Geology)

Opponent: Assoc. Prof., Ph.D. Niels Balling, University of Aarhus, Denmark

The thesis will be defended at the University of Tartu, Estonia, on Novem-
ber 16th, 1998 at 14.15

The publication of this dissertation is granted by the University of Tartu

CONTENTS

LIST OF ORIGINAL PUBLICATIONS	6
ABSTRACT	7
1. INTRODUCTION	8
2. HEAT FLOW DENSITY AND TEMPERATURE DATA IN ESTONIA	12
3. DISCUSSION	14
3.1. Influence of groundwater flow	14
3.2. Implications of recent climatic changes to heat flow density.....	21
3.3. Geothermics in the lithospheric scale	23
4. CONCLUSIONS	27
5. ACKNOWLEDGEMENTS	28
6. REFERENCES	29
SUMMARY IN ESTONIAN: Eesti ja Soome eelkambriumilise aluskorra ja fanerosoiilise settekatte geotermilised uuringud.....	35
APPENDIX. Table of heat flow density data.....	37
PUBLICATIONS	49

LIST OF ORIGINAL PUBLICATIONS

- I **Jõeleht, A.**, 1997. Temperature and heat flow in Estonia. In: S. Hurter (ed.) Atlas of geothermal resources in Europe. European Commission, Directorate General XII — Science, Research and Development. (In press).
- II **Jõeleht, A.** and Kukkonen, I. T., 1996. Heat flow density in Estonia — Assessment of palaeoclimatic and hydrogeological effects. *Geophysica*, 32 (3): 291–317.
- III **Jõeleht, A.** and Kukkonen, I. T., 1998. Thermal properties of granulite facies rocks in the Precambrian basement of Finland and Estonia. *Tectonophysics*, 291: 195–203.
- IV Kukkonen, I. T. and **Jõeleht, A.**, 1996. Geothermal modelling of the lithosphere in the central Baltic Shield and its southern slope. *Tectonophysics*, 255: 25–45.

ABSTRACT

This thesis presents temperature and heat flow density data from Estonia and discusses factors affecting heat flow density — mainly convective heat transfer by groundwater flow and changes of ground surface temperature in the past. It also presents data on radiogenic heat production of middle crustal granulite facies rocks and lithospheric geothermal modelling of the central part and southern slope of the Baltic Shield.

Groundwater flow was found to have only minor influence on geothermal field, although simple Peclet number analysis suggests more pronounced disturbances. In the carbonate rock outcrop areas this can be attributed to hydraulic conductivity structure which forces the flow to take place close to the surface. The groundwater flow in southern Estonia in the Devonian exposure area is effectively reduced by a relatively thick cover of low hydraulic conductivity glacial till together with semi-permeable aquitards. Another sources of disturbance on heat flow density are Holocene climatic changes. The influence of permafrost and groundwater flow under the ice sheet during the Weichselian glaciation may also have produced thermally relevant phenomena, and they must be investigated in detail in future.

No relationship between seismic P-wave velocity and radiogenic heat production of granulite facies rocks was observed. This suggests that seismic data is not useful for direct estimation of middle and lower crustal heat production. Heat production is very probably not negligible in the middle and lower crust and may vary widely. Thermal modelling suggests that surface heat flow density is mainly controlled by crustal, especially upper crustal heat production while lithosphere thickness is only of minor significance. Application of volatile bearing peridotite solidus temperature at the lithosphere/asthenosphere boundary was found to be useful approach providing more stable modellings of temperatures and heat flow densities than those based on constant mantle heat flow density as the boundary condition.

1. INTRODUCTION

The basic observables in geothermics are subsurface temperature, thermal conductivity of rocks and heat flow density. Temperature is measured in boreholes, whereas heat flow density is calculated as a product of temperature gradient and thermal conductivity of rocks intersected by the hole.

The mean heat flow density of continents is 65 mW/m^2 (Pollack *et al.*, 1993). The heat flow density in Estonia is mostly less than 40 mW/m^2 and only in the northeast the values are close to the continental mean. The level of heat flow density in any area is related to many contributing factors, such as heat production of the (basement) rocks (e.g. Roy *et al.*, 1968; Birch *et al.*, 1968), tectonothermal age of the rocks (e.g. Polyak and Smirnov, 1968; Vitorello and Pollack, 1980; Sclater *et al.*, 1980; Uyeda, 1988), lithosphere and crustal thickness (e.g. Ballard and Pollack, 1987; Nyblade and Pollack, 1993a,b), convective heat transfer (e.g. Majorowicz *et al.*, 1984; Lewis and Beck, 1977; Clauser and Villinger, 1990), and palaeoclimatic conductive disturbances (e.g. Shen *et al.*, 1995; Beck, 1992; Clauser and Mareschal, 1995; Beck *et al.*, 1992; Beltrami and Mareschal, 1991; Mareschal and Vasseur, 1992; Wang *et al.*, 1992; Štulc, 1998; Majorowicz and Šafanda, 1998; Veliciu and Šafanda, 1998; Bodri and Čermák, 1998; Rajver *et al.*, 1998; Kukkonen *et al.*, 1998) as well as structural effects (Kohl and Rybach, 1996; Kukkonen and Clauser, 1994) and topographic effects (e.g. Powell *et al.*, 1988; Šafanda, 1994).

The aims of this thesis are to summarize data on Estonian geothermics, to analyse thermal conditions in both upper crustal and full lithospheric scales and to discuss the effect of climatic changes and groundwater flow on subsurface temperatures. A list of both previously published and new heat flow density determinations in Estonia is given as an Appendix.

The thesis is based on four papers and their major contents are summarized below.

Paper I

Jõelet, A., 1998. **Temperature and heat flow in Estonia.** In: S. Hurter (ed.) **Atlas of geothermal resources in Europe.** European Commission, Directorate General XII — Science, Research and Development. Lovell Johns Ltd. (in press).

In this paper the geothermal data of Estonia are presented as temperature maps and cross-sections and a table of heat flow density data. Due to the quite low heat flow from the Precambrian basement and the small thickness of sedimentary rocks the groundwater temperatures in the Phanerozoic aquifers are below 15°C

and do not represent useful geothermal resources in terms of typical “Hot wet rock” techniques. However, these formations could well be used for producing geothermal energy for space heating with heat exchanger techniques. Potential targets can also be found in the basement for “Hot dry rock” applications. Temperature at 250 m depth varies from about 8°C to 15°C and at 500 m depth from 11°C to 16.5°C. The higher temperature values (11°C and 14°C at 250 and 500 m depths, respectively) in northern Estonia can be attributed to the thermal blanketing effect caused by the low thermal conductivity of the Lower Cambrian clays, which attain a thickness of about 100 m. In southern Estonia the increased temperatures at the top of the basement (>13°C) are related only to a deeper location of the basement than in northern Estonia. Heat flow density data are presented for boreholes deeper than 200 metres, to exclude data from shallow boreholes that may often be disturbed by water flow or site specific perturbations. Similarly to the Baltic Shield, Estonia can be described as a relatively low heat flow density area. The apparent heat flow density in Estonia varies from 22 to 62 mW/m² and its mean value is 35 mW/m². Palaeoclimatically corrected heat flow density values vary between about 28 and 68 mW/m² and the mean value is 42 mW/m².

Paper II

Jöeleht, A. and Kukkonen, I. T., 1996. Heat flow density in Estonia — Assessment of palaeoclimatic and hydrogeological effects. *Geophysica*, Vol. 32 (3): 291–317.

This paper presents heat flow density determinations from six boreholes in northern and western Estonia. The mean heat flow density values range from 20 to 40 mW/m². All holes display a vertical variation in apparent heat flow densities from 15 to 52 mW/m². Since most of the holes are shallow and therefore sensitive to surficial disturbances, the effects of palaeoclimatic ground temperature changes and heat transfer by groundwater flow were studied with the aid of numerical modelling. The palaeoclimatic models suggested that the measured vertical variation might be partly attributed to the palaeoclimatic effects, but when the corrections were applied to the measured data they did not entirely eliminate the vertical variation in heat flow density. This is probably due to thermal conductivity structures that deviate from the assumed half-space conditions and the palaeoclimatic ground temperature history used in the models. 2-dimensional fluid and heat transfer simulations indicate that the thermal effect of regional flow systems is less than 5 mW/m² in most of Estonia. Larger perturbations may occur in SE Estonia, where the hydraulic gradient is higher.

Paper III

Jöeleht, A. and Kukkonen, I. T., 1998. Thermal properties of granulite facies rocks in the Precambrian basement of Finland and Estonia. *Tectonophysics*, 291: 195–203.

Results of heat production, thermal conductivity and P-wave velocity measurements of 252 rock samples from five granulite facies areas in Finland and Estonia are presented. These compositionally mainly intermediate Archean and Paleoproterozoic metamorphic rocks have relatively high heat production values. Mean values averaged by areas range from 0.57 to 2.24 $\mu\text{W}/\text{m}^3$. The lowest values are in the Varpaisjärvi area, which is the oldest, most mafic and where the highest metamorphic pressure occurred (8–11 kbar), whereas the highest heat production is found in the Turku granulite belt where the metamorphic pressure was 4–6 kbar. The heat production decreases with the increase of the metamorphic pressure. However, a general numerical relationship cannot be presented because of considerable variations in heat production data. The data suggest no relationship between heat production and P-wave velocity. The mean thermal conductivity of granulites at room temperature varies from 3.0 to 3.5 $\text{W}/(\text{m}\cdot\text{K})$. Slightly elevated thermal conductivity values in the Varpaisjärvi and Lapland granulite areas can be attributed to higher sillimanite and quartz contents, respectively.

Paper IV

Kukkonen, I. T. and Jöeleht, A., 1996. Geothermal modelling of the lithosphere in the central Baltic Shield and its southern slope. *Tectonophysics*, 255: 25–45.

Lithospheric temperature and heat flow density were studied in the central Baltic Shield and its subsurface continuation to the south. A transect trends from eastern Finland to southern Estonia. It runs from a low heat flow density ($\leq 30 \text{ mW}/\text{m}^2$) thick (150–190 km) lithosphere area to an area with thinner (110–150 km) lithosphere with slightly elevated heat flow density (35–55 mW/m^2). Numerical 2-D conductive models were constructed in which peridotite solidus temperatures were assigned to those depths which correspond to the seismically determined lithosphere/asthenosphere boundary. Upper crustal heat production values were taken from literature or from new measurements. Middle and lower crustal lithologies were estimated with the aid of the deep seismic V_P/V_S data, and corresponding heat production values were adapted from global xenolith averages and from data for granulites cropping out in other Precambrian areas. The results of the modelling suggest that the lithosphere and Moho depth variations are only weakly reflected in the measured surface heat flow density data,

which are mainly controlled by heat sources in the upper crust. The simulated heat flow densities at 50 km depth (approximately at the Moho) are relatively low and range from 12 mW/m² at the Archaean northeastern end to 19 mW/m² on the Proterozoic southwestern end of the transect. Simulated temperatures at 50 km depth increase from northeast to southwest, ranging from 450–550°C in eastern Finland to about 650°C in Estonia. Sensitivity of the simulations to parameter changes was studied by varying the heat production and thermal conductivity values. The extreme values for the Moho temperature estimates thus obtained may be about 50 K lower or 100 K higher than the values above. The corresponding sensitivity of heat flow density at the Moho is about ±6 mW/m² and at the surface ±5–20 mW/m², respectively.

2. HEAT FLOW DENSITY AND TEMPERATURE DATA IN ESTONIA

Extensive temperature loggings in Estonian boreholes started in 1974 by the Geological Survey of Estonia and in 1978 by the Institute of Geology of Estonian Academy of Sciences (Юрима, 1984; Юрима и Эрг, 1984). These measurements were made mainly for general geological and hydrogeological purposes. The uppermost part of sections is usually very well studied (readings were taken every 2.5–10 metres), while the measurement interval in the deeper part was up to 50 metres. Often such a sparse interval of readings do not allow to recognize borehole specific perturbations coming from water movements in boreholes (e.g. Drury *et al.*, 1984; Drury, 1989).

Very many heat flow density determinations in Estonia were made by the Institute of Geochemistry and Geophysics of Belorussian Academy of Sciences under the leadership of Gennadi Urban (Урбан и др., 1991; Урбан, 1989; Урбан и Цыбуля, 1988) who has been active in Latvia and Lithuania, too (Урбан, 1989, 1991; Урбан и Цыбуля, 1988). In addition to results of Urban *et al.* (Урбан и др., 1991) and those published in Papers I and II, few more results exist (Гордиенко и Завгородняя, 1985; Moiseenko and Chadovich, 1992). However, these are only first order estimates based on a single thermal gradient and thermal conductivity values for boreholes penetrating through distinctly different lithologies (clay, sandstone, siltstone, limestone). The list of published heat flow density determinations in Estonia is given in the Appendix.

Urban *et al.* (Урбан и др., 1991) established two heat flow density anomalies — low heat flow density in the central Estonia and high in northeastern Estonia. The anomaly in the central Estonia is based on three boreholes of which one (Keava) is obviously disturbed by water flow in borehole (Fig. 1) and should not be used for heat flow density measurement. Unfortunately, the other two (Kõnnu and Lelle) were not logged to the bottom of boreholes and it is not possible to decide whether they are influenced by water movements. In any case, all three boreholes are located on or very close to a northeast-southwest directional thrust zone where rocks are fractured. Thus, if the low heat flow density anomaly exists, it might be much more local and limited to fracture zones. The elevated heat flow density in northeastern Estonia is a western continuation of a larger heat flow density anomaly in the Sankt-Peterburg region (Гордиенко и др., 1984; Gordienko *et al.*, 1985).

The heat flow density in Estonia is in a general agreement with surrounding areas (Balling, 1995; Čermák *et al.*, 1993, Čermák and Hurtig, 1979; Gordienko *et al.*, 1985; Hurtig *et al.*, 1992; Kukkonen, 1993).

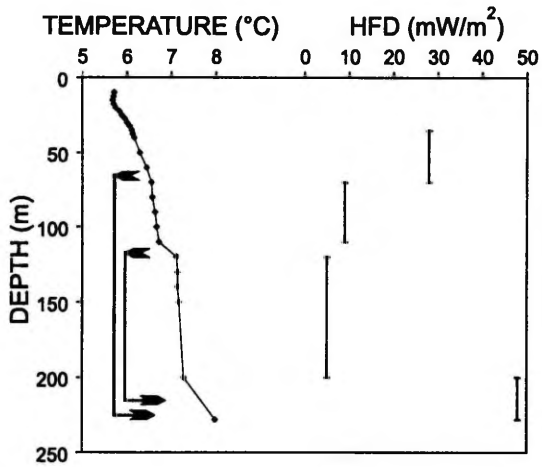


Figure 1. Temperature (A. Schmied, pers. comm.) and heat flow density (Урбан и др., 1991) in the Keava borehole. Arrows indicate depths of groundwater inflow and outflow from the borehole. The uppermost part of temperature log seems to be affected by recent climatic changes.

3. DISCUSSION

3.1. Influence of groundwater flow

In this chapter, factors relevant for interpreting the subsurface thermal field in Estonia are discussed. The most important factors are convective heat transfer by groundwater flow (both present and past conditions during glaciations) and palaeoclimatic conductive disturbances produced by climatically induced variations in ground surface temperature. Further, a discussion on the representativity of the available data on a lithospheric scale is given.

Natural groundwater flow

The natural flow of groundwater and related heat transfer were numerically modelled in Paper II. Here the discussion is continued with the aid of Peclet number analysis and simple numerical models of typical hydrogeological structures in Estonia.

Groundwater flow in a porous medium, such as the sedimentary rocks in Estonia, can be described by Darcy's law

$$v = \frac{dh}{dl} k \quad (1)$$

where v is the Darcy velocity (m/s), dh/dl is the hydraulic gradient (dimensionless) and k is the hydraulic conductivity (m/s). These two main parameters control the water flow. The hydraulic gradient provides the driving force of the flow and the hydraulic conductivity determines the flow velocity and its spatial distribution.

Although many kinds of Estonian sedimentary rocks are highly permeable, hydraulic gradients are relatively small (Perens and Vallner, 1997). Are these parameters large enough to produce heat flow density anomalies?

To estimate the magnitude of convective heat transfer, the dimensionless Peclet number can be used. The Peclet number is a ratio of heat transferred by convection to that transferred by conduction (Bredehoeft and Papadopulos, 1965). For 2-dimensional groundwater flow, the Peclet number can be defined as:

$$Pe = \frac{\beta k (dh/dl) DA}{\alpha_m} \quad (2)$$

where β is the ratio of the heat capacity of the fluid to the heat capacity of the fluid saturated medium (dimensionless), D (m) and A (dimensionless) are the thickness and aspect ratio of the flow system and α_m is the thermal diffusivity of the medium (m^2/s) (van der Kamp and Bachu, 1989). If the absolute value of the

Peclet number is greater than unity then the system is convection dominated, if less than unity then the system is conduction dominated. A practical threshold value for convective disturbance, which can be recognized in geothermal data under favourable conditions, is 0.1.

In most of Estonia, the hydraulic gradient as estimated from topography ranges from 0.01 to 0.0001 being mostly over 0.001. Typical hydraulic conductivity values of bedrock aquifers varies between $1 \cdot 10^{-5}$ and $1 \cdot 10^{-4}$ m/s (Perens and Vallner, 1997). Assuming aquifer's thickness 100–400 metres and moderate flow distances (tens of kilometres) gives Peclet numbers mainly exceeding 0.1. This would indicate a variation in heat flow density values depending on the elevation of the site, as the heat carried away by recharging water in higher elevations is released by discharging water in lowlands. However, such dependence is not supported by the data (Fig. 2).

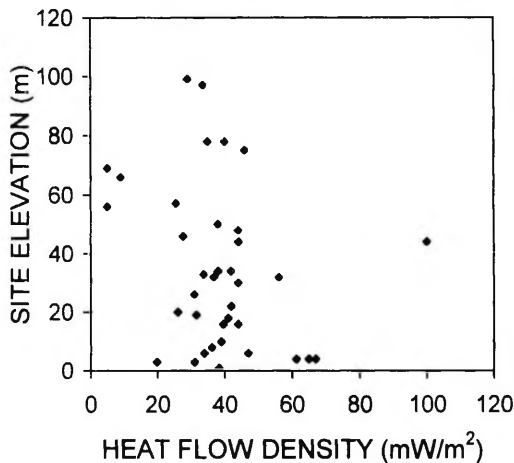


Figure 2. Heat flow density *versus* site elevation. The low heat flow density values (<10 mW/m²) at 60–70 metres altitude are from boreholes that are located on or near major fracture zones.

A number of different permeability structures typical for Estonia were investigated with schematic models (Fig. 3) using the numerical code SHEMAT (Clauser, 1988; Clauser and Villinger, 1990). In all models, a constant hydraulic head and temperature were assigned to upper boundary and 40 mW/m² heat flow density to lower boundary. No flow of heat or fluid was allowed through other boundaries.

In carbonate rocks the main reason for a lack of thermal anomalies is the decrease of hydraulic conductivity with depth. Investigations in Pandivere Upland in northern Estonia (Перенс, 1984), Saaremaa and Muhu islands (Perens *et al.*, 1994) and elsewhere in Estonia (see Paper II) suggest a decrease of hydraulic conductivity according to a power law (Fig. 4). The hydraulic conductivity of

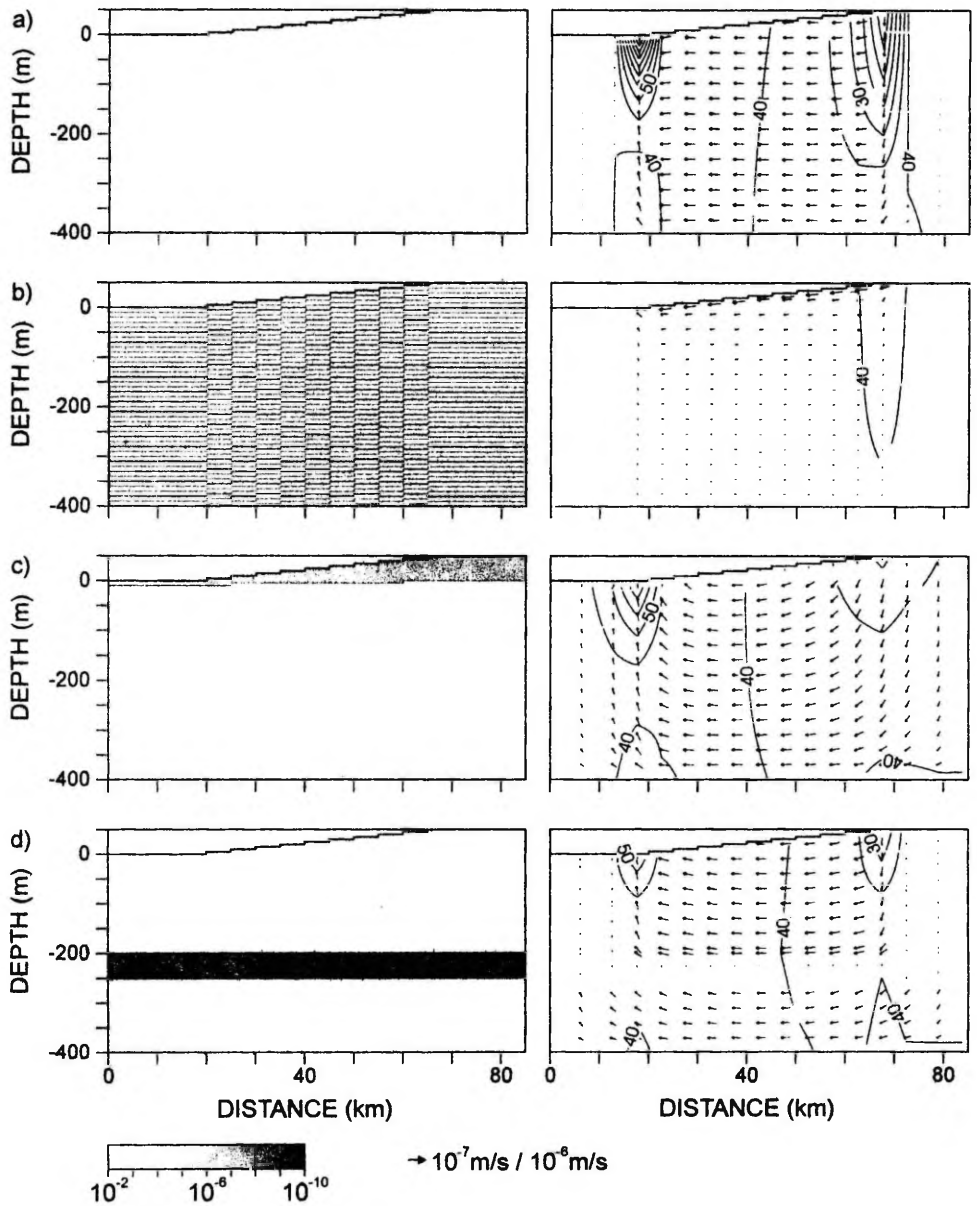


Figure 3. A series of 2-dimensional models on the left and corresponding simulated heat flow density (mW/m^2 ; curves) and Darcy velocity (m/s ; arrows) on the right. Models represent flow systems which are driven by hydraulic gradient of 0.001 (50 m height difference over a 50 km distance). The hydraulic conductivity of model b) decreases gradually according to curve in Fig. 4.

deeper parts of carbonate rocks is not low, but in the uppermost part it is much higher. The decrease of hydraulic conductivity over one order of magnitude in first tens of metres forces most of the flow to be close to the surface (Fig. 3b). Since the water flow is nearly horizontal in the uppermost strata, no significant heat flow density perturbations result. In vertical fracture zones the high hydraulic conductivity continues deeper and heat transfer by advection may be very large. For example, Kõnnu, Lelle and Keava boreholes in central Estonia (Урбан и др., 1991; Appendix) are located at relatively high elevations on or close to major NE-directional fracture zones.

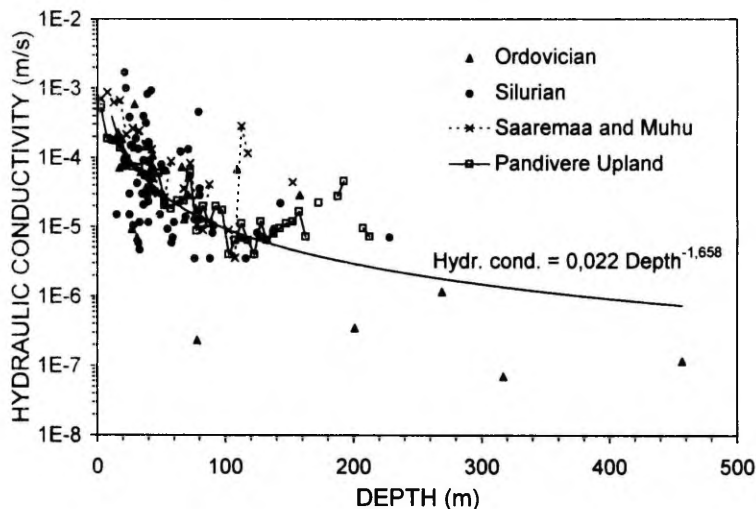


Figure 4. Hydraulic conductivity *versus* depth. The decrease of hydraulic conductivity with depth is fitted by power law to Ordovician and Silurian data of Paper II. The variations of mean hydraulic conductivity from Pandivere Upland (Перенс, 1984) and Saaremaa and Muhu Islands (Perens *et al.*, 1994) are given, too.

The highest topographic variations in Estonia are in the southern parts of the country. There are exposed Devonian sandstones and siltstones which have rather high hydraulic conductivity, but there are also thick Quaternary sediments which have much lower hydraulic conductivity. According to Perens and Vallner (1997) the hydraulic conductivity of Quaternary loamy-sandy till varies from $1 \cdot 10^{-9}$ to $1 \cdot 10^{-5}$ m/s. Fig. 3c presents a model where the overlying layer has hydraulic conductivity three orders of magnitude lower than underlying strata. The thickness of upper layer increases from 10 m at lower elevations to 50 m at higher elevations. This feature is typical to the Otepää and Haanja Uplands. The effect of a covering low-permeability layer can be attributed to recharge and discharge taking place not only close to the slope, but over a wider area. The amplitude of heat flow density anomaly depends on the thickness of low conductivity layer and in Fig. 3c the anomaly in discharge area would be smaller if the thickness would be larger there, too.

The third reason why we do not see large convective heat flow density anomalies is the effect of aquitards. The aquitards with hydraulic conductivity only couple orders of magnitude lower than the surrounding aquifers cannot effectively diminish flow below them. This is because of layered strata where the thickness of layers and thus the area perpendicular to flow is much smaller than the recharge area (perpendicular to flow direction of recharging water). In a 2-dimensional flow assuming a hydraulic conductivity contrast of two orders of magnitude the same amount of water that flows horizontally through an area of 0.1 km² in a 100 m thick aquifer penetrates an aquitard over the area of 10 km². If the flow is three-dimensional (relatively smaller recharge area), the hydraulic conductivity contrast is higher or the confined aquifer is thicker, then due to smaller Darcy flow the heat transfer by convection is also smaller.

Fig. 3d presents a case which is analogous to the Devonian area in southern Estonia where a fifty metres thick Narva Stage acts as the aquitard. The hydraulic conductivity of aquitard is $5 \cdot 10^{-10}$ m/s which is typical value for these rocks (Perens and Vallner, 1997). Although neither covering till layer nor deeper aquitard alone can explain the lack of heat flow density anomalies in southern Estonia, but in case of their co-effect the variations do not exceed 10% of the conductive heat flow density.

Groundwater flow during glaciations

The water of the Cambrian-Vendian aquiferous complex recharged during the last glaciation. This is suggested by low $\delta^{18}\text{O}$ values (18–20‰) and ¹⁴C age determinations (up to 33 430 years; Mokrik, 1997). But the mechanism of recharge is not clear. Mokrik (1997) proposes that during Late Weichselian up to 200 m thick permafrost was formed, which prevented direct recharge of the aquiferous complex from the north. Further, he assumes that during the Middle Weichselian (Denekamp Interstadial, in particular) western Estonia was not covered by ice and glacial waters could intrude, because there the Lontova and Lükati Stages are represented with permeable sandstones. However, it is not clear what is the driving force of such water flow. According to pollen and spore compositions, this was a dry periglacial period (Лийвранд, 1986; Liivrand, 1991; Raukas and Kajak, 1997) and the altitude of ice lake (i.e. hydraulic head) in the area was not high. Under such moderate flow conditions that are similar to present day ones it takes tens of thousands of years for water to flow distances of more than 100 kilometres to reach eastern Estonia. Moreover, the area was not covered by ice, but the climate was still cold. Estimates from ice cores of Greenland (Johnsen *et al*, 1992; Holmlund and Fastook, 1995) suggest that during most of the Weichselian the temperature was 7–12 K colder than at present (the present ground surface temperature in Estonia is 5–7°C). Thus, the conditions may have been favourable for formation of permafrost, which permits groundwater recharge through frozen sediments.

Boulton *et al.* (1996) and Piotrowski (1997) have modelled groundwater flow under and outside the glaciers in northwestern Europe. They found that hydraulic heads and flow velocities were far above their modern values and relatively shallow aquifers are completely flushed during glaciations. Due to frictional, strain and geothermal heating, most of the glacier's base reaches melting temperature and the ice thickness determines meltwater hydraulic heads. Thus, the recharge of aquifers could be much better explained by groundwater flow under the ice sheet where was enough meltwater under high pressure. The only constraint is permafrost — was there enough time for thawing and recharge of the Cambrian-Vendian aquiferous complex?

The thickness of permafrost depends on the ground surface temperature and duration of cold periods, and on the porosity of rocks. In general, the coldest temperatures occur in front of the ice sheet margin. Estonia has been a glacier's marginal area for several times before and during the Weichselian glaciation as is suggested by different till layers and interstadial sediments between them. Kajak *et al.* (Каяк и др., 1981) received ages 39700–31200 years for the intertill organic material containing a layer of the Peedu section, southeastern Estonia. This seems to be approximately the time range when, at least southern Estonia was not covered by ice. The age of underlying till layer of the Peedu section is 40000 years and older and at the Valga valley till is 43000 years old (Каяк и др., 1981). There is no information when the “ice free” period ended, but probably it coincides with the glacier's extension at about 28000 years ago. Thus, there might have been up to 12000 years long period when ground surface temperature in Estonia was between 0°C and –5°C.

Both formation and thawing of permafrost depend on the porosity of rocks. The effect is related to the latent heat of water — the higher the water content in the rock, the higher must be energy loss or absorption before phase change takes place. This means that in porous medium the temperature changes at about 0°C are slower than at other temperatures or in non-porous medium. If the permafrost is thicker than 10–15 metres (depending on thermal diffusivity of frozen rock) then the rate of thinning at the base of permafrost can be characterized by approximate relation (Lachenbruch, 1982):

$$\frac{\partial Z}{\partial t} \approx \frac{q}{LP} \quad (3)$$

where q is the heat flow density at the base of permafrost, L is the latent heat of ice per unit volume ($3.0 \cdot 10^8 \text{ J/m}^3$) and P is the porosity of rock. Assuming 20% porosity of sand- and siltstones of the Cambrian-Vendian aquifer system and 40 mW/m^2 heat flow density, the corresponding thawing rate at the base of permafrost is about 2 cm/a. For rock porosities of 10% (typical value for carbonate rocks) and 30% (Cambrian clays), the thawing rates are 4 cm/a and 1.4 cm/a, respectively.

Calculations with finite difference method (J. Šafanda, pers. comm.) at the outcrop area of the Cambrian-Vendian aquifer system (assuming 100 metres of sandstone with 20% porosity laying on the non-porous basement) give the maximum thickness of frozen rocks from 115 m to 365 m depending on surface temperature during interstadial (-5°C to -10°C) and the length of ice-free period (2000 to 10000 years). Despite of large differences in permafrost thickness (by a factor of 3.2), the melting times have less variations (2900 to 5500 years, i.e. by a factor of 1.9). This can be explained with quicker temperature increase in basement rocks with negligible water content. It is highly probable that in areas where the Cambrian-Vendian aquifer system is covered by other rocks, the thawing of the Cambrian-Vendian part was shorter, because the depth to the bottom of frozen beds is smaller.

The molten conditions under the glacier are supported also by a fact that in Estonia, there are no ribbed moraines, which are believed to form at the transition zone between molten and frozen beds (Hättestrand 1997, 1998; Hättestrand and Kleman, 1998). The closest areas where these moraines are widely distributed are about 400 kilometres northwest of Estonia in central Sweden and western Finland (Hättestrand and Kleman, 1998; Kleman *et al.*, 1997).

Thus, during the Late Weichselian the base of a glacier at the Cambrian-Vendian outcrop area in Estonia has been at molten state for about 11000 years. During this time the hydraulic head was controlled by thickness of ice. Piotrowski and Kraus (1997) investigated compaction of soft sediments under the glacier in northwestern Germany and concluded that pore water pressure was close to ice floatation point, especially in areas of low hydraulic conductivity. Although the Cambrian-Vendian aquifer system itself has high hydraulic conductivity, it is surrounded by areas of low hydraulic conductivity and therefore the hydraulic head in outcrop area of aquifer system was probably also close to floating point (90% of ice thickness). Different reconstructions of ice sheet have yielded different results, but mostly the maximum thickness range from 2400 to 2800 metres (Lambeck, 1995; Elverhøi *et al.*, 1993; Denton and Hughes, 1981), i.e. the hydraulic head was at least 2150 metres above rock surface while at the nearest marginal area (about 500 km to southeast) the hydraulic head corresponded to topography (150–300 metres above the present sea level). If we also account for postglacial uplift (200 m) and for present depth of the Cambrian-Vendian aquifer system (100 m bsl) we get a mean hydraulic gradient at least 0.0031. Taking hydraulic conductivity of the Cambrian-Vendian aquifer system as $5 \cdot 10^{-5}$ m/s we get a particle velocity of water $7.75 \cdot 10^{-7}$ m/s, i.e. at least 270 kilometres during 11000 years. This flow distance seems to be supported by hydrochemical investigations which show an increase of salinity (transition from fresh glacier meltwater to pre-existing more saline water) of the Cambrian-Vendian aquifer system in the southern Estonia (Perens and Vallner, 1997; Tšeban, 1975).

3.2. Implications of recent climatic changes to heat flow density

Plotting the Estonian heat flow density data as a function of depth (Fig. 5), an interesting result is obtained. The data in the uppermost 200 metres shows an increasing trend depth from 0–20 mW/m² to 30–50 mW/m², whereas values determined at deeper holes seem to settle at about 40 mW/m².

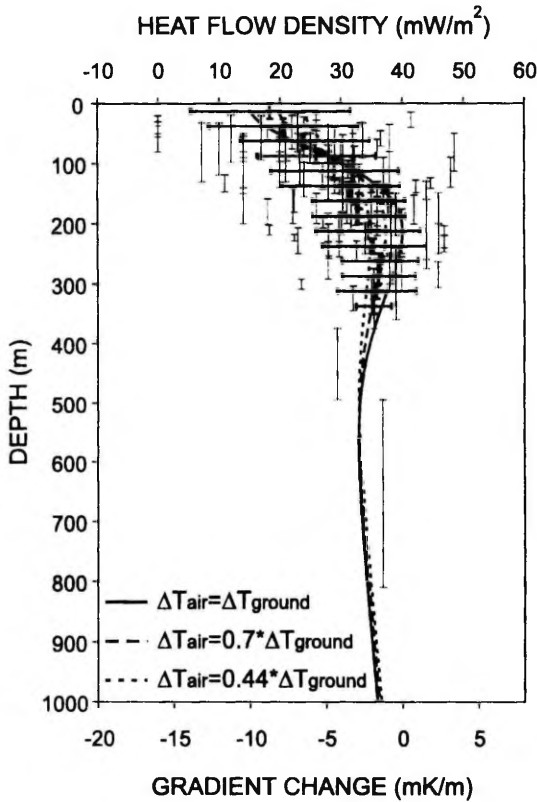


Figure 5. Heat flow density variations by depth intervals and temperature gradient changes due to change of climate. Heavy lines indicate mean values and standard deviations for 25 metre depth intervals. The figure does not include data from northeastern Estonia, from boreholes that are obviously disturbed by water flow and from boreholes of northern coastal areas which might be disturbed by human activities. Calculations of climatic perturbations are based on the model in Table 1, Paper II, except for most recent cold period that ended 135 years ago, and which had one degree lower air temperature. In different models the air temperature changes are converted to ground surface temperature changes by multiplying with 0.44, 0.7 or 1.0. The curves of temperature gradient changes can be taken as vertical heat flow density variations assuming 40 mW/m² “basal” heat flow density and 2.5 W/m/K as thermal conductivity.

Large variations at certain depth can be attributed to several disturbing factors, such as possible differences of steady-state heat flow density between different areas, unrecognized convective disturbances, local terrain effects (e.g. different land use histories, etc.) and uncertainty in thermal conductivity measurements. However, it is claimed here that generally the vertical heat flow density variation can be attributed to conductive palaeoclimatic disturbances by the Late Holocene climatic changes. The basal heat flow density can be assumed to be approximately 40 mW/m^2 in Estonia except for northeastern Estonia (data are not included in Fig. 5).

Here like in Paper II, forward modelling was used in studying the palaeoclimatic effects. In geothermics, inversion methods have recently become very popular for revealing past climatic variations from geothermal temperature profiles (Shen *et al.*, 1995; Beck, 1992; Clauser and Mareschal, 1995; Beck *et al.*, 1992; Beltrami and Mareschal, 1991; Mareschal and Vasseur, 1992; Wang *et al.*, 1992; Štulc, 1998; Majorowicz and Šafanda, 1998; Veliciu and Šafanda, 1998; Bodri and Čermák, 1998; Rajver *et al.*, 1998; Kukkonen *et al.*, 1998). Simultaneous use of many boreholes gives better results than studies based on single boreholes (Pollack *et al.*, 1996). Also forward techniques can give very good results, if they use many boreholes and take geological settings into account (e.g. Kukkonen and Šafanda, 1996). Inversion methods have been tested also with the Estonian boreholes using singular value decomposition (Mareschal and Beltrami, 1992; Beltrami and Mareschal, 1995) and least squares inversion in functional space (Shen and Beck, 1991; 1992) codes, but so far the results have been unsatisfactory. This can be attributed to the strong, but often unknown thermal conductivity variations and other disturbing factors. However, more detailed work with selected data sets might be more successful.

The instrumental records of annual mean air temperature at every weather station in Estonia suggest $0.7\text{--}1.0^\circ\text{C}$ total increase since the middle of the last century (Jaagus, 1997). The increase, however, has not been uniform. Mostly it happened before 1890 whereas after this there are no long-term changes. Only during the last decade temperature has grown again, but most of the temperature loggings were made earlier.

The heat flow density data proves that the climate was cold also before 1830s when first instrumental recording started in Estonia, suggesting that in general the climatic model in Paper II is more likely to be correct. The cold period from 1830s to 1890s alone can produce only heat flow density variations of up to few mW/m^2 and cannot be responsible for such a big decrease in heat flow density in the upper part of the cross-section.

The heat flow density data also suggest that air temperature and ground surface temperature might be more closely related to each other than was proposed in Paper II (Fig. 5). Probably the obtained constant which was used to convert air temperature to ground surface temperature (0.44, Paper II) shows better the variety of site specific conditions, but reflect worse air-ground tem-

perature coupling. The more plausible value for this constant is between 0.7 and 1.0. The first is obtained in Finland (Kukkonen, 1987) similarly to Estonia, but represents much larger range of latitudes. The second characterizes a situation where changes in mean air and ground temperature are equal.

3.3. Geothermics in the lithospheric scale

Representativity of measured heat flow density data

Any geothermal modelling is dependent on surface heat flow density values. But how representative can data from uppermost few hundred metres be for the whole crust or lithosphere? In an one-dimensional steady-state case the heat flow density should decrease with depth by an amount of heat produced by the decay of radioactive elements above the depth of measurement. However, deep drillings have proven that often this is not the case. The superdeep hole in the Kola Peninsula shows an increase of heat flow density from 30 mW/m² in the uppermost 1 km to about 50 mW/m² at 5–6 km depth (Kremenetsky and Ovchinnikov, 1986). In spite of the fact that about 7 km deep Siljan hole in Sweden is drilled to granites with relatively high heat production, the geothermal gradient is remarkably constant (Balling *et al.*, 1990; Balling, 1995; Balling and Nielsen, 1997). A significant change in heat flow density is observed in the 9 km deep KTB hole in Germany (Huenges and Zoth, 1991) and in the Vorotilovo (Popov *et al.*, 1998), Ural and Tyumen holes (Popov *et al.*, 1996) in Russia.

But not only the deep data indicate that surface heat flow density data are biased. Heat flow density measurements in up to 800 metres deep boreholes in eastern Karelia have apparently given conductive heat flow density values less than 12 mW/m² (Kukkonen *et al.*, 1998), which are even lower than what is often thought to be the mantle heat flow density.

There are three main reasons that may cause such disturbed heat flow density patterns: 1) convective heat transfer by flowing water, 2) ground surface temperature changes in the past and 3) structural features of the borehole site, namely refraction (channelling) of heat flow to rocks with higher thermal conductivity. The low heat flow density in shallow boreholes could be also attributed to minimal crustal heat production, but it does not explain vertical heat flow density variations.

In convective heat transfer, water carries heat away from one place and releases it in another place. For example, the high heat flow density in the sedimentary part of the Rheingraben can be attributed to groundwater flow (Clauser and Villinger, 1990; Schellschmidt and Schulz, 1991). Note that there the situation is opposite to the previous cases — heat flow density decreases significantly with depth in the discharge area of the flow system.

In areas where crust consists of layers with varying thermal conductivity that are tilted, refraction anomalies may occur. It is found to be important in KTB (Kohl and Rybach, 1996) and Kola (Kukkonen and Clauser, 1994) holes. However, it does not explain all the anomalies at these sites and the effect of heat refraction is negligible in horizontally layered areas.

Depending on the thermal diffusivity of rocks the largest temperature perturbations due to the Weichselian glaciation are at about 1.5 kilometres. Shallower than this depth the temperature gradient is smaller than undisturbed gradient and deeper the gradient is higher with maximum gradient at about 2.5–3.5 km. This holds fairly well for many of the above mentioned sites. The greater depth of maximal heat flow density in the Kola hole is at least partly due to heat refraction (Kukkonen and Clauser, 1994), but there are also two additional possible factors that may contribute. Firstly, Kohl (1998) studied the effect of water flow on climatic signal at the KTB and he found that downwards moving water does not “wash out” climatic signal, but it shifts it deeper. Thus, analogously the climatic perturbations in Kola may have been transported deeper by groundwater flow that does not have to be as big as was predicted by Kukkonen and Clauser (1994).

The second factor is related to the use of advanced palaeoclimatic models. The better fitting between measured data and models could be achieved if models would have different surface temperatures during glaciations. For example, models can assume the ground surface temperature during Elsterian and Saalian glaciations (possibly earlier too, but their contribution is very small) much lower than it was during Weichselian glaciation, especially its latest stage. During the Late Weichselian the deep hole area was covered by glacier and ground surface temperature was probably close to melting temperature while during earlier times of Weichselian the area was mainly exposed to cold climate (Hättestrand, 1998; Holmlund and Fastook, 1995). Anyway, the climatic history of Kola deephole site is very complicated since during glaciations this area has been at glacier central, flow and border areas, which all have different thermal conditions.

Heat production in lithosphere

It is known that in general, heat production decreases with depth. In comparison to mafic rocks, the felsic rocks, which are dominating the upper part of the crust, are enriched in heat producing radioactive elements. Unfortunately, this is only a general trend in the crustal scale and since we cannot measure *in situ* the heat production of Earth's deeper parts we must find other ways to estimate their contribution to terrestrial heat flow.

In 1960's a linear relationship was found between heat flow density Q and heat production of outcropping rocks A_s at a certain area (Roy *et al.*, 1968; Birch *et al.*, 1968)

$$Q = Q_r + D A_s. \quad (4)$$

Q_r is the "reduced heat flow", the heat coming below of layer with thickness D . Lachenbruch (1968) showed that there is a variety of models that can explain heat flow density–heat production relationship, but according to three most commonly used models the heat production decreases with depth linearly, exponentially or with a step. The most favoured has been the exponential model where the heat production A at the depth z is (Lachenbruch, 1968):

$$A(z) = A_s e^{-\frac{z}{D}} \quad (5)$$

where D is the depth where heat production has decreased to 1/e-th of its value at the surface. However, the data from the Kola deep borehole in Russia (Кременецки и Овчинников, 1986) and KTB in Germany (Pribnow and Winter, 1997) suggest that heat production is mainly linked to the rock types being more or less constant within one rock type. Furlong and Chapman (1987) showed also that the decrease does not have to be exponential since 2-dimensional (and 3-dimensional, too) models with homogeneous rock bodies give similar results. The Earth is more complicated and cannot be characterized with simple exponential decrease of heat production or with one high heat production layer above the rest of the Earth where heat production is negligible.

We must know the shape of rock bodies and their heat production. The first can be often received from seismic studies, but as shown in Paper III, the exact values of the second cannot be received because of too large error limits in P-wave velocity–heat production relationship. Actually, the heat production variations are also large if we use estimates based on lithology. This means that geothermal models must be accompanied with error estimates. One way to improve results is to use Monte Carlo modelling technique, where randomly existing high and low values are eliminated in the final result. The second way is to get data from other independent sources which would fix temperatures at certain depth. This allows to "interpolate" temperatures between two known values.

Lithospheric geothermal model of southeastern part of the Baltic Shield

The geothermal model of lithosphere in Paper IV is based on assigning fixed temperature at the seismically determined lithosphere/asthenosphere boundary. Using this boundary condition, we get much less variable temperature estimates from greater depths than by assuming the constant heat flow density in the mantle. The use of volatile-bearing peridotite solidi at the lower boundary seems to give the best results (Paper 4; Kukkonen, 1998; Kukkonen *et al.*, 1997).

In recent years, kimberlites from eastern Finland have been found. The age of kimberlite pipes is Cambrian or Ordovician (Tyni, 1997; Peltonen *et al.*, in prep.). By measuring pressure and temperature data of xenoliths we can get a new independent temperature-depth estimates to check our models.

The results of thermobarometry show that the geotherm in Paper IV is very close to the xenolith based geotherm deviating only up to 100°C (Kukkonen and Peltonen, 1998). This is within the temperature and depth error limits which for xenoliths are $\pm 50^\circ\text{C}$ and ± 10 km, respectively. However, none of xenolith samples show signs of partial melting suggesting that the petrological lithosphere continues to at least 230 km depth in eastern Finland i.e., about 50 km deeper than the seismically determined lithosphere/asthenosphere boundary. Kukkonen and Peltonen (1998) proposed that the seismically determined lithosphere corresponds to rheological lithosphere that is rigid and deeper of which the creep strength of rocks has decreased below 1–10 Mpa (Ranalli, 1995) and rocks are ductile. However, there are no signs of flow and the deeper part has been interpreted as thermal boundary layer that moves with lithosphere (Kukkonen and Peltonen, 1998).

Although there is no partial melting, the xenolith-based geotherm is very close to volatile bearing peridotite solidi at about 200 km depth in eastern Finland. This shows that application of constant temperature at the lower boundary of lithosphere models is useful a approach, but the methods for temperature estimation still have to be refined.

4. CONCLUSIONS

The present dissertation has provided the following conclusions:

* On the basis of heat flow density data compiled into updated maps and lists of all available measurements, it can be concluded, that in most of Estonia heat flow density varies mostly between 30 and 45 mW/m². The slight elevation of heat flow density in northeastern Estonia reaching 50–60 mW/m² is interpreted as a continuation of increased heat flow density area in northwestern Russia.

* Present-day convective heat transfer has only minor influence to heat flow density. Due to the hydraulic conductivity structure in carbonate rocks, the groundwater flow is forced to take place close to the surface. In terrigenous rocks the groundwater flow is reduced by co-effect of low hydraulic conductivity Quaternary sediments and permeable aquitards, which neither can be responsible for the reduction alone.

* All aquifers in the Phanerozoic sedimentary cover were recharged during glaciations. Very likely permafrost existed in Estonia, but it disappeared under the ice sheet where basal temperature reached the pressure melting point.

* Shallow (<400 m) heat flow density data is strongly influenced by climatic ground temperature changes during the Holocene. Average vertical variation in heat flow density values agrees well with forward models of palaeoclimatic conductive disturbances in the subsurface.

* Investigations of granulite facies rocks suggest that the heat production may vary widely in the middle and lower crust and only ranges of variation tend to decrease with depth. Therefore thermal models should not be presented for single sets of “best” parameter variations, but also include error estimations and variations of parameter values.

* There seems to be no relationship between heat production and seismic P-wave velocity in granulite facies rocks of Estonia and Finland which prevents using deep seismic sounding data in estimation of heat production.

* Variation of lithosphere thickness, which ranges from about 110 km in Estonia to more than 200 km in eastern Finland is only weakly reflected in the surface heat flow density variations, but it does have an effect on the lower crustal and subcrustal thermal regime, particularly on temperature. Surface heat flow density is mainly controlled by crustal, particularly upper crustal heat production.

* Lithospheric thermal models can be improved by using fixed temperatures as a lower boundary condition, while surface heat flow density can be used as an independent parameter to check the validity of models. Temperature at the seismic lithosphere/asthenosphere boundary in the southeastern part of the Baltic Shield appears to be at the solidus temperature of volatile-bearing peridotite.

5. ACKNOWLEDGEMENTS

I am grateful to all colleagues who helped me to get up to date with new literature. My special thanks belong to Ilmo T. Kukkonen (Geological Survey of Finland) for co-operation and critical comments to all my works; to Volli Kalm (University of Tartu) for support; to Jan Šafanda (Academy of Sciences of the Czech Republic) who helped me with permafrost calculations; to Kalle Kirsimäe (University of Tartu) for fruitful discussions on various topics; to Andreas Schmidt (Geological Survey of Estonia) for providing Estonian borehole temperature data; and to Ivar Puura (University of Tartu) for revising English. Paper I was supported by European Commission's JOULE programme (contract JOU2-CT 920115/1).

6. REFERENCES

- Ballard, S. and Pollack, H. N., 1987. Diversion of heat by Archean cratons: a model for southern Africa. *Earth and Planetary Science Letters*, 85: 253–264.
- Balling, N., 1995. Heat flow and thermal structure of the lithosphere across the Baltic Shield and northern Tornquist Zone. *Tectonophysics*, 244: 13–50.
- Balling, N., Eriksson, K. G., Landström, O., Lind, G. and Malmqvist, D., 1990. Thermal measurements from the deep Gravberg-1 well. Swedish State Power Board, 57, 13 pp.
- Balling, N. and Nielsen, S. B., 1997. Results of high precision temperature logging in deep boreholes in the Siljan Ring Structure, Central Sweden. Europrobe-Svekalapko 2nd workshop, Lammi, Finland, November 27–30, pp. 20.
- Beck, A. E., 1992. Inferring past climate change from subsurface temperature profiles: some problems and methods. *Palaeogeography, Palaeoclimatology, Palaeoecology*, 98: 73–80.
- Beck, A. E., Shen, P. Y., Beltrami, H., Mareschal, J.-C., Šafanda, J., Sebagenzi, M. N., Vasseur, G. and Wang, K., 1992. A comparison of five different analyses in the interpretation of five borehole temperature data sets. *Palaeogeography, Palaeoclimatology, Palaeoecology*, 98: 101–112.
- Beltrami, H. and Mareschal, J.-C., 1991. Recent warming in eastern Canada inferred from geothermal measurements. *Geophys. Res. Lett.*, 18: 605–608.
- Beltrami, H. and Mareschal, J.-C., 1995. Resolution of ground temperature histories inverted from borehole temperature data. *Global Planet. Change.*, 11: 57–70.
- Birch, F., Roy, R. F. and Decker, E. R., 1968. Heat flow and thermal history in New England and New York. In: E. Zen, W. S. White, J. B. Hadley and J. B. Thompson (Editors), *Studies of Appalachian Geology: Northern and maritime*. Interscience, New York, 437–451.
- Bodri, L. and Čermák, V., 1998. Last 250 years climate reconstruction inferred from geothermal measurements in the Czech Republic. *Tectonophysics*, 291: 251–261.
- Boulton, G. S., Caban, P. E., van Gijssel, K., Leijnse, A., Punkari, M. and van Weert, F. H. A., 1996. The impact of glaciation on the groundwater regime on Northwest Europe. *Global and Planetary Change*, 12: 397–413.
- Bredehoeft, J. D. and Papadopoulos, I. S., 1965. Rates of vertical groundwater movements estimated from the Earth's thermal profile. *Water Resources Research*, 1:325–328.
- Čermák, V., Balling, N., Kukkonen, I. and Zui, V.I., 1993. Heat flow in the Baltic Shield — results of the lithospheric geothermal modelling. *Precamb. Res.*, 64: 53–65.
- Čermák, V. and Hurtig, E., 1979. Heat flow map of Europe. In: V. Čermák and L. Rybach (Eds.), *Terrestrial heat flow in Europe*. Colour enclosure, Springer-Verlag, Berlin, Heidelberg, New York.
- Clauser, C., 1988. Untersuchungen zur Trennung der konduktiven und konvektiven Anteile im Wärmetransport in einem Sedimentbecken am Beispiel Des Oberrheintalgrabens. *Fortschritt-Berichte VDI, Reihe 19, Nr. 28*, 124 pp. (Dissertation).
- Clauser, C. and Mareschal, J. C. 1995. Ground temperature history in Central Europe from borehole temperature data. *Geophys. J. Int.*, 121, 805–817.

- Clauser, C. and Villinger, H., 1990. Analysis of conductive and convective heat transfer in a sedimentary basin, demonstrated for the Rheingraben. *Geophysical Journal International*, 100, 393–414.
- Denton, G. H. and Hughes, T. J., 1981. *The last great ice sheets*. John Wiley and Sons, 484 pp.
- Drury, M. J., 1989. Fluid flow in crystalline crust: detecting fractures by temperature logs. In: A. E. Beck, G. Garcen and L. Stegena (Editors), *Hydrogeological Regimes and Their Subsurface Thermal Effects*. Geophysical Monograph 47, Am. Geophys. Union, Washington, pp. 129–135.
- Drury, M., Jessop, A. M. and Lewis, T. J., 1984. The detection of groundwater flow by precise temperature measurements in boreholes. *Geothermics*, 13: 163–174.
- Elverhøi, A., Fjeldskaar, W., Solheim, A., Nyland-Berg, M. and Russwurm, L., 1993. The Barents Sea ice sheet — A model of its growth and decay during the last ice maximum. *Quaternary Science Reviews*, 12: 863–873.
- Furlong, K. P. and Chapman, D. S., 1987. Crustal heterogeneities and the thermal structure of the continental crust. *Geophys. Res. Lett.*, 14: 314–317.
- Gordienko, V. V., Zavgorodnyaya, O. V., Moiseenko, U. I. and Smyslov, A. A., 1985. Heat flow at the southern slope of the Baltic Shield. *Geophysical Journal*, 6: 365–376.
- Hättestrand, C., 1997. Ribbed moraines in Sweden — distribution pattern and paleo-glaciological implications. *Sedimentary Geology*, 111: 41–56.
- Hättestrand, C., 1998. The glacial geomorphology of central and northern Sweden. *Sveriges Geologiska Undersökning, Ser. Ca 85*, 47 pp.
- Hättestrand, C. and Kleman, J., 1998. Ribbed moraine formation. *Quaternary Science Reviews* (in press).
- Holmlund, P. and Fastook, J., 1995. A time dependent glaciological model of the Weichselian ice sheet. *Quaternary International*, 27: 53–58.
- Huenges, E. and Zoth, G., 1991. KTB Oberpfalz VB: temperature, thermal conductivity and heat flow density. *Scientific Drilling*, 2, 81–89.
- Hurtig, E., Čermák, V., Haenel, R. and Zui, V. (Editors), 1992. *Geothermal atlas of Europe*. Gotha, Hermann Haack, 156 pp.
- Jaagus, J., 1997. Climatic trends in Estonia during the period of instrumental observations and climate scenarios. In: J.-M. Punning (Editor), *Estonia in the system of global climate change*. Institute of Ecology, Publication, 35–48.
- Johnsen, S. J., Clausen, H. B., Dansgaard, W., Fuhrer, K., Gundestrup, N., Hammer, C. U., Iversen, P., Jouzel, J., Stauffer, B. and Steffensen, J. P., 1992. Irregular glacial interstadials recorded in a new Greenland ice core. *Nature*, 359: 311–313.
- Kleman, J., Hättestrand, C., Borgström, I. and Stroeven, A., 1997. Fennoscandian palaeoglaciology reconstructed using a glacial geological inversion model. *Journal of Glaciology*, 43 (144): 283–299.
- Kohl, T., 1998. Palaeoclimatic temperature signals — can they be washed out? *Tectonophysics*, 291: 225–234.
- Kohl, T. and Rybach, R., 1996. Thermal and hydraulic aspects of the KTB drill site. *Geophys. J. Int.*, 124: 756–772.
- Kremenetsky, A. A. and Ovchinnikov, L. N., 1986. The Precambrian continental crust: Its structure, composition and evolution as revealed by deep drilling in the USSR. *Precambrian Research*, 33: 11–43.

- Kukkonen, I., 1987. Vertical variation of apparent and palaeoclimatically corrected heat flow densities in the Central Baltic Shield. *J. Geodynamics*, 8: 33–53.
- Kukkonen, I. T., 1993. Heat flow map of northern and central parts of the Fennoscandian Shield based on geochemical surveys of heat producing elements. *Tectonophysics*, 225: 3–13.
- Kukkonen, I. T., 1998. Temperature and heat flow density in a thick cratonic lithosphere: The SVEKA transect, central Fennoscandian Shield. *J. Geodynamics*, 26: 111–136.
- Kukkonen, I. T. and Clauser, C., 1994. Simulation of heat transfer at the Kola deephole site — Implications for advection, heat refraction and paleoclimatic effects. *Geophysical Journal International*, 116: 409–420
- Kukkonen, I. T., Golovanova, I. V., Khachay, Yu.V., Druzhinin, V. S., Kosarev, A. M. and Schapov, V. A., 1997. Low geothermal heat flow of the Urals fold belt — implication of low heat production, fluid circulation or palaeoclimate? *Tectonophysics*, 276: 63–85.
- Kukkonen, I. T., Gosnold, W. and Šafanda, J., 1998. Anomalously low heat flow density in eastern Karelia, Baltic Shield: a possible palaeoclimatic signature. *Tectonophysics*, 291: 235–249.
- Kukkonen, I. T. and Peltonen, P., 1998. Xenolith-controlled geotherm for the central Fennoscandian Shield: Implications for lithosphere-asthenosphere relations. *Tectonophysics* (Submitted).
- Kukkonen, I. T. and Šafanda, J., 1996. Structure and palaeoclimate: the most important factors controlling subsurface temperatures in crystalline rocks. A case history from Outokumpu, eastern Finland. *Geophys. J. Int.*, 126: 101–112.
- Lachenbruch, A. H., 1968. Preliminary geothermal model of the Sierra Nevada. *J. Geophys. Res.*, 73: 6977–6989.
- Lachenbruch, A. H., 1982. Permafrost, heat flow, and the geothermal regime at Purdhoe Bay, Alaska. *J. Geophys. Res.*, 87, B11: 9301–9316.
- Lambeck, K., 1995. Constraints on the Late Weichselian ice sheet over the Barents Sea from observations of raised shorelines. *Quaternary Science Reviews*, 14: 1–16.
- Lewis, T. J. and Beck, A. E., 1977. Analysis of heat-flow data — detailed observations in many holes in a small area. *Tectonophysics*, 41: 41–59.
- Liivrand, E., 1991. Biostratigraphy of the Pleistocene deposits in Estonia and correlations in the Baltic region. Stockholm Univ. Dept. Quaternary Res. Report 19, Stockholm, 114 pp.
- Majorowicz, J. A., Jones, F. W., Lam, H. L. and Jessop, A. M., 1984. The variability of heat flow both regional and with depth in southern Alberta, Canada: Effect of groundwater flow? *Tectonophysics*, 106: 1–29.
- Majorowicz, J. A. and Šafanda, J., 1998. Ground surface temperature history from inversions of underground temperatures — a case study of the Western Canadian Sedimentary Basin. *Tectonophysics*, 291, 287–298.
- Mareschal, J.-C. and Beltrami, H., 1992. Evidence for recent warming from perturbed geothermal gradients: examples from eastern Canada. *Clim. Dyn.*, 6: 135–143.
- Mareschal, J.-C. and Vasseur, G., 1992. Ground temperature history from two deep boreholes in Central France. *Palaeogeography, Palaeoclimatology, Palaeoecology*, 98: 185–192.

- Moiseenko, U. I. and Chadovich, T., 1992. Heat flow density data in: E. Hurtig, V. Čermák, R. Haenel and V. Zui, (Editors), Geothermal atlas of Europe. Gotha, Hermann Haack.
- Mokrik, R., 1997. The palaeohydrogeology of the Baltic Basin — Vendian & Cambrian. Tartu University Press, Tartu, 138 pp.
- Nyblade, A. A. and Pollack, H. N., 1993a. A comparative study of parameterized and full thermal-convection models in the interpretation of heat flow from cratons and mobile belts. *Geophys. J. Int.*, 113: 747–751.
- Nyblade, A. A. and Pollack, H. N., 1993b. A global analysis of heat flow from Precambrian terrains: Implications for the thermal structure of Archean and Proterozoic lithosphere. *Journal of Geophysical Research*, 98 (B7): 12207–12218.
- Perens, R., All, T. ja Lelgus, M., 1994. Siluri karbonaatkivimite veejuhtivusest Saaremaal vooluhulga-karotaaži andmetel. *Bull. of the Geological Survey of Estonia*, 4: 36–43.
- Perens, R. and Vallner, L., 1997. Water-bearing formation. In: A. Raukas and A. Teedumäe (Editors), *Geology and mineral resources of Estonia*. Estonian Academy Publishers, Tallinn, p. 137–145.
- Piotrowski, J. A., 1997. Subglacial hydrology in north-western Germany during the last glaciation: Groundwater flow, tunnel valleys and hydrological cycles. *Quaternary Science reviews*, 16: 169–185.
- Piotrowski, J. A. and Kraus, A., 1997. Response of sediment to ice sheet loading in northwestern Germany: effective stresses and glacier-bed stability. *Journal of Glaciology*, 43: 495–502.
- Pollack, H. N., Hurter, S. J., and Johnson, J. R., 1993. Heat flow from the Earth's interior: Analysis of the global data set. *Reviews of Geophysics* 31: 267–280.
- Pollack, H. N., Shen, P. Y. and Huang, S., 1996. Inference of ground surface temperature history from subsurface temperature data: Interpreting ensembles of borehole logs. *Paegoph*, 147: 537–550.
- Polyak, B. G. and Smirnov, Y. B., 1968. Relationships between terrestrial heat flow and tectonics of continents. *Geotectonics*, 4: 205–213.
- Popov, Y. A., Pimenov, V. P., Pevzner, L. A., Romushkevich, R. A. and Popov, E. Y., 1998. Geothermal characteristics of the Vorotilovo deep borehole drilled into the Puchezh-Katunk impact structure. *Tectonophysics*, 291: 205–223.
- Popov, Y., Popov, E., Romushkevich, R., Pevzner, L. and Karasyova, T., 1996. Geothermic parameters of sections of the Ural and Tyumen superdeep boreholes. Abstracts, The Fourth International Workshop "Heat Flow and the Structure of the Lithosphere", Castle of Třešt', Czech Republic, June 9–15, pp. 97–98.
- Powell, W. G., Chapman, D. S., Balling, N. and Beck, A. E., 1988. Continental heat flow density. In: R. Haenel, L. Rybach and L. Stegena (Editors), *Handbook of terrestrial heat flow density determination*. Kluwer, Dordrecht, p. 167–222.
- Pribnow, D. and Winter, H., 1997. Radiogenic heat production in the upper third of continental crust from KTB, *Geophysical Research Letters*, 24: 349–352.
- Rajver, D., Šafanda, J. and Shen, P.Y., 1998. The climate record inverted from borehole temperatures in Slovenia. *Tectonophysics*, 291: 263–276.
- Ranalli, G., 1995. *Rheology of the Earth*. Chapman & Hall, London, 413 pp.

- Raukas, A. and Kajak, K., 1997. Quaternary cover. In: A. Raukas and A. Teedumäe (Editors), *Geology and mineral resources of Estonia*. Estonian Academy Publishers, Tallinn, pp. 125–136.
- Roy, R. F., Blackwell, D. D. and Birch, F., 1968. Heat generation of plutonic rocks and continental heat flow provinces. *Earth and Planetary Science Letters*, 5: 1–12.
- Šafanda, J., 1994. Effects of topography and climatic changes on the temperature in borehole GFU-1, Prague. *Tectonophysics*, 239: 187–197.
- Schellschmidt, R. and Schulz, R., 1991. Hydrothermic studies in the hot dry rock project at Soultz-Sous-Forêts. *Geotherm. Sci. Tech.*, 3, 217–238.
- Slater, J. G., Jaupart, C. and Galson, D. A., 1980. The heat flow through oceanic and continental crust and the heat loss of the Earth. *Rev. Geophys. Space Phys.*, 18: 269–311.
- Shen, P. Y. and Beck, A. E., 1991. Least squares inversion of borehole temperature measurements in functional space. *J. Geophys. Res.*, 96, 19965–19979.
- Shen, P. Y. and Beck, A. E., 1992. Paleoclimate change and heat flow density inferred from temperature data in the Superior Province of the Canadian Shield. *Palaeogeogr., Palaeoclimatol., Palaeoecol.*, 98: 143–165.
- Shen, P. Y., Pollack, H. N., Huang, S. and Wang, K., 1995. Effects of subsurface heterogeneity on the inference of climate change from borehole temperature data: Model Studies and field examples from Canada. *J. Geophys. Res.*, 100 (B4): 6383–6396.
- Štulc, P., 1998. Combined effect of topography and hydrogeology on subsurface temperature — implications for aquifer permeability and heat flow. A study from the Bohemian Cretaceous basin. *Tectonophysics*, 284: 161–174.
- Tšeban, E., 1975. Eesti NSV põhjavesi ja selle kasutamine. Valgus, Tallinn, 166 lk.
- Tyni, M., 1997. Diamond prospecting in Finland — a review. In: H. Papunen (Editor), *Mineral deposits: Research and exploration, where do they meet? Proceedings of the Fourth Biennial SGA Meeting, Turku, Finland*, A.A. Balkema, Rotterdam, pp. 789–791.
- Uyeda, S., 1988. Geodynamics. In: R. Haenel, L. Rybach and L. Stegena (Editors), *Handbook of terrestrial heat flow density determination*. Kluwer, Dordrecht, p. 317–351.
- Van der Kamp, G. and Bachu, S., 1989. Use of dimensional analysis in the study of thermal effects of various hydrogeological regimes. In: A. E. Beck G. Garcen and L. Stegena (Editors), *Hydrogeological Regimes and Their Subsurface Thermal Effects*. Geophysical Monograph 47, Am. Geophys. Union, Washington, pp. 23–28.
- Veliciu, S. and Šafanda, J., 1998. Ground temperature history in Romania inferred from borehole temperature data. *Tectonophysics*, 291: 277–286.
- Vitorello, I. and Pollack, H. N., 1980. On the variation of continental heat flow with age and the thermal evolution of continents. *J. Geophys. Res.*, 85: 983–995.
- Wang, K., Lewis, T. J. and Jessop, A. M., 1992. Climatic changes in central and eastern Canada inferred from deep borehole temperature data. *Palaeogeogr., Palaeoclimatol., Palaeoecol.*, 98: 129–141.
- Гордиенко, В. В. и Завгородняя, О. В., 1985. Определение теплового потока на Восточно-Европейской платформе. Доклады АН СССР, Сер. Б, О2: 10–13.

- Гордиенко, В. В., Завгородняя, О. В., Моисеенко, У. И. и Смыслов, А. А., 1984. Тепловой поток южного склона Балтийского щита. Геофизический журнал, 6: 31–7.
- Каяк, К. Ф., Раукас, А. В. и Хютт, Г. И., 1981. Опыт изучения разновозрастных морен Эстонии термолюминесцентным методом. Геология плейстоцена Северо-Запада СССР, с. 3–11.
- Кременецки, А. А. и Овчинников, Л. Н., 1986. Геохимия глубинных пород. Наука, Москва, 260 с.
- Лийвранд, Э. Д., 1986. Условия накопления четвертичных отложений в погребенной долине Пуртсе на северо-востоке Эстонии. В кн.: Палинология четвертичного периода. Наука, Москва, с. 140–147.
- Перенс, Р., 1984. Изучение фильтритрованных свойств силурийско-ордовикской карбонатной толщи Эстонии с помощью расходографии. В кн.: Л. К. Валлнер (ред.), Методы анализа и обработки гидрогеологических данных для прогноза ресурсов подземных вод. Таллинн, с. 100–104.
- Урбан, Г., 1989. Тепловой поток и радиогенная теплогенерация отдельных структур кристаллического фундамента Балтийской синеклизы. Изв. АН Эстонии, Геол., 38: 155–160.
- Урбан, Г., 1991. Новые определения теплового потока в пределах тепловой аномалии Балтийской синеклизы. Изв. АН Эстонии, Геол., 40: 24–32.
- Урбан, Г. и Цыбуля, Л., 1988. Тепловое поле Рижского плутона. Изв. АН Эстонии, Геол., 37: 49–54.
- Урбан, Г., Цыбуля, Л., Козел, В. и Шмидт, А., 1991. Геометрическая характеристика северной части Балтийской синеклизы. Изв. АН Эстонии, Геол., 40: 112–121.
- Юрима, М. Х., 1984. Применение методов геогидротермии для изучения водовмещающей толщи Эстонии. В кн.: Л. К. Валлнер (ред.), Методы анализа и обработки гидрогеологических данных для прогноза ресурсов подземных вод. Таллинн, с. 216–221.
- Юрима, М. и Эрг, К., 1984. Геотемпературное поле Эстонии на мелкомасштабных картах. Академия наук ЭССР, Институт геологии, Таллинн, 44 л.

EESTI JA SOOME EELKAMBRIUMILISE ALUSKORRA JA FANEROSOILISE SETTEKATTE GEOTERMILISED UURINGUD

Kokkuvõte

Käesolevas dissertatsioonis on toodud Eesti maasisese temperatuuri ja soojusvoo tiheduse andmestik. Käsitletakse ka peamisi soojusvoo tihedust mõjutavaid faktoreid, s.o. põhjavee liikumisega kaasnevat konvektiivset soojuskannet ja minevikus toimunud maapinnatemperatuuride muutusi. Samuti tuuakse ära keskkoorde kuuluvate granuliitse faatsiese kivimite radiogeense soojustootlikkuse andmed ning Balti kilbi keskosa ja lõunanõlva litosfääri geotermiline mudel.

Põhjavee liikumine mõjutab ainult vähesel määral maasisest soojusvälja, kuigi Peclet' arvud eeldaksid enamat. Karbonaatkivimite filtratsiooniliste omaduste kahanemine sügavuti põhjustab maapinnalähedase vee voolamise, mis ei tekita suuri soojusvälja häireid. Lõuna-Eestis devoni avamusel kahandab põhjavee voolu suhteliselt paksu, väikese filtratsioonikoefitsiendiga moreenkatte ja poolläbilaskvate veepidemete koosmõju. Soojusvoo tiheduse vertikaalseid muutusi põhjustavad ka holotseeni jooksul toimunud kliima muutused. Viimase mandrijäätumisaegse igikeltsa ja liustikualuse põhjavee voolamise mõju vajab alles uurimist.

Kristalse aluskorra granuliitse faatsiese kivimites ei sõltu radiogeenne soojustootlikkus seismiliste pikilainete leviku kiirusest, s.t. seismilisi andmeid ei tohi kasutada kesk- ja alakoore kivimite soojustootlikkuse hindamiseks. Viimane varieerub laialt, kuid tal on arvestatavad väärtused. Termiline modelleerimine näitab, et maapinna soojusvoo tihedust kontrollib peamiselt maakoore, eriti üla-koore kivimite soojustootlikkus ja litosfääri paksus on vähem tähtis. Modelleerimine näitab ka, et piirtingimusena fluide sisaldava peridotiidi solidustemperatuuri kasutamine litosfääri ja astenosfääri piiril annab mudelite sügavamas osas täpsemaid temperatuuri ja soojusvoo tiheduse tulemusi, võrrelduna mudelitega, kus vahevööst tulev soojusvoo tihedus on pandud konstantseks.

APPENDIX

Table of heat flow density data

Legend:

TC — thermal conductivity (W/(m·K)); HP — radiogenic heat production ($\mu\text{W}/\text{m}^3$); HF — heat flow density (mW/m^2); References: 1) Paper II, 2) this work, 3) Moiseenko and Chadovich, 1992, 4) Урбан и Цыбуля, 1988, 5) Урбан и др., 1991.

No.	Site		Lat. N	Long. E	Elev.	Min depth	Max depth	Temp. grad.	No. temp.	TC	No. TC	HP	No. HP	Meas. HF	Error of estim	Corr. HF	Ref.	Publ. year
1	Loksa	853	59°35.3'	25°43.6'	8	32	130							36	10	45	1	1996
								32	53	36.1	10	1.45		52.3	60.2			
								53	82	14.9	13	2.27		33.8	45.9			
								82	94	16.2	5	1.56		25.3	33.1			
2	Rohuneeme	6-2	59°34'	24°48'	3	20	116							20	4	29	1	1996
								20	64	16.3	18	1.25		20.4	28			
								64	92	8.8	12	1.72		15.1	24.1			
								92	116	9.3	11	2.57		23.9	36			
3	Saviranna	F502	59°30.1'	25°02.2'	16	32	208							44			6	1991
								32	73	41.5		1.24		51				
								73	101	25.7		1.74		45				
								101	163	14.5		2.57		37				
								163	208	15.6		2.8		44				
3	Saviranna	F502	59°30.1'	25°02.2'	16	40	212							40	11	48	1	1996
								40	93	38.9	23	1.24		48.2	54.4			
								93	116	14.7	10	1.74		25.6	32.9			
								116	148	13.0	14	2.57		33.4	42.1			
								148	212	15.0	25	3.41	5	5.25	6	51.2		
4	Maardu	F530	59°27.9'	25°04.6'	30	60	260							44			5	1991
								30	60	80	26.0		1.2		31			
								30	80	120	27.2		1.71		47			
								30	120	160	12.8		2.48		32			
								30	160	260	14.2		3.07		44			
5	Kopli	798	59°27.8'	24°39.6'		25	200	24					40			3	1979	

No.	Site		Lat. N	Long. E	Elev.	Min depth	Max depth	Temp. grad.	No. temp.	TC	No. TC	HP	No. HP	Meas. HF	Error of estim	Corr. HF	Ref.	Publ. year
6	Kuusalu	987a	59°27.1'	25°25.2'	44	50	155							44	11	51	2	
						50	113	37.3	25	1.3				48.6		54.2		
						113	130	29.9	8	1.74				52		58.1		
						130	155	12.7	11	2.5				31.9		39.5		
7	Jöelähtme	8-1	59°27.0'	25°10.5'	33	51	218							34	11	40	1	1996
						51	130	33.6	32	1.25				42		47.4		
						130	152	10.2	9	1.72				17.5		23		
						152	188	12.0	15	2.53				30.4		37.4		
						188	218	17.2	9	2.6				44.7		51.2		
8	Meriküla	914	59°25.1'	27°58.4'	4	15	208							61		67	2	
						15	78	49.7	27	1.3				64.7		71.2		
						78	109	19.7	23	2.06				40.5		48.9		
						109	150	48.4	18	1.56				75.5		80.7		
						150	208	30.7	24	1.91				58.7		63.8		
8	Meriküla	914	59°25.1'	27°58.4'	4	15	200							67			5	1991
						15	35	37.5		1.31				49				
						35	80	51.8		1.49				77				
						80	110	19.3		2.06				40				
						110	150	45.2		1.56				71				
						150	200	31.2		1.91				60				
8	Meriküla	914	59°25.1'	27°58.4'	4	25	200	34		1.9				65			3	1979
9	Kunda		59°25'	26°30'		25	230	30		1.66				50			3	1979
10	Vasavere		59°25'	27°20'		25	150	34		1.76				60			3	1979
11	Keila-Joa	4-2	59°24'	24°19'	32	73	180							37		42	2	
						73	127	34.9	23	1.3				45.3		50.5		
						127	148	14.5	9	1.73				25.1		30.6		
						152	180	13.6	12	2.53				34.3		41.3		
12	Kuusalu		59°22'	25°20'		50	180	20		1.6				32			3	1979
13	Tõrma	8531	59°19'	26°16'	87	60	100									40	5	1991
14	Kehra		59°17'	25°20'		25	200	28		1.67				47			3	1979

No.	Site		Lat. N	Long. E	Elev.	Min depth	Max depth	Temp. grad.	No. temp.	TC	No. TC	HP	No. HP	Meas. HF	Error of estim	Corr. HF	Ref.	Publ. year
15	Vintse	2-2	59°16.5'	23°52.5'	3	14	200							31		41	2	
						14	40	17.3	11	2.39	3			41.5		57.7		
						45	71	14.6	11	2.5	1			36.5		52.2		
						71	142	24.8	30	1.3				32.2		38.9		
						142	200	10.8	23	2.04				22.1		30.1		
16	Aruvalla	1001a	59°15.3'	25°02.9'	46	17	64	13.2		1.99				26		38	5	1991
17	Nabala	7-1	59°15'	24°53'	46	70	250							28		32	2	
						70	89	11.2	8	2.15				24		34.1		
						89	95	21.9	4	0.97				21.2		25.5		
						95	124	12.7	13	2.46				31.2		40.6		
						124	142	23.8	8	1.88				44.7				
						142	190	29.0	20	1.3				37.7		41.7		
						190	207	15.7	8	1.73				27.1		31.8		
						207	250	9.1	19	2.53				23		29.6		
18	Lasila		59°14.6'	26°11.8'		35	350							37			5	1991
						35	149	17.5		2.17				38				
						149	200	19.0		1.86				35				
						200	250	33.0		1.41				46				
						250	289	15.4		2.48				38				
						289	350	11.5		3.07				35				
19	Nõmmemaa	1-2	59°09'	23°45'	19	32	219							32		40	2	
						32	90	13.2	24	2.55	8			33.6		45.9		
						90	97	30.7	4	0.97				29.7		33.7		
						97	128	10.9	14	2.65	2			28.9		38.6		
						128	149	18.6	10	2.28	1			42.3		49.5		
						149	169	28.5	11	1.3				37		40.7		
						169	203	15.9	14	2.04				32.5		37.7		
						203	219	7.2	8	2.53				18.3		24.3		

No.	Site		Lat. N	Long. E	Elev.	Min depth	Max depth	Temp. grad.	No. temp.	TC	No. TC	HP	No. HP	Meas. HF	Error of estim	Corr. HF	Ref.	Publ. year
20	Lohu	5-1	59°08'	24°47'	57	78	263							26		32	2	
						78	135	10.8	24	2.15			23.3	31.5				
						139	181	9.1	18	2.46			22.4	29.4				
						181	218	23.1	16	1.3			30.1	33.3				
						218	229	12.9	5	1.73			22.4	26.5				
21	Varesmetsa	6168	59°07.0'	27°26.8'	48	9	110							44			5	1991
						9	93	28.0		2.12			59					
						93	110	17.6		2.47			44					
						20	94	7.2		2.37			17	32	5	1991		
						23	119						50	5	1991			
22	Inka	969	59°06.8'	23°50.4'	17	48	90	10.2		2.01				21				
						48	90	21.7		2.29			50					
						90	119						51		5	1991		
						40	60	16.5		1.93			32					
						40	90	11.0		2.05			23					
23	Iisaku	14	59°06'	27°18'		90	150	5.2		2.04				10				
						150	180	17.3		1.52			26					
						200	250	27.0		1.8			49					
						250	290	33.5		1.74			58					
						310	344	17.6		2.74			48					
24	Tudulinna	24	59°03'	27°09'		50	130							56			5	1991
						50	80	18.7		2.1			39					
						80	110	28.0		2.05			57					
						110	130	23.0		2.34			54					
						107	312						34	39	2			
25	Jaama	3. 23	59°02.9'	27°44.5'	32	107	211	14.8	43	2.15				31.7		38.2		
						211	255	12.1	19	2.46			29.7		35.4			
						255	312	30.7	24	1.3			39.9		43			
						107	211	14.8	43	2.15			31.7		38.2			
						211	255	12.1	19	2.46			29.7		35.4			
26	Ramma	974	59°01.4'	26°02.0'	97	107	211	14.8	43	2.15				31.7		38.2		
						211	255	12.1	19	2.46			29.7		35.4			
						255	312	30.7	24	1.3			39.9		43			
						107	211	14.8	43	2.15			31.7		38.2			
						211	255	12.1	19	2.46			29.7		35.4			

No.	Site		Lat. N	Long. E	Elev.	Min depth	Max depth	Temp. grad.	No. temp.	TC	No. TC	HP	No. HP	Meas. HF	Error of estim	Corr. HF	Ref.	Publ. year
27	Ellavere	594	59°00.5'	25°59.9'	99	17	150							29			5	1991
						17	50	10.6		2.2		23						
						50	97	6.4		2.25		14						
						97	150	11.3		2.54		29						
28	Risti	1121a	59°00.0'	24°06.2'	40	30	160									33	5	1991
						30	55	0				0		33				
						55	97	8.6		2.36		20		33				
						97	160	11.9		2.37		28		33				
29	Förby	F369	58°59.9'	23°08.8'	1	130	306							38	5	46	2	
						130	159	14.4	12	2.18		31.4		40.3				
						159	170	28.3	4	1.35		38.2		43.2				
						170	264	15.4	38	2.48		38.2		46.4				
						264	306	14.7	17	3.12	5	2.08	5	45.9		55.5		
30	Soovälja	K1	58°59.5'	22°46.3'	6	32	814							34	3	42	1	1996
						32	130	2.6	40	2.74	12		7.2		21.4			
						130	275	18.0	59	2.44	14		44		51.8			
						275	375	12.3	42	2.87	10		35.4		44			
						375	495	11.4	49	2.58	11		29.4		37.4			
						495	810	12.6	126	2.93	29	1.94	27	36.8		44.1		
31	Taebla	F349	58°57.2'	23°45.6'	10	40	360							39			5	1991
						40	80	10.1		2.28		23						
						80	150	15.9		2.37		38						
						150	220	20.9		1.85		39						
						220	240	43.0		1.1		47						
						240	285	15.8		2.48		39						
285	360	14.5		2.7		39												

No.	Site		Lat. N	Long. E	Elev.	Min depth	Max depth	Temp. grad.	No. temp.	TC	No. TC	HP	No. HP	Meas. HF	Error of estim	Corr. HF	Ref.	Publ. year
32	Keava	936	58°57'	24°57'	69	35	228							5			5	1991
						35	70	12.6		2.22		28						
						70	110	4.2		2.19		9						
						120	200	2.0		2.36		5						
33	Haapsalu	985	58°56.1'	23°31.4'	6	19	247							48			5	1991
						19	98	5.1		2.28		12						
						98	155	10.5		2.3		24						
						155	204	16.3		2.18		36						
34	Maidla	1307	58°56.0'	24°07.5'	34	50	300							47			5	1991
						50	100	10.0		2.51		25						
						100	200	15.0		2.17		33						
						200	254	17.6		1.58		28						
35	Maidla	1307	58°56.0'	24°07.5'	34	254	300	18.5		2.04				47			5	1991
						254	300	18.5		2.04		38						
						52	320					29		35	2			
						52	183	11.9	54	2.55		30.3		40.4				
						183	188	28.8	4	0.97		27.9		30.7				
						188	230	11.8	17	2.53		29.7		36.5				
						230	292	21.4	26	1.3		27.9		31.2				
292	309	9.3	8	2.53		23.5		30.2										
36	Kirimäe	F350	58°55.6'	23°45.6'	16	309	320	14.7	6								5	1991
						309	320	14.7	6									
37	Koluvere	971	58°53.8'	24°06.2'	26	60	100	14.7		2.2				32		47	5	1991
						34	200							31				
						34	130	8.3		2.47		21						
					130	200	14.3			2.2			31					

No.	Site		Lat. N	Long. E	Elev.	Min depth	Max depth	Temp. grad.	No. temp.	TC	No. TC	HP	No. HP	Meas. HF	Error of estim	Corr. HF	Ref.	Publ. year
38	Tooma	1052	58°53.2'	26°12.1'	78	20	250							40			5	1991
						20	76	9.8		2.22				22				
						81	122	12.7		2.17				28				
						122	176	13.0		2.54				33				
						176	250	21.0		1.89				40				
39	Lelle	1254	58°51.3'	25°01.7'	66	34	177							9			5	1991
						34	71	5.4		2.78				15				
						71	128	2.3		2.2				5				
						128	177	4.1		2.2				9				
40	Jõgeva	1302	58°45.7'	26°21.9'	75	22	201							46			5	1991
						22	39	8.8		2.78				24				
						39	98	13.6		2.17				29				
						99	143	12.5		2.18				27				
						149	201	19.0		2.43				46				
41	Kõnnu	300	58°43.6'	24°50.6'	56	40	245					0.82	3	5			5	1991
						40	105	0						0				
						105	171	1.5		2.41				4				
						171	245	2.7		2.23				6				
42	Võhma		58°35'	25°30'	50		400							38			3	1979
43	Are	171	58°31.9'	24°35.4'	18	60	250					0.71	6	41			5	1991
						60	90	10		3.05				30				
						90	140	22.8		2.2				48				
						140	200	6.7		2.16				14				
						200	250	15.4		2.19				34				
44	Tori-Jõesuu	188	58°29.6'	24°53.5'	20	28	76							26			5	1991
45	Ramsi	H-420	58°24.7'	25°35.7'	78	60	210							35			5	1991
						30	50	0						0				
						60	90	13.3		2.67				36				
						110	160	11.4		2.78				32				
						160	210	14.4		2.46				35				

No.	Site		Lat. N	Long. E	Elev.	Min depth	Max depth	Temp. grad.	No. temp.	TC	No. TC	HP	No. HP	Meas. HF	Error of estim	Corr. HF	Ref.	Publ. year
46	Viki	532	58°21.1'	22°05.1'	22	153	201	16.8		2.5				42			4	1988
47	Tartu	422	58°21.2'	26°41.6'	72	45	100	12.2		2.1				26		38	5	1991
48	Pärnu	383	58°21'	24°40'		37	190							51			5	1991
						20	37	-						-				
						37	60	9.1		2.25				20				
						60	80	0						0				
						90	120	17.0		2.33				40				
						120	160	22.8		2.29				52				
						160	190	24.3		2.5				61				
49	Pärnu	330	58°19.4'	24°44.7'		20	188							40			5	1991
						20	60	8.2		2.25				19				
						60	90	0						0				
						90	140	17.8		2.24				40				
						140	188	27.7		2.48				69				
50	Viljandi		58°19'	25°28'		40	220							36			5	1991
						40	60	7.5		2.4				18				
						60	80	12		2.2				26				
						80	160	0						0				
						160	180	30.5		2.34				71				
						180	220	14.2		2.5				36				
51	Pärnu	345	58°16'	24°44'		20	210							35			5	1991
						20	54	12		2.27				27				
						54	90	5		2.75				14				
						100	130	14		2.25				32				
						130	160	16.7		2.17				36				
						160	180	14.5		2.46				36				
						180	210	12.7		2.87				36				
52	Elva		58°13.5'	26°25.0'	60	50	150									49	5	1991
						50	90	16.8		1.89				32		49		
						90	150	18		2.04				37		49		

PUBLICATIONS

Jõelet, A., 1997.
Temperature and heat flow in Estonia.
In: S. Hurter (ed.) Atlas of geothermal resources in Europe.
European Commission, Directorate General XII — Science,
Research and Development. (In press).

TEMPERATURE AND HEAT FLOW IN ESTONIA

Argo Jõelet

Institute of Geology, University of Tartu,
Vanemuise 46, Tartu 51014, Estonia, e-mail ajoeleht@math.ut.ee

Introduction

Estonia is situated on the southern slope of the Baltic Shield, which has been described as a relatively low heat flow area (Urban *et al.*, 1991; Jõelet and Kukkonen, 1996), as well as the Baltic Shield itself (Balling, 1995; Čermák *et al.*, 1993; Kukkonen, 1987, 1988). The thickness of the Phanerozoic sedimentary rocks that cover the Early Proterozoic basement, increases from 150 m in the north to 600–700 m in the south. The sedimentary cover is represented by Vendian, Cambrian, Ordovician, Silurian and Devonian sediments. Geothermally the most interesting aquifers are in Cambrian and Vendian sandstones and siltstones. Due to the quite low heat flow from the Precambrian basement and the small thickness of sedimentary rocks the groundwater temperatures in the Phanerozoic aquifers are below 15°C and do not represent useful geothermal resources in terms of typical “Hot wet rock” techniques. However, these formations could well be used for producing geothermal energy for space heating with heat exchanger techniques. Potential targets can also be found in the basement for “Hot dry rock” applications.

Temperature, heat flow density and heat production data

The temperature maps are based on data by Savitskii *et al.* (1977), Jurima and Erg (1984) and Jõelet and Kukkonen (1996; 1995 unpubl. data). Only data from holes that are deeper than 2/3 of the nominal depths of the maps were used in compiling the temperature maps.

In the maps of temperatures at 250 and 500 m depths the high temperature values (11°C and 14°C, respectively) in northern Estonia can be attributed to the thermal blanketing effect caused by the low thermal conductivity of the Lower Cambrian clays (about 1.3 W/K/m), which attain a thickness of about 100 m. In southern Estonia the increased temperatures at the top of the basement are related only to a bigger depth of the basement than in northern Estonia.

The heat flow density data (Table 1) was compiled from Urban *et al.* (1991) and Jõelet and Kukkonen (1996; 1995 unpubl. data). Since the details of the corrections applied by Urban *et al.* (1991) have not been reported, only their apparent heat flow density values were included in the present study. The apparent heat flow density in Estonia varies from 22 to 62 mW/m² (Table 1) and its mean value is 35 mW/m².

Paleoclimatic corrections of the geothermal gradient were calculated with homogeneous half-space models. The ground surface temperature history applied in the corrections is described in detail in Jõelet and Kukkonen (1996). The greatest calculated temperature perturbations (up to –3°C) are due to glaciations and they occur at

about 1500 m depth. Paleoclimatically corrected heat flow density values vary between about 28 and 68 mW/m² and the mean value is 42 mW/m².

The Estonian Precambrian basement is represented by metamorphic rocks of the amphibolite and granulite facieses as well as the granulites with retrograde overprint under amphibolite facies conditions (Hölttä and Klein, 1991). The heat production values of the Estonian Precambrian basement are given. In general the mean heat production values decrease with increasing metamorphic grade from 3.23 $\mu\text{W}/\text{m}^{-3}$ in the amphibolite facies to 1.26 $\mu\text{W}/\text{m}^{-3}$ in the granulite facies whereas granulite facies rocks with a retrograde overprint under amphibolite facies conditions have intermediate values (mean 2.09 $\mu\text{W}/\text{m}^{-3}$) (Kukkonen and Jöeleht, 1996).

Hydrogeological effects

In earlier investigations temperature measurements in Estonia have been made in 250–350 m deep holes and in the lower part of the holes (>150 m) readings have been taken only at every 50 m. Such data does not necessarily allow identification of hydrogeologically disturbed temperature logs. However, numerical fluid and heat transfer simulations have indicated that heat transfer by groundwater flow is not generally significant, although small disturbances may exist at shallow depths (Jöeleht and Kukkonen, 1996). These disturbances (up to 10 mW/m²) are due to the high hydraulic permeability (up to $5 \cdot 10^{-12}$ m²) of the sedimentary rocks, but the disturbances are constrained to depths above 200 m. In southern Estonia the increased hydraulic gradient (up to 0.02) due to higher topographic variations may produce greater heat flow density disturbances. Therefore, in the current heat flow density maps only data from boreholes deeper than 200 m has been used.

Urban *et al.* (1991) reported a low heat flow density area (less than 10 mW/m²) in central Estonia. It was based on measurements made in boreholes, which are in the vicinity of major fracture zones of NE-SW and NW-SE directions. These zones are up to 10 km wide and in detail consist of many smaller fracture zones. The increased permeability creates local groundwater recharge systems and downward flowing water may produce heat flow minima at these small depths (0–250 m). Moreover, some of these boreholes for which low heat flow density values have been reported, are obviously disturbed by water flow in the holes as well.

Geothermal potential of Estonia

Small thickness of the sedimentary cover and the relatively low heat flow density are responsible for the lack of geothermally useful aquifers. Geothermal energy is used for local heating only in installation near Tallinn, northern Estonia (L. Savitskii, Geological Survey of Estonia, personal comm., 1994). For Hot Dry Rock technique northeastern Estonia is the most potential area and temperatures of 30°C can be expected at depths of about 1 km. The origin of increased heat flow density in the area is not yet well understood. Since there is no thermally important regional groundwater flow, the anomaly can be more likely attributed to crustal heat sources in the basement.

Acknowledgements. This data compilation was partly supported by Socomine, contract JOU2-CT920115/1. I am grateful to I. Kukkonen (Geological Survey of Finland) for a constructive review of the manuscript.

References

- Balling, N., 1995. Heat flow and thermal structure of the lithosphere across the Baltic Shield and northern Tornquist Zone. *Tectonophysics*, 244, 13–50.
- Čermák, V., Balling, N., Kukkonen, I. and Zui, V.I., 1993. Heat flow in the Baltic Shield — results of the lithospheric geothermal modelling. *Precambrian Research*, 64, 53–65.
- Kukkonen, I.T., 1987. Vertical variation of apparent and paleoclimatically corrected heat flow densities in the central Baltic Shield. *Journal of Geodynamics*, 8, 33–53.
- Kukkonen, I.T., 1988. Terrestrial heat flow and radiogenic heat production in Finland, the central Baltic Shield. *Tectonophysics*, 156, 59–74.
- Kukkonen, I.T. and Jöeleht, A., 1996. Geothermal modelling of the lithosphere in the central Baltic Shield and its southern slope. *Tectonophysics*, in press.
- Hölttä, P. and Klein, V., 1991. PT-development of granulite facies rocks in southern Estonia. *Geological Survey of Finland, Special Paper 12*, 37–47.
- Jöeleht, A. and Kukkonen, I.T., 1996. Heat flow in Estonia — Assessment of palaeoclimatic and hydrological effects. (Submitted to *Geophysica*).
- Jurima, M. and Erg, K., 1984. Geotemperaturnoe pole Estoni na melko mastabnyh kartah. Tallinn, 44 pp. (in Russian, unpublished report in the Geological Fund of Estonia).
- Savitskii, L.A., Belkina, V.Y., Savitskaya, L.O., Jurima, M.H., Jaani, A.E. and Yashtshuk, S.D., 1977. Svodnyi otshet po izutsheniyu rezhima podzemnyh vod na territoriy ESSR. Tallinn, 637 pp. (in Russian, unpublished report in the Geological Fund of Estonia).
- Urban, G., Tsybulia, L., Cozel, V. and Schmidt, A., 1991. A geothermic characterization of the northern part of the Baltic Syncline. *Proceedings of the Estonian Academy of Sciences, Geology*, 40, 112–121.

Table 1. Heat flow data in Estonia.

No.	Site	Hole	Latitude (N)	Longitude (E)	Q (mW/m ²)	Qpaleocorr. (mW/m ²)	Reference
1.	Kärdla	K-1	58°59'	22°40'	34	42	1
2.	Förby	F-369	59°00'	23°09'	38	46	1
3.	Jõeähtme	8-1	59°27'	25°10'	34	40	1
4.	Saviranna	F-502	59°30'	25°03'	40	48	1
					43	51	2
5.	Loksa	853	59°35'	25°44'	36	45	1
6.	Haapsalu	985	58°57'	23°35'	27	37	2
7.	Are	171	58°33'	24°38'	31	40	2
8.	Maidla	1307	58/57'	24°11'	29	37	3
					31	38	2
9.	Lasila		59°16'	26°16'	38	43	2
10.	Tooma	1052	58°53'	26°19'	32	37	2
11.	Võru		57°52'	27°03'	22	28	2
12.	Meriküla	914	59°26'	28°00'	61	67	3
					62	68	2
13.	Maardu	530	59°28'	25°06'	41	48	2
14.	Koluvere	971	58°55'	24°10'	25	35	2
15.	Taebla	349	58°58'	23°47'	37	47	2
16.	Tudulinna	24	59°03'	27°09'	35	39	2
17.	Jõgeva	1302	58°41'	26°27'	33	40	2
18.	Pärnu	345	58°16'	24°44'	28	36	2
19.	Pärnu	383	58°21'	24°40'	45	54	2
20.	Ramsi	H-420	58°19'	25°36'	34	40	2
21.	Keila-Joa	4-2	59°24'	24°19'	37	42	3
22.	Nabala	7-1	59°15'	24°53'	28	32	3
23.	Nõmmemaa	1-2	59°09'	23°45'	32	40	3
24.	Ramma	974	59°03'	26°05'	34	39	3
25.	Lohu	5-1	59°08'	24°47'	26	32	3
26.	Vintse	2-2	59°17'	23°53'	31	41	3

References:

- 1) Jõeäht and Kukkonen, 1996
- 2) Urban *et al.*, 1991
- 3) Jõeäht and Kukkonen, 1995 (unpubl. data)

Jõelet, A. and Kukkonen, I. T., 1996.
Heat flow density in Estonia — Assessment of palaeoclimatic and
hydrogeological effects.
Geophysica, 32 (3): 291–317.

Heat Flow Density in Estonia - Assessment of Palaeoclimatic and Hydrogeological Effects

A. Jõelehr¹ and I.T. Kukkonen²

¹ Institute of Geology, University of Tartu, Vanemuise 46, EE2400 Tartu, Estonia
(previously at: Geological Survey of Estonia, Pikk 67, EE0001 Tallinn, Estonia)

² Geological Survey of Finland, Betonimiehenkuja 4, FIN-02150 Espoo, Finland

(Received: November 1995; Accepted: May 1996)

Abstract

New measurements of heat flow density have been made in six boreholes in northern and western Estonia. The mean heat flow values range from 20 to 40 mW m⁻². All holes display a vertical variation in apparent heat flow densities from 15 to 52 mW m⁻². Since most of the holes are shallow and therefore sensitive to surficial disturbances, the effects of palaeoclimatic ground temperature changes and heat transfer by groundwater flow were studied with numerical models. Forward modelling of palaeoclimatic effects was made with a homogeneous half-space model in which the assumed climate history covered glaciations during the past million years, the Holocene, and the recent climatic warming. The influence of the sea cover after deglaciation was also included. The palaeoclimatic models suggested that the measured vertical variation might be partly attributed to the palaeoclimatic effects, but when the corrections were applied to the measured data they did not entirely eliminate the vertical variation in heat flow density. This is probably due to thermal conductivity structures that deviate from the assumed half-space conditions and the palaeoclimatic ground temperature history used in the models. Fluid and heat transfer in the subsurface were simulated with finite difference techniques. The simulation results of a 2-dimensional model indicate that the thermal effect of regional flow systems is less than 5 mW m⁻² in most of Estonia. Larger perturbations may occur in the southeast of the country, where the hydraulic gradient is higher.

Key words: geothermics, paleoclimatic, hydrogeology, drill holes, Estonia

1. Introduction

Geothermal information on Estonia, which lies on the southern slope of the Baltic (Fennoscandian) Shield, is based on heat-flow density (HFD) measurements provided by Urban *et al.* (1991). According to them, heat flow density is generally about 40 mW m⁻², but there are considerable local anomalies. Borehole depths range from 60

to 350 m. Most of the boreholes are in the Phanerozoic sediments; only five reach the Precambrian basement. The data used by *Urban et al.* (1991) were originally produced for hydrogeological purposes to characterize aquifer temperatures. Therefore, the depth interval between temperature readings in single boreholes varied from 2.5 to 50 m. Although *Urban et al.* (1991) did not report any thermal conductivity measurements in detail their data suggest that the average sampling interval was 20 m.

Geothermal logs are sensitive to convective and conductive disturbances such as shallow groundwater circulation and transient conductive disturbances created by palaeoclimatic changes in ground surface temperatures. These effects have not yet been discussed with reference to the area of Estonia.

We here present a palaeoclimatic ground temperature history for the study area compiled from various proxy and meteorological data. The data were used to calculate the palaeoclimatic disturbances to HFD data with half-space models.

The thermal effects of groundwater circulation in Phanerozoic sediments are discussed with the aid of numerical modelling. A 2-dimensional finite difference simulation of fluid and heat transfer in the subsurface is presented for a 230-km-long transect running from Haanja, southern Estonia, to Võsu, northern Estonia.

Finally we present new temperature, fluid resistivity and thermal conductivity data from six boreholes in northern and western Estonia, ranging from 110 to 810 m in depth.

2. *Palaeoclimatic effects on subsurface temperatures*

Climatic temperature changes at the ground surface propagate downwards to the subsurface, creating transient disturbances in the geothermal gradient. Due to the poor thermal diffusivity of rocks, the disturbances persist in the bedrock for a long time. To obtain an undisturbed steady-state heat flow density value, the measured values should therefore be corrected for ground surface temperature histories (e.g. *Beck*, 1977). Conversely, subsurface temperature logs can be applied to reconstruct the past ground surface temperature history (e.g. *Čermák et al.* 1993).

The surface temperature history of Estonia during the last million years (Table 1) was compiled from the literature. Deglaciation in the study area took place at 11 500 BP (*Donner and Raukas*, 1989). The periods of earlier glaciations and deglaciations were adapted from studies conducted in Finland (*Kukkonen*, 1987) using the oxygen-isotope curve of ocean sediments (*Shackleton and Opdyke*, 1976), which represents the variation in the ice volume in glaciers. The surface temperature under the ice sheets was assumed to represent pressure melting, that is, -1°C . The value is the same as in *Jessop* (1971) and *Kukkonen* (1987) for the Canadian and Baltic Shields, respectively.

Palaeontological (Iversen, 1944) and palaeobotanical (Donner, 1978) studies indicate that 8000-5000 years ago the air temperature was +2°C higher than it is today. The warmer period (+1 °C) continued until 2500 BP (Aaby, 1976). Little is known about "the Little Climatic Optimum" (700-1300 AD) and "the Little Ice Age" (1300-1700 AD) in the Shield area and so data on western Europe (Bell and Walker, 1992) were used. Regular meteorological temperature observations were started in Estonia in 1828. The air temperature is reported to have increased by 0.5°C since the end of the last century (Jaagus, 1994).

Table 1. Ground surface temperature changes relative to present values in Estonia. The data were compiled from various geological, proxy and meteorological sources (see text). The time of deglaciation (t_g) and the ground temperature difference between glaciation and the present (ΔT_g) were determined for each site on the basis of its deglaciation history. For northern and western Estonia, the values are 11500 years and -7 K, respectively. Outside the given $t_i - t_{i+1}$ intervals the ground surface temperature was assumed to be equal to its present value.

ΔT_i	t_{i+1}	t_i
-0.2	95	295
-0.9	295	695
0.4	695	1295
0.4	2500	5000
0.9	5000	8000
ΔT_g	t_g	30000
"	40000	45000
"	60000	75000
"	126000	194000
"	240000	290000
"	340000	357000
"	429000	471000
"	479000	533000
"	573000	671000
"	680000	716000
"	732000	794000
"	803000	848000

The ground surface temperature is not the same as the air temperature, although these parameters are often linearly correlated (Kukkonen, 1987). The relation between air and surface temperatures was determined from data published by the Estonian Meteorological and Hydrological Institute (Prokhorov, 1970). Annual mean soil

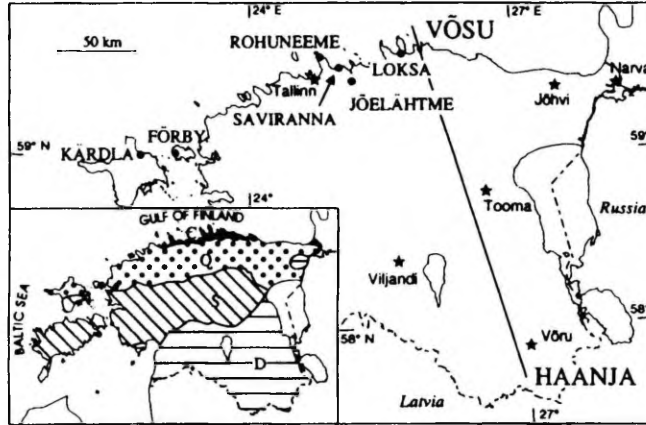


Fig. 1. Location of meteorological stations (stars) and new heat flow density measurement sites (dots; Table 3), the cross-section used for hydrogeological modelling and the main outcropping stratigraphic units in Estonia: C, Cambrian, O, Ordovician, S, Silurian and D, Devonian.

temperatures at a depth of 40 cm at six meteorological stations (Fig. 1) and corresponding air temperatures at the same stations for the period 1952-1965 were used for regression analysis. The air temperatures range from 3.0 to 6.7°C and surface temperatures at a depth of 40 cm from 5.3 to 7.6°C. To avoid over-representation of some temperature intervals, the data were divided into 0.5°C air temperature intervals for which corresponding average ground temperature values were then calculated. The following regression line was obtained (Fig. 2):

$$T_s = 0.44 T_a + 4.49, \quad (1)$$

where T_s and T_a are annual mean surface and air temperatures (°C), respectively. Eq. (1) was further used to convert palaeoclimatic air temperature estimates based on various geological, botanical and other proxy indicators to surface temperatures.

When the Weichselian ice sheet had already retreated to the north, coastal areas were still covered by sea. Because of glacio-isostatic uplift of the lithosphere, the Baltic Sea retreated westwards and northwards, exposing new land areas. Depending on the location and present elevation above sea level, the time of retreat ranges in Estonia from 9000 years BP in more elevated areas to 1000 years BP in areas close to the present shore line.

Recent studies in the Baltic Proper and in the Gulf of Finland (Kullenberg, 1981; Haapala and Alenius, 1994) show that at depths exceeding 50 m the seawater temperature is close to +4°C, with annual variations of a few tenths of a degree. In shallower depths, the water is effectively mixed and the sea bottom temperatures more or less follow the air temperature variations. Due to the lack of more accurate

information, we assume that the present ground surface temperature and the sea surface temperature at the same location are equal (+6 °C) and that the sea bottom temperature varies linearly from 4°C (50 m) to the prevailing surface temperatures at zero sea depth.

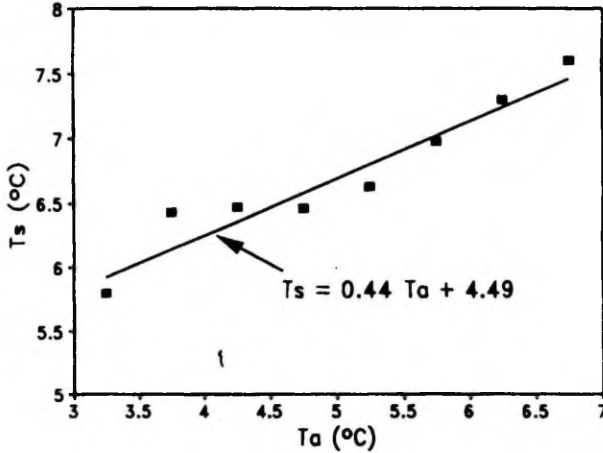


Fig. 2. Annual mean air temperature versus ground temperature in Estonia at 40 cm depth below the ground surface. Data from the six stations of the Estonian Meteorological and Hydrological Institute for 1952-1965. The points represent mean values of ground temperatures calculated from the original annual mean temperature data arranged into groups of 0.5°C intervals of air temperature. The regression line corresponds to Eq. (1).

General palaeoclimatic ground surface temperature histories were constructed separately for northern and western Estonia. The temperature histories were approximated with stepwise changes (Table 1). The surface temperature variation was calculated as a function of sea depth and air temperature. Air temperatures were converted to ground temperatures with Eq. (1).

The subsurface thermal responses to the palaeoclimatic ground surface temperature histories were calculated with a homogeneous half-space model with constant diffusivity (*s*). The subsurface temperature $\Delta T(z,t)$ and gradient disturbances $\Delta \Gamma(z,t)$ due to several instantaneous changes in surface temperature ΔT_i during the time period $t_{i+1} < t < t_i$ are (Carslaw and Jaeger, 1959; Jaeger, 1965; Čermák, 1976):

$$\Delta T(Z)_i = \Delta T_i \left(\operatorname{erf} \frac{Z}{\sqrt{4st_i}} - \operatorname{erf} \frac{Z}{\sqrt{4st_{i+1}}} \right) \tag{2}$$

and

$$\Delta \Gamma(Z)_i = \Delta T_i \left[(\pi st_i)^{-1/2} \exp(-z^2/4st_i) - (\pi st_{i+1})^{-1/2} \exp(-z^2/4st_{i+1}) \right]. \tag{3}$$

A thermal diffusivity of $1 \cdot 10^{-6} \text{ m}^2 \text{ s}^{-1}$ was used for all models.

In general, the results of models for different parts of Estonia (Fig. 3) are similar, since there are no significant differences between ground surface temperature histories. The results suggest that the palaeoclimatic effect reduces the geothermal gradient by 3–6 mK m^{-1} in the uppermost 200 m, which is the depth interval most affected by temperature changes during the Holocene.

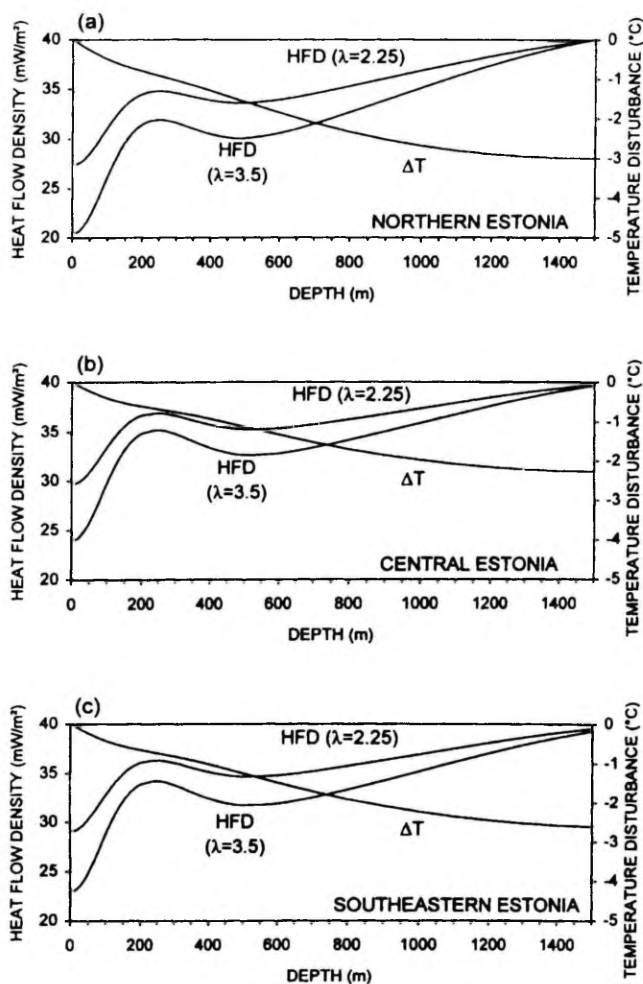


Fig. 3. Theoretical palaeoclimatic temperature disturbance and heat flow density *versus* depth curves calculated from the ground temperature history in Table 1. Calculations were made for (a) northern and western, (b) central and (c) southeastern Estonia. The HFD curves were calculated for sedimentary cover (thermal conductivity $2.25 \text{ W m}^{-1} \text{ K}^{-1}$) and for the Precambrian basement ($3.5 \text{ W m}^{-1} \text{ K}^{-1}$) by assuming a basal heat flow density of 40 mW m^{-2} .

Deeper down the palaeoclimatic effect diminishes, and is mainly due to glaciations. The effects extend down to a depth of 1200 m, below which the gradient changes are less than 1 mK m^{-1} . Theoretical palaeoclimatic temperature disturbance and heat flow-depth curves are also presented in Fig. 3. Due to the Holocene temperature changes, the palaeoclimatic effect is less than 3 mK m^{-1} at depths between 150 and 400 m. If we assume that the palaeoclimatic histories are correct, the result indicates that, even at shallow depths, heat flow density measurements may yield values close to those of undisturbed situations. Depending on conductivity, the deviation would not be more than $5\text{-}7 \text{ mW m}^{-2}$.

In detail, the modelling suggests slight differences between northern and western coastal areas, the central Estonian upland and southeastern Estonia. The temperature perturbations in central Estonia are smaller than those in southeastern Estonia. In central Estonia, the present surface temperature is lower ($< 5^\circ\text{C}$) than elsewhere (5.5°C in southeastern Estonia and 6°C in northern and western coastal areas) and surface temperature changes between the present and glaciations are relatively smaller. The disturbances in heat flow density do not, however, differ by more than $4\text{-}5 \text{ mW m}^{-2}$ (Fig. 3).

The ice sheet withdraw later in northern and western Estonia than in the southwest, and so the modelling gave the largest temperature perturbations for these areas. Since the coastal areas were covered by sea after deglaciation, the calculated gradient changes depend on the elevations of the borehole sites. For instance, in the Rohuneeme and Fõrby holes, drilled very close ($< 30 \text{ m}$) to the shoreline, the gradient perturbations are about 1 mK m^{-1} in the uppermost 300 m. This is more than in Jõelähtme and Saviranna, which are situated farther away from the shore, at elevations of 32 and 16 m, respectively (Fig. 4).

3. *Hydrogeological effects on subsurface temperatures*

Quaternary sediments cover the Phanerozoic deposits ranging from Vendian to Devonian on Precambrian basement. The basement depth increases rather monotonously from north to south, from 150 m on the shore of the Gulf of Finland to 600 m in southern Estonia (Koistinen, 1994). Aquifers suitable for water production are usually only a few tens of meters thick. The sedimentary rocks are very poorly consolidated and, with the exception of the Lower Cambrian clay formation, have rather high hydraulic conductivities (about $10^{-5}\text{-}10^{-4} \text{ m s}^{-1}$). These Lontova stage clays have much lower hydraulic conductivities (mean value $5 \cdot 10^{-14} \text{ m s}^{-1}$; Pirrus and Saarse, 1979). The hydraulic conductivities of other Phanerozoic sediments were

determined from the specific yield data listed in *Tšeban* (1975) and *Arkhangelskiy* (1966):

$$k = 130q/(m \cdot 86400) \quad (4)$$

where k is hydraulic conductivity (m s^{-1}), q specific yield ($\text{l s}^{-1} \text{m}^{-1}$) and m the thickness (m) of the measured interval.

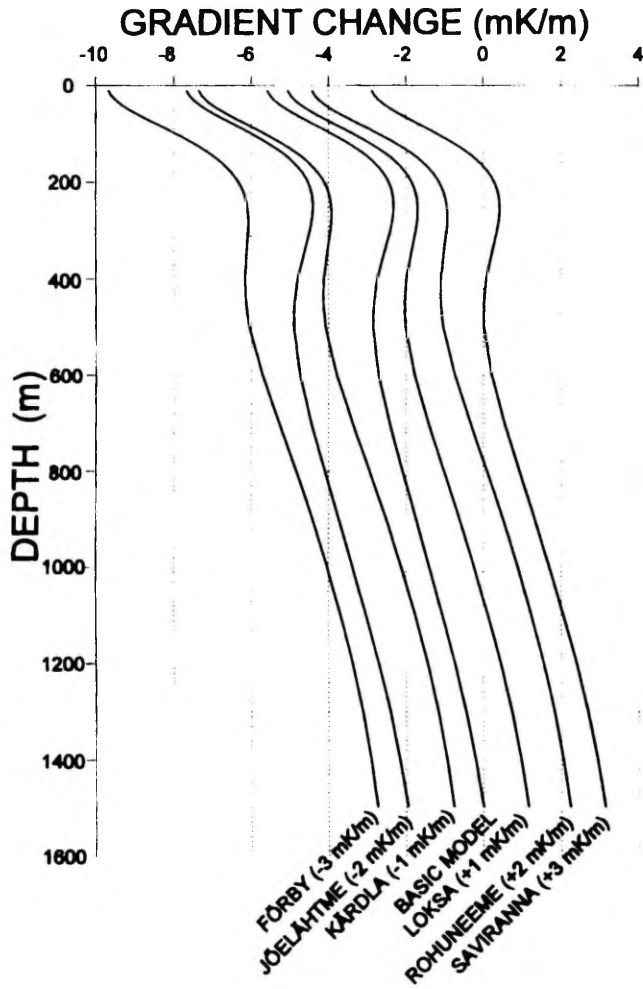


Fig. 4. Simulated temperature gradient changes produced by palaeoclimatic ground temperature variations at the sites of new geothermal measurements. For clarity, the curves were displaced by -3 - $+3 \text{ mK m}^{-1}$ from the general model for northern Estonia.

The calculated hydraulic conductivity values for the Cambrian-Vendian aquifer range from $6.8 \cdot 10^{-6} \text{ m s}^{-1}$ to $1.1 \cdot 10^{-4} \text{ m s}^{-1}$, with a mean of $5.4 \cdot 10^{-5} \text{ m s}^{-1}$. For the Cambrian-Ordovician aquifer the mean is $4.8 \cdot 10^{-5} \text{ m s}^{-1}$, and for the Ordovician and Silurian strata $8.3 \cdot 10^{-5}$ and $9.6 \cdot 10^{-5} \text{ m s}^{-1}$, respectively. In the Ordovician and Silurian strata the hydraulic conductivity decreases downwards (Fig. 5) due to increased fracturing in the uppermost parts of these mainly calcareous sediment deposits. Further down, lithostatic pressure reduces the size of fracture apertures and conductivity can be attributed to other hydraulically connected porous textures. Other stratigraphic units have more or less constant hydraulic conductivity with depth (Fig. 5).

The area of Estonia is characterized by low topography, most of the country being less than 100 m above sea level. The regional hydraulic gradients estimated from topography range from 0.01 to 0.0001, depending on the assumed flow distances. Locally, there are higher elevations in the north and southeast of the country, and higher flow gradients may occur.

Since the hydraulic conductivities are high and the sediment beds are continuous over long distances without any major tectonic breaks, advective heat transfer may be large enough to affect subsurface temperatures. We have investigated the thermal effects of the Estonian hydrogeological system with numerical simulations of coupled heat and fluid transfer by assuming a porous medium. The numerical code SHEMAT (Clauser, 1988; Clauser and Villinger, 1990) was used for the simulations, which applies finite difference techniques to the numerical solutions.

A north-south transect running from Haanja to Võsu was chosen for modelling (Fig. 1), and general hydrogeological model was constructed from the geological and hydrogeological profiles of Tšeban (1975). The 2-dimensional model is 600 m deep and 230 km long. The discretization applied was 25 m in the vertical dimension and 5 km in the horizontal. The length of the model is justified by the need to investigate the existence of large-scale flow systems in the sediment aquifers as suggested by the hydraulic head variation maps of Tšeban (1975).

The thermal conductivity of the sedimentary rocks was assumed to be $2.25 \text{ W m}^{-1}\text{K}^{-1}$ except in the clays of the Lower Cambrian Lontova stage, which have a value of $1.5 \text{ W m}^{-1}\text{K}^{-1}$ (Urban *et al.*, 1991). Porosity was 10% and heat production $0.5 \mu\text{W m}^{-3}$ throughout. The thermal and hydraulic properties used in simulation are given in Table 2.

Topographic variation was not included in the model, but each upper boundary node was assigned a constant hydraulic head following the topography and the measured head variation (Tšeban, 1975).

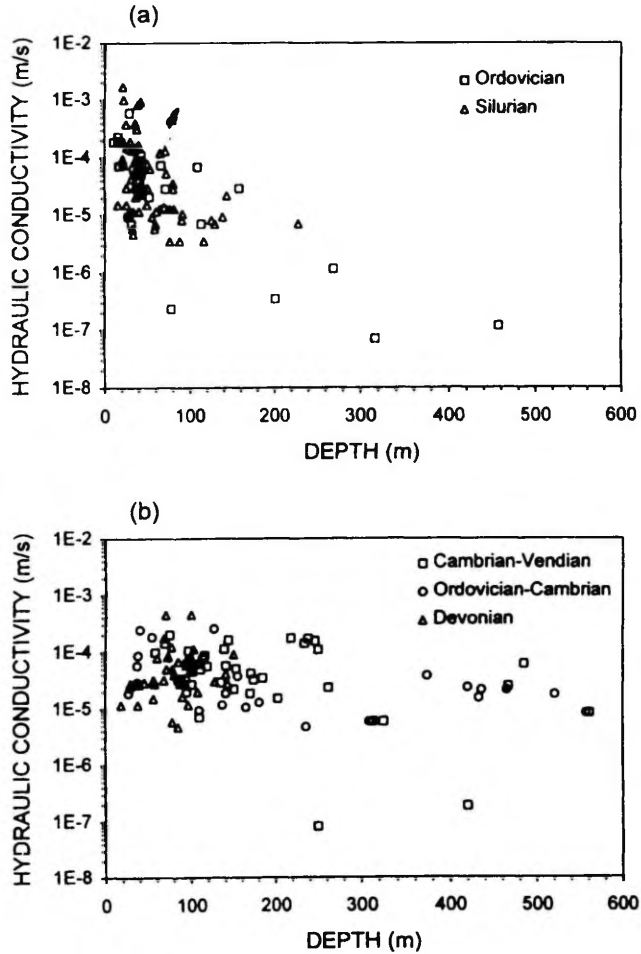


Fig. 5. Hydraulic conductivity versus depth estimated from the transmissivity data of *Tšeban* (1975) and *Arkhangelskiy* (1966). In (a) the Ordovician and Silurian strata the hydraulic conductivity decreases with depth, in (b) the Vendian-Cambrian, Cambrian-Ordovician and Devonian sediments there is no significant change with depth.

The following boundary conditions were set:

- (1) Top: constant temperature (5 °C) and constant head (following topography) adapted from the maps of *Tšeban* (1975). The head varied from about 160 m a.s.l. in the Haanja area to zero on the shore of the Gulf of Finland (Fig. 6).
- (2) Bottom: Constant heat flow density (40 mW m⁻²) and no fluid flow.
- (3) Lateral boundaries: No flow of heat or fluid was allowed.

Table 2. Hydraulic and thermal properties of different stratigraphic units used to simulate groundwater flow in the bedrock. Domain numbers refer to Fig. 6.

Stratigraphic unit / Depth	Hydraulic conductivity m/s	Thermal conductivity $\text{Wm}^{-1}\text{K}^{-1}$	Domain number
Devonian	$5 \cdot 10^{-5}$	2.25	1
Silurian			
0-100 m	$5 \cdot 10^{-5}$	2.25	2
100-200 m	$1 \cdot 10^{-5}$	2.25	3
Ordovician			
0-100 m	$5 \cdot 10^{-5}$	2.25	4
100-200 m	$1 \cdot 10^{-5}$	2.25	5
200-300 m	$5 \cdot 10^{-7}$	2.25	6
> 300 m	$1 \cdot 10^{-7}$	2.25	7
Cambrian-Ordovician	$5 \cdot 10^{-5}$	2.25	8
Lontova clays	$1 \cdot 10^{-14}$	1.5	9
Cambrian-Vendian	$5 \cdot 10^{-5}$	2.25	10
Precambrian	$1 \cdot 10^{-8}$	3.50	11

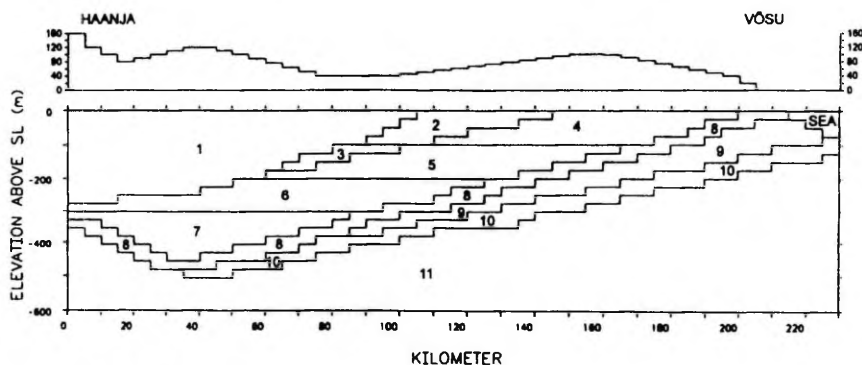


Fig. 6. The cross-section and hydraulic head variations on the transect used for simulating groundwater flow (Fig. 1). The domain numbers are as in Table 2.

The model results (Fig. 7) suggest that there are regional groundwater flow systems. The Cambrian-Vendian aquifer covered by Lontova clays recharges in southern Estonia and discharges to the Gulf of Finland. In other aquifers the groundwater flow directions follow the topography. The model further suggests that the thermal field is not markedly disturbed by groundwater flow, and that the thermal effects are less than 5 mW m^{-2} in most parts of the model. The highest heat flow

density differences are confined to the uppermost 100-150 m. However, in the southern part of the transect, which has thick Devonian and Ordovician layers and where the hydraulic head reaches 160 m, the model suggests heat flow highs of up to $60\text{--}70\text{ mW m}^{-2}$ in the groundwater discharge areas. The situation would be different if the overlying strata had much lower hydraulic conductivities than the values applied here. We used hydraulic conductivity values measured in boreholes originally drilled and investigated for water production purposes, not regional groundwater flow studies. The high conductivity aquifers may therefore be over-represented in the data.

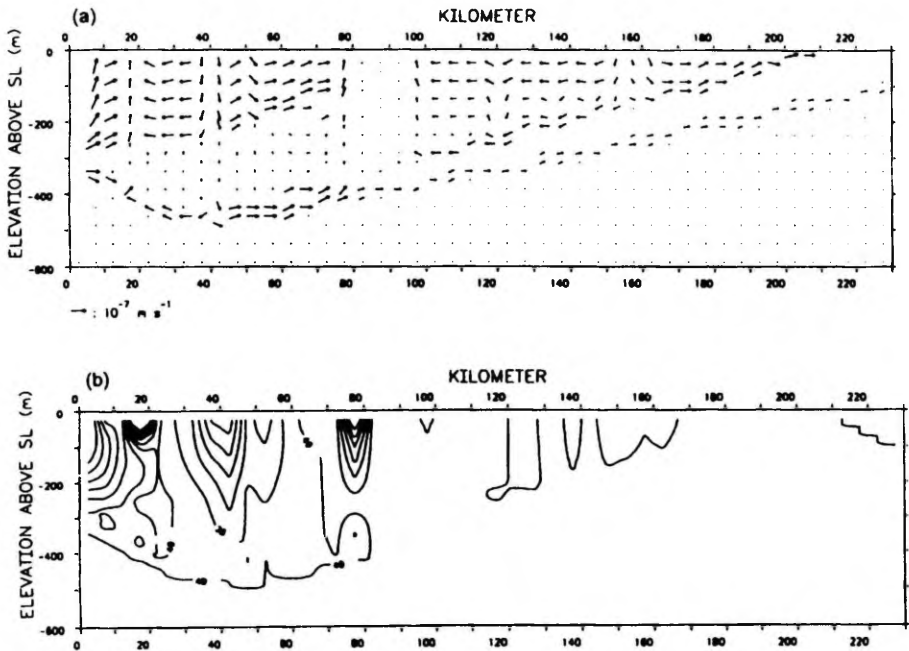


Fig. 7. The simulated (a) Darcy velocity and (b) heat flow density in the transect. The scale of Darcy velocity is logarithmic-exponential.

4. *New measurements of heat flow density*

More than 150 holes have been drilled in the Estonian terrain to the Precambrian basement, but practically all are cemented or the casing has not been preserved. The number of open holes suitable for geothermal loggings is thus very small, and most of them are very shallow (< 100 m).

Six holes (Table 3, Fig. 1) were chosen for this study following two criteria: 1) they should be as deep as possible, and 2) they should reach the Precambrian basement.

The Precambrian basement was reached in all boreholes except that at Rohuneeme. At Loksa the hole was blocked at 132 m, and only 2 m of the Precambrian basement could be logged. At Jöelähtme, logging covered about 25 m of the Precambrian, but at Saviranna and Förby 60 m and 40 m, respectively. The deepest logging was made at Kärkla, where the drill hole penetrated about 300 m of the Precambrian basement under a meteorite impact crater (800 m below surface).

Temperature was measured with equipment constructed at the Geological Survey of Finland. The measuring element was a temperature-sensitive microcircuit (Analog Device 590H) capable of an absolute accuracy of 0.1°C and a resolution of 0.01°C. Temperature readings were taken at 2.5 m depth intervals.

Table 3. Sites of new heat flow density measurements (see also Fig. 1).

Hole	No.	Location		Elevation (m)	Depth (m)	Drilling year
		N	E			
Kärkla	K-1	58° 59'	22° 40'	6.0	815	1990
Förby	F369	59° 00'	23° 09'	1.0	306	1987
Jöelähtme	8-1	59° 27'	25° 10'	32.5	218	1991
Saviranna	F502	59° 20'	25° 03'	16.0	212	1979
Loksa	853	59° 35'	25° 44'	7.5	157	1989
Rohuneeme	6-2	59° 34'	24° 48'	2.8	116	1991

The electrical resistivity of drill hole fluid was logged with a two-wire cable and a resistivity meter. The reading interval was 5 m. Because of the casing structures at the borehole top, fluid resistivity could not be measured at Jöelähtme and Loksa. All drill hole loggings were made during August 1993.

The drill cores were sampled at 10 m intervals wherever possible. Thermal conductivity was measured at the Geological Survey of Finland with the divided bar method on rock disks cut perpendicular to the core samples. Vendian and Cambrian clays, sandstones and siltstones are very poorly consolidated and their conductivities could not be measured with the divided bar apparatus. The conductivity data from *Urban et al.* (1991) were used for these sections.

Heat flow densities were determined with the interval technique using mean conductivity and temperature gradient, but also with the Bullard technique (temperature-thermal resistance plots).

The geothermal gradient and heat flow density values for both apparent and palaeoclimatically corrected values are given in Table 4. The palaeoclimatic corrections were calculated for each borehole using the technique referred above. The local sea regression histories were taken into account in the borehole corrections, and are shown

in Fig. 8. Bathymetric data were taken from *Donner and Raukas (1992)*, *Hyvärinen et al. (1992)*, *Kessel and Raukas (1979)*, *Linkrus (1962)* and *Ratas (1977)*.

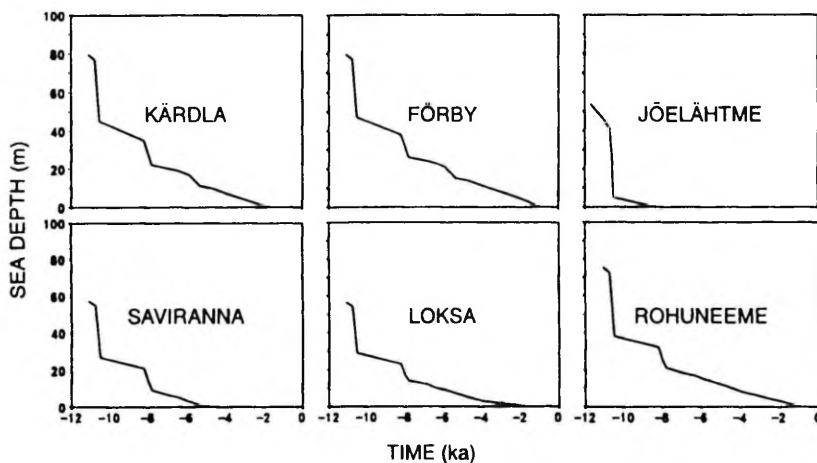


Fig. 8. Sea regression histories at the borehole sites.

Sections of drillholes obviously disturbed by water flow in the hole itself (see Appendix and e.g., *Drury et al.*, 1984) were not included in the heat flow density calculations. A detailed description of logging results is given in the Appendix.

Both apparent and palaeoclimatically corrected heat flow densities vary markedly with depth (Table 4). However, the mean heat flow density values are close to each other (34–40 and 40–48 mW m^{-2} , respectively), except in the Rohuneeme, where they are 20 and 30 mW m^{-2} .

5. Discussion

Palaeoclimatic models do not seem to eliminate the vertical variation in heat flow density nor do corrections reduce the standard deviation of the mean heat flow values (Table 4). There are two explanations for this: 1) the palaeoclimatic model is not quite correct, and/or 2) the heat transfer is not purely conductive. A homogeneous half-space is by no means the best model for a layered sedimentary environment, and the values of palaeoclimatic corrections should therefore be taken only as approximations.

Efforts should be made not only to include the geological structures more carefully in the models, but also to take many local climatic and artificial effects into account. The land-use history of a site may contain relevant information about ground surface temperature changes. For instance, deforestation and soil cultivation may have changed the ground temperatures by 1–2°C, which equals or even exceeds climatic warming during the last 200–400 years. The ground surface temperature may differ for

several tenths of a degree depending on the present vegetation cover (forest or open fields). Vegetation types changed gradually during the Holocene.

Table 4. Apparent and palaeoclimatically corrected heat flow densities.

Hole	ΔZ	Γ	$\Delta\Gamma$	λ	Q	Q'
Kärdla	32-130	2.6±0.1	-5.2	2.74±0.20	7.2	21.4
	130-275	18.0±0.1	-3.2	2.44±0.19	44.0	51.8
	275-375	12.3±0.1	-3.0	2.87±0.57	35.4	44.0
	375-495	11.4±0.0	-3.1	2.58±0.50	29.4	37.4
	495-810	12.6±0.3	-2.5	2.93±0.59	36.8	44.1
mean of interval 275-810 m					33.9±3.2	41.9±3.1
Förby	130-159	14.4±0.3	-4.1	2.18	31.4	40.3
	159-170	28.3±1.3	-3.7	1.35	38.2	43.2
	170-264	15.4±0.2	-3.3	2.48	38.2	46.4
	264-306	14.7±0.3	-3.1	3.12±0.48	45.9	55.5
mean					38.4±5.1	46.4±5.7
Jöelähtme	51-130	33.6±0.4	-4.3	1.25	42.0	47.4
	130-152	10.2±0.4	-3.2	1.72	17.5	23.0
	152-188	12.0±0.2	-2.8	2.53	30.4	37.4
	188-218	17.2±0.6	-2.5	2.60±0.23	44.7	51.2
mean					33.7±10.8	39.8±10.9
Saviranna	40-93	38.9±0.7	-5.0	1.24	48.2	54.4
	93-116	14.7±0.3	-4.2	1.74	25.6	32.9
	116-148	13.0±0.2	-3.4	2.57	33.4	42.1
	148-212	15.0±0.1	-2.9	3.41±0.09	51.2	61.0
mean					39.6±10.5	47.6±10.9
Loksa	32-53	36.1±1.1	-5.4	1.45	52.3	60.2
	53-82	14.9±0.7	-5.3	2.27	33.8	45.9
	82-94	16.2±1.6	-5.0	1.56	25.3	33.1
	94-130	17.5±0.4	-4.3	1.91	33.4	41.6
mean					36.2±9.9	45.2±9.8
Rohuneeme	20-64	16.3±0.3	-6.1	1.25	20.4	28.0
	64-92	8.8±0.2	-5.2	1.72	15.1	24.1
	92-116	9.3±0.2	-4.7	2.57	23.9	36.0
mean					19.8±3.6	29.4±5.0

Legend

ΔZ - depth interval (m);

Γ - geothermal gradient (mK m^{-1});

$\Delta\Gamma$ - palaeoclimatic correction (mK m^{-1});

λ - thermal conductivity ($\text{W m}^{-1}\text{K}^{-1}$), values without standard deviation are from *Urban et al.* (1991) from nearby holes;

Q and Q' - apparent and palaeoclimatically corrected heat flow densities (mW m^{-2}).

Numerical simulation of groundwater circulation in the bedrock indicates that there are regional groundwater flow systems. Their existence can be mainly attributed to the high hydraulic conductivity of all sediments (excluding the Lontova clays). However, the small thickness of sedimentary rocks is responsible for small heat flow density disturbances. The thicker sedimentary cover in southern Estonia allows groundwater to flow at greater depth. These flow systems are driven by the greater topographic variation. The particularly low apparent heat flow values in western Estonia reported by *Urban et al.* (1991) can be attributed to a very local recharge of the aquifers, or even to flow in the holes. These postulates are supported by the fact that the holes are situated above or very close to major 10-20-km-wide fracture zones which affect both the Precambrian basement and the sedimentary cover (*Norman and Solovjova*, 1982, unpublished report in the Geological Fund of Estonia).

The low apparent heat flow density values measured under the Lontova clays at Jõelähtme, Saviranna, Loksa and Rohuneeme (see Appendix) may be due to the southward migration of seawater in these layers. Seawater intrusion is caused by extensive pumping of water from the Cambrian-Vendian aquifer during the last 50 years. Geothermal investigations may provide a valuable tool for the modelling and experimental testing of the above, as yet unproven, hypothesis.

6. Conclusions

According to the present forward modellings of palaeoclimatic effects, the greatest changes can be expected in northern and western Estonia, but the amplitude of perturbations depends on the location and elevation of the borehole site. In coastal areas, in the uppermost part of the cross-section (0-100 m), the apparent heat flow density has declined by 10-15 mW m⁻² due to past climatic changes. In central and southeastern Estonia, the perturbations are smaller at these depths (7-10 mW m⁻²). At depths of 150-400 m the palaeoclimatic effects are less than 5-7 mW m⁻².

Regional groundwater flow does not seem to cause significant thermal disturbances. Perturbations higher than 5 mW m⁻² occur only in the uppermost 100 m and in areas where the hydraulic gradient exceeds 0.002.

Probably owing to the distinctly layered structure in the boreholes, and to the relatively scarce data on thermal conductivity, particularly from less consolidated sections of boreholes, the vertical heat flow density variations cannot be explained by either the present palaeoclimatic models or regional groundwater flow. Terrain effects, and groundwater flow effects such as sea water intrusion to Cambrian sediments also need to be studied in detail.

The heat flow density mean values presented here are in agreement with earlier data on geothermal conditions in Estonia. The average heat flow density in Estonia is 35-40 mW m⁻².

Acknowledgements

This work was carried out as a cooperation project by the Geological Survey of Estonia and the Geological Survey of Finland. We are grateful to V. Klein (GSE) and to L. Eskola (GSF) for their support; to L. Savitsky, R. Perens and A. Schmidt (GSE) for discussions on hydrogeology; to K. Suuroja (GSE) for enabling us to take samples of the Kärđla holes; to C. Clauser, S. Hurter (Niedersächsisches Landesamt für Bodenforschung, Hannover) and an anonymous referee for their constructive reviews of the manuscript; and to G. Häkli for revising the English.

References

- Aaby, B., 1976. Cyclic climatic variations over the past 5500 years reflected in raised bogs. *Nature*, **263**, 281-284.
- Arkhangelskiy, B.N. (Ed.), 1966. *Gidrogeologia SSSR, Estonskaja SSR*. 30, Nedra, Moscow, 302 p. (in Russian).
- Beck, A.E., 1977. Climatically perturbed temperature gradients and their effect on regional and continental heat flow means. *Tectonophysics*, **41**, 17-39.
- Bell, M. and M.J.C. Walker, 1992. Late Quaternary Environmental Change: physical and human perspectives. Longman, 273 p.
- Carlslaw, H.S. and J.C. Jaeger, 1959. *Conduction of heat in solids*. Clarendon Press, Oxford, 386 p.
- Čermák, V., 1976. Palaeoclimatic effect on the underground temperature and some problems of correcting heat flow. In: A. Adám (Ed.), *Geoelectric and Geothermal Studies*. KAPG Geophys. Monogr. Akademiai Kiadó, Budapest, 59-66.
- Čermák, V., N. Baling, I. Kukkonen and V.I. Zui, 1993. Heat flow in the Baltic Shield - results of the lithospheric geothermal modelling. *Precambrian Research*, **64**, 53-65.
- Clauser, C., 1988. Untersuchungen zur Trennung der konduktiven und konvektiven Anteile im Wärmetransport in einem Sedimentbecken am Beispiel Des Oberrheintalgrabens. Fortschritt-Berichte VDI, Reihe 19, Nr. 28, 124 p. (Dissertation).
- Clauser, C. and H. Villinger, 1990. Analysis of conductive and convective heat transfer in a sedimentary basin, demonstrated for the Rheingraben. *Geophys. J. Int.*, **100**, 393-414.
- Donner, J., 1978. Suomen kvartäärigeologia. Helsingin yliopisto, geologian laitos, geologian ja paleontologian osasto, 264 p.

- Donner, J. and A. Raukas, 1989. On the Geological History of the Baltic Ice Lake. *Proc. Estonian Acad. Sci., Geology*, **38**, 128-137.
- Donner, J. and A. Raukas, 1992. Baltiyskoe lednikovoe ozero. In: A. Raukas and H. Hyvärinen (Eds), *Geology of the Gulf of Finland*. Tallinn, 262-276. (in Russian).
- Drury, M.J., A.M. Jessop and T.J. Lewis, 1984. The detection of groundwater flow by precise temperature measurements in boreholes. *Geothermics*, **13**, 163-174.
- Haapala, J. and P. Alenius, 1994. Temperature and salinity statistics for the Northern Baltic Sea 1961-1990. *Finnish Marine Research*, **262**, 51-121.
- Hyvärinen, H., A. Raukas and H. Kessel, 1992. Yoldievoe i Eheneysovoe morya. In: A. Raukas and H. Hyvärinen (Eds), *Geology of the Gulf of Finland*. Tallinn, 276-283. (in Russian).
- Iversen, J., 1944. *Viscum*, *Hedera* and *Ilex* as climatic indicators. *Geologiska Föreningens Stockholm Förhandlingar*, **66**, 463-483.
- Jaagus, J., 1994. Muutused Eesti kliimas. In: *Meteoroloogia ja klimatoloogia uurimistööst Eestis*. (in press).
- Jaeger, J.C., 1965. Application of the theory of heat conduction to geothermal measurements. In: H.K. Lee (Ed.), *Terrestrial Heat Flow*. Geophys. Monogr., Am. Geophys. Union, **8**, 7-23.
- Jessop, A.M., 1971. The distribution of glacial perturbation of heat flow in Canada. *Can. J. Earth Sci.*, **8**, 162-166.
- Kessel, H. and A. Raukas, 1979. The Quaternary History of the Baltic. Estonia. In: V. Gudelis and L.-K. Königsson (Eds), *The Quaternary History of the Baltic*. *Acta Univ. Ups. Symp. Univ. Ups. Ann. Quing. Cel.*: **1**. Uppsala, 127-146.
- Koistinen, T. (Ed.), 1994. Precambrian basement of the Gulf of Finland and surrounding area, 1: 1mill. Geological Survey of Finland, Espoo.
- Kukkonen, I.T., 1987. Vertical variation of apparent and palaeoclimatically corrected heat flow densities in the Central Baltic Shield. *J. Geodyn.*, **8**, 33-53.
- Kullenberg, G., 1981. Physical oceanography. In: A. Voipio (Ed.) *The Baltic Sea*. Elsevier, Amsterdam, 135-181.
- Linkrus, E., 1962. Valgejõe alamjooksu oru geomorfoloogiast. *EGS Aastaraamat*, 28-45.
- Lewis, T. and K. Wang, 1992. Influence of terrain on bedrock temperatures. *Global Planet. Change*, **98**, 87-100.
- Pirrus, E. and L. Saarse, 1979. Fiziko-mekhanitsheskie svoistva Kembriiskih glin Severnoi Estonii. *Proc. Estonian Acad. Sci., Geology*, **28**, 68-74. (in Russian).
- Prokhorov, Z.P. (Ed.), 1970. Spravotshnik po klimatu SSSR, Estonskaya SSR. Meteorologicheskie dannye za otdelnye gody, **I**, Temperatura vozduha i potshvy. Tallinn, 355 p. (in Russian).
- Puura, V. and K. Suuroja, 1992. Ordovician impact crater at Kärđla, Hiiumaa Island, Estonia. *Tectonophysics*, **216**, 143-156.
- Ratas, U., 1977. Vormsi loodusest. Valgus, Tallinn, 59 p.

- Shackleton, N.J. and N.D. Opdyke, 1976. Oxygen isotope and paleomagnetic stratigraphy. *Quat. Res.*, **3**, 39-55.
- Tšeban, E., 1975. Eesti NSV põhjavesi ja selle kasutamine. Valgus, Tallinn, 166 p.
- Urban, G., L. Tsybulia, V. Cozel and A. Schmidt, 1991. Geotermicheskaya kharakteristika severnoy chasti Baltyskoy sineklisy. *Proc. Estonian Acad. Sci., Geology*, **40**, 112-121. (in Russian).

APPENDIX

The following gives details of the logging results of the six boreholes measured in 1993.

Kärdla, Hiiumaa Island

K-1, drilled in 1990, is currently the deepest borehole in Estonia. It is situated in the centre of a meteorite crater formed about 455 Ma ago (*Puura and Suuroja, 1992*). This impact structure has a diameter of 4 km. The drillhole intersects post-impact Quaternary and Ordovician sediments, underlain by various allochthonous and autochthonous impact breccias (Fig. 9). At a depth of 512 m, it reaches the Precambrian basement, which is heavily fractured due to the impact. The shock effects decline with depth, but are still present at the borehole bottom.

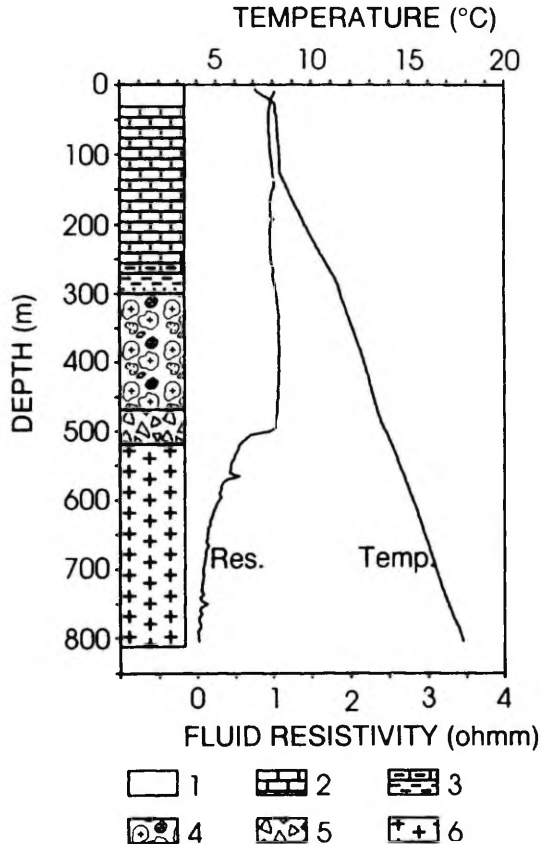


Fig. 9. Temperature and fluid resistivity at the Kärdla borehole. Cross-section: 1. overburden (Q), 2. limestone (O₂tt-O₃ad), 3. transition from sandstone to marl (O₂pl), 4. allochthonous impact breccia (O₂krd), 5. autochthonous impact breccia (O₂krd), 6. basement (PR₁).

The temperature log shows several intervals with distinctly differing gradients. The depths of gradient changes coincide with the main lithological and stratigraphic boundaries. The highest gradient was recorded at the interval 6-32 m (52 mK m^{-1}). This can be attributed partly to the low thermal conductivity of Quaternary glacial till and partly to annual temperature variations at these shallow depths. Below this zone, a very low gradient of 2.6 mK m^{-1} was measured to a depth of 130 m. Deeper down the gradient is more or less normal and varies from 10 to 19 mK m^{-1} .

Thermal conductivity was measured from core samples of the logged hole for the deeper part ($> 360 \text{ m}$) and from the cores of the neighbouring hole, K-18, for the upper part. Hole K-18 is situated only 400 m to the northeast of hole K-1, and the sediment stratigraphy is similar to that in K-1. Therefore, we assume that the K-18 samples are representative of the hole K-1 section as well.

Heat flow density is not uniform with depth. The Bullard diagram (Fig. 10) shows several sections with different apparent heat flow values. The variations below 275 m may be due to the small water flows in a hole, or to biased conductivity values. Heat flow values at depths above 400 m in particular were based on thermal conductivities measured on K-18 samples. The mean heat flow density between 275 and 800 m is 42 mW m^{-2} .

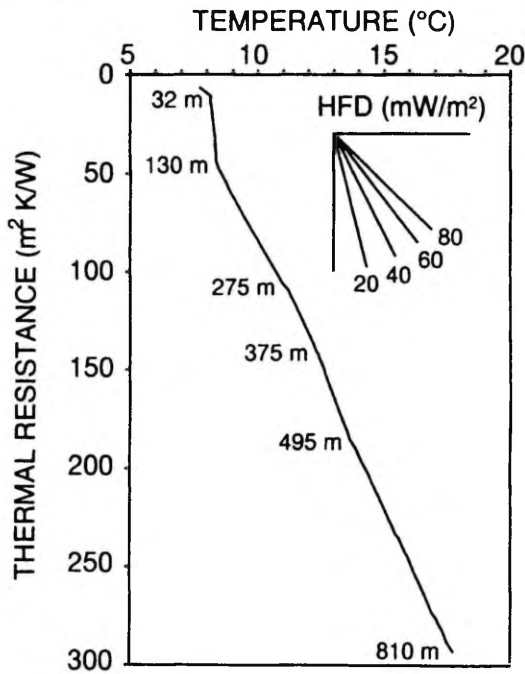


Fig. 10. Bullard diagram of the Kärđla borehole. Numbers next to curve refer to depths.

The variation does not, however, seem to follow the calculated palaeoclimatic variations (Fig. 4), at least those calculated with half-space models. The measured temperature log could of course be interpreted with a ground surface temperature history, but this would mean that the temperatures were at least 2°C lower 100-700 years ago than they are today. Such a long and cold period has not been reported.

Förby, Vormsi Island

The borehole (F369) is situated on the western shore of Vormsi, only about 20 m from the shoreline. This 306-m deep hole was drilled in 1987. The Precambrian basement was intersected for 42 m at depths of 264-306 m. On top of the basement there are Vendian, Cambrian and Ordovician sediments (Fig. 11).

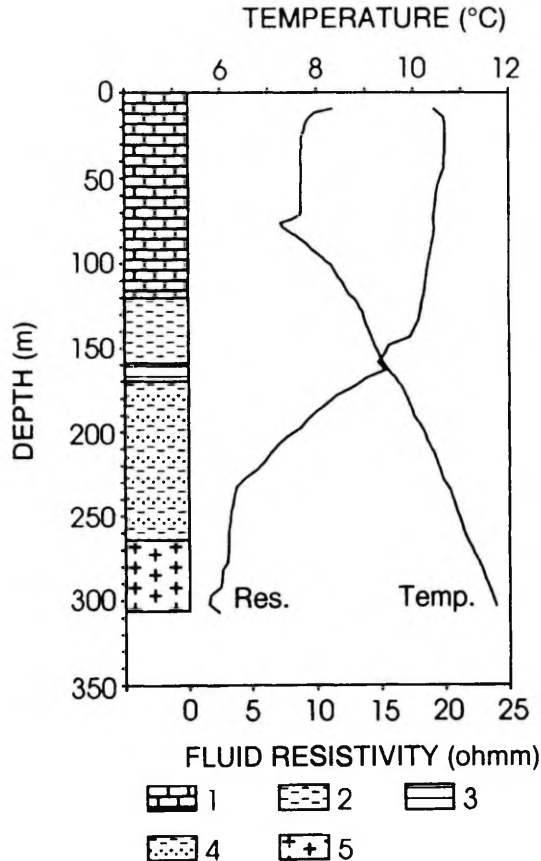


Fig. 11. Temperature and fluid resistivity at the Förby borehole. Cross-section: 1. limestone (O₂pk_r-O₃mo), 2. siltstone (E₁ts-O₁kl), 3. silty clay (E₁lk), 4. intercalating beds of sandstone and siltstone (V-E₁sr), 5. basement (PR₁).

In the upper part of the temperature log (< 130 m) the gradient is very disturbed and neither heat flow determinations nor palaeoclimatic corrections were made. The perturbations may be caused by water flowing in the hole. The low temperature peak at 65 m seems to be a product of cold water entering the hole. Above this depth, the temperature gradient is very low. It could also be attributed to water flowing in the hole, or to the existence of a horizontal heat flow component produced by the adjacent shoreline. If the sea bottom temperatures differ from the ground temperatures on shore, horizontal temperature gradients will be generated. These may produce very disturbed heat flow values (Lewis and Wang, 1992).

In the lower part of the hole (> 130 m), the temperature is less disturbed and gradient changes can be more or less attributed to thermal conductivity differences.

Thermal conductivity was measured on seven samples of Ordovician limestone and five samples of the Precambrian basement. In the middle part of the section, the data of Urban *et al.* (1991) on comparable stratigraphic units were used.

Below 130 m, both apparent and palaeoclimatically corrected heat flow densities increase with depth from 31 and 40 to 46 and 56 mW m⁻², respectively (Table 4). Average values are 38 and 46 mW m⁻².

Jõelähtme, northern Estonia

The Jõelähtme drillhole (8-1) penetrates Lower Ordovician, Cambrian and Vendian sediments down to the Precambrian basement (Fig. 12). The hole is 218 m deep and was drilled in 1991.

There do not seem to be any significant water flow effects on the temperature log. The increased gradient between 50 m and 130 m can be explained by the lower thermal conductivity of the Lontova clays (about 1.25 Wm⁻¹K⁻¹; Urban *et al.*, 1991) than of the Cambrian sands (about 2.5 W m⁻¹K⁻¹). In the sedimentary part below the clays, the temperature gradient does not vary very much (10-12 mK m⁻¹).

The ground surface temperature history at Jõelähtme is mainly dictated by glaciations and Holocene climatic changes. The influence of sea bottom temperatures is small, because the Baltic Ice Lake and the early Baltic Sea retreated from the hole site more than 8000 years ago (Fig. 8).

The apparent heat flow densities vary from 17 mW m⁻² in Voronka siltstones to more than 40 mW m⁻² in Lontova clays and Precambrian basement. This variation cannot be attributed to neither the regional groundwater flow discussed earlier or palaeoclimatic changes. The mean apparent and palaeoclimatically corrected heat flow densities are 34 mW m⁻² and 40 mW m⁻², respectively.

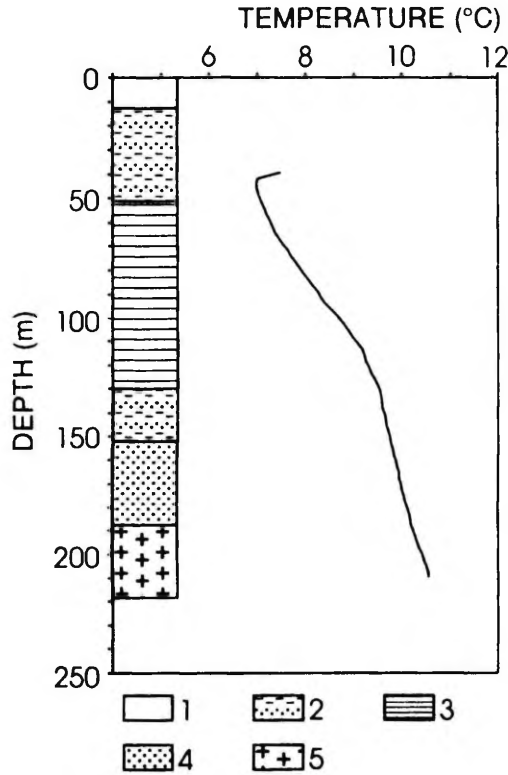


Fig. 12. Temperature at the Jõelähtme borehole. Cross-section: 1. overburden (Q), 2. intercalating beds of sandstone and siltstone ($\text{E}_1\text{lk-O}_1\text{kl}$ and V_2vr), 3. silty clay (E_1ln), 4. sandstone (V_2gd), 5. basement (PR₁).

Saviranna, northern Estonia

The hole (F502) is 212 m deep and reaches 64 m to the Precambrian basement, which is represented by granites of the Naissaare intrusion (Fig. 13). The hole is in a cliff near the coast.

The shape of the temperature curve is very similar to the Jõelähtme temperature log. This is to be expected, because the distance between the two holes is less than 15 km and their stratigraphies are similar. The differences in palaeoclimatic models are connected with hole site elevations and the withdrawal of the sea, which took place about 5000 years ago.

The heat flow density variations are very similar to those in the Jõelähtme hole. The higher mean heat flow density values (40 and 48 mW m^{-2}) can be attributed to the heat production of granite, which is higher than that of the gneissic basement rocks at Jõelähtme.

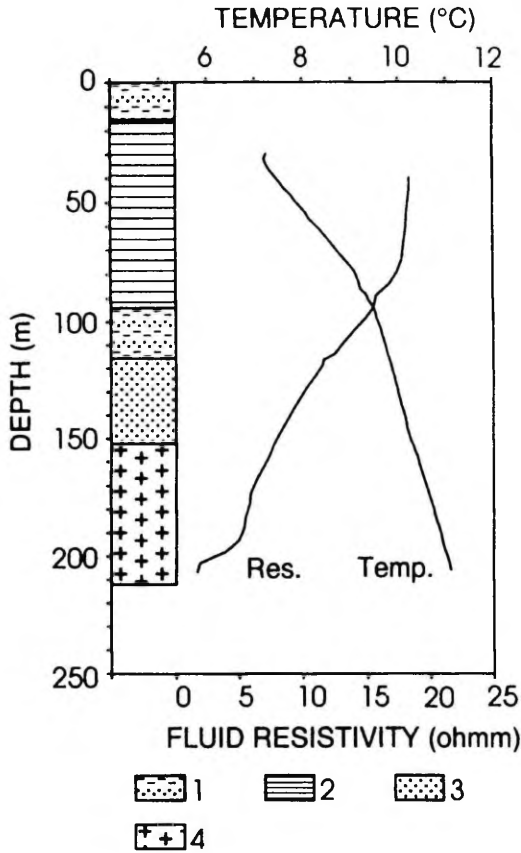


Fig. 13. Temperature and fluid resistivity at the Saviranna borehole. Cross-section: 1. intercalating beds of sandstone and siltstone (E₁lk and V₂vr), 2. silty clay (E₁ln), 3. sandstone (V₂gd), 4. basement (PR₁).

Loksa, northern Estonia

The 157-m deep hole (853) was drilled in 1989. In 1993 we only reached a depth of 132 m, where there was a blockage. The stratigraphy is represented by Quaternary, Cambrian and Vendian sediments and the Precambrian basement.

The temperature gradient changes (Fig. 14) correlate with the stratigraphic units, but the available thermal conductivity data do not support an explanation based exclusively on conductivity variations. However, the conductivities measured on other holes in the vicinity (Urban *et al.*, 1991) may not be representative.

As in previous holes, the heat flow density varies with depth. Below the Lontova clays flow values are low. The palaeoclimatic models do not explain this variation. The mean heat flow density values are 36 and 45 mW m⁻².

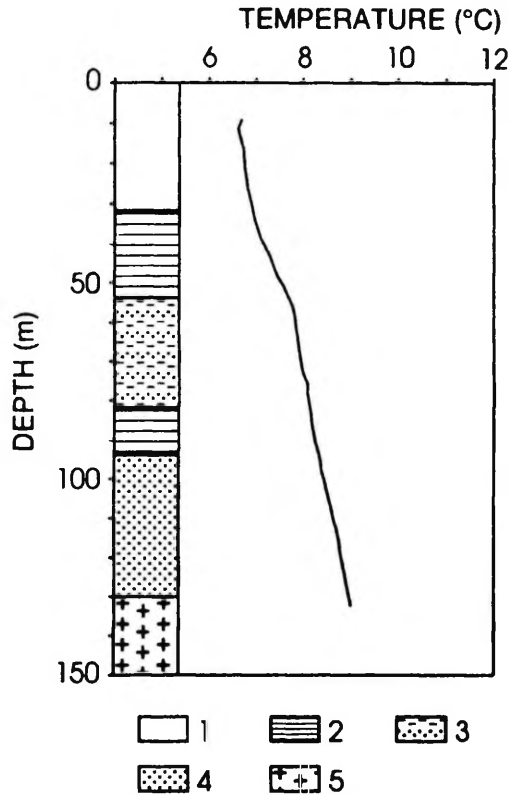


Fig. 14. Temperature at the Loksa borehole. Cross-section: 1. overburden (Q), 2. silty clay (E_{1In} and V_{2kt}), 3. intercalating beds of sandstone and siltstone (V_{2vr}), 4. sandstone (V_{2gd}), 5. basement (PR_1).

Rohuneeme, northern Estonia

The Rohuneeme hole (6-2) was drilled in 1991 only 25 m from the sea shore. The stratigraphy of the intersection is represented by Cambrian and Vendian sediments (Fig. 15).

On the temperature log the main gradient change at 65 m depth is related to the boundary of Lontova clays and Voronka siltstones, and can be at least partly attributed to the conductivity contrast between these stratigraphic units.

The apparent heat flow density varies from 15 to 24 $mW m^{-2}$. As discussed above for Förby the proximity of the shoreline may have created non-vertical heat flow components resulting in low apparent heat flow density at these very shallow depths.

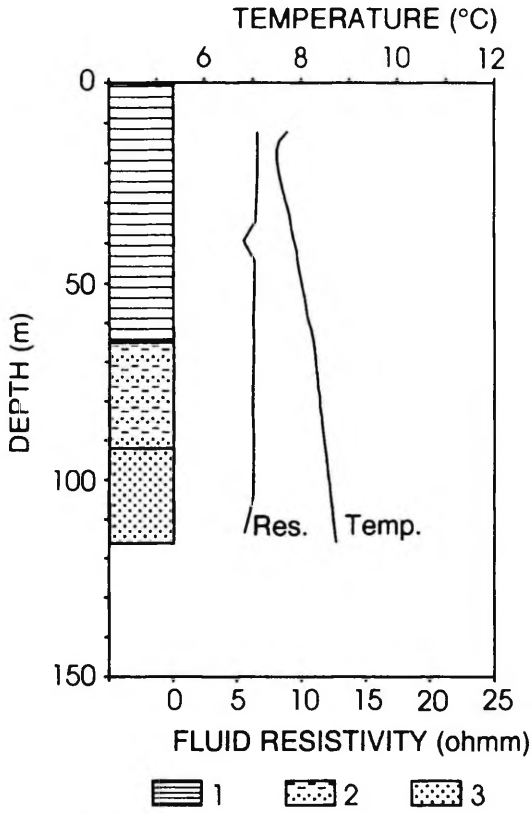


Fig. 15. Temperature and fluid resistivity at the Rohuneeme borehole. Cross-section: 1. silty clay (E_{1ln}), 2. intercalating beds of sandstone and siltstone (V_{2vr}), 3. sandstone (V_{2gd}).

Jöeleht, A. and Kukkonen, I. T., 1998.
Thermal properties of granulite facies rocks
in the Precambrian basement of Finland and Estonia.
Tectonophysics, 291: 195–203.



ELSEVIER

Tectonophysics 291 (1998) 195–203

TECTONOPHYSICS

Thermal properties of granulite facies rocks in the Precambrian basement of Finland and Estonia

A. Jöeleht^{a,*}, I.T. Kukkonen^b

^a Institute of Geology, University of Tartu, Vanemuise 46, EE2400 Tartu, Estonia

^b Geological Survey of Finland, P.O. Box 96, FIN-02151 Espoo, Finland

Received 31 December 1996; accepted 27 June 1997

Abstract

We present results of heat production, thermal conductivity and P-wave velocity measurements of 252 rock samples from five granulite facies areas in Finland and Estonia. These compositionally mainly intermediate Archaean and Palaeoproterozoic metamorphic rocks have relatively high heat production values. Mean values averaged by areas range from 0.57 to 2.24 $\mu\text{W m}^{-3}$. The lowest values are in the Varpaisjärvi area, which is the oldest and most mafic and where the highest metamorphic pressure occurred (8–11 kbar), whereas the highest heat production is found in the Turku granulite belt where the metamorphic pressure was 4–6 kbar. The heat production decreases with the increase of the metamorphic pressure. However, a general numerical relationship cannot be presented because of considerable variations in heat production data. There is no significant difference in the metamorphic temperatures of the studied granulites and therefore no dependence on temperature is found. Further, our data suggest no relationship between heat production and P-wave velocity. The mean thermal conductivity of granulites varies from 3.0 to 3.5 $\text{W m}^{-1} \text{K}^{-1}$. Slightly elevated thermal conductivity values in the Varpaisjärvi and Lapland granulite areas can be attributed to higher sillimanite and quartz contents, respectively. © 1998 Elsevier Science B.V. All rights reserved.

Keywords: granulite; heat sources; thermal properties; Baltic Shield

1. Introduction

Modelling vertical variation in temperature and heat flow density demands data on the distribution of heat producing elements in the Earth's crust and thermal conductivity of these rocks. However, the deeper we go the less we know about rock properties. Often properties of outcropping rocks have been applied for upper crust. For middle and lower crust, data from other sources have to be used. One

commonly applied technique is the empirical P-wave velocity–heat production relationship (Rybach and Buntebarth, 1984), but the general validity of the relationship is still a controversial issue (Fountain, 1986, 1987; Rybach and Buntebarth, 1987; Kern and Siegismund, 1989; Čermák et al., 1990; Huenges, 1997). Another approach is provided by investigating granulite facies terrains and xenoliths. Since the granulite xenoliths in general have more mafic compositions (Rudnick and Presper, 1990) and higher p–T conditions than granulites exposed in high-grade terrains (Rudnick, 1992) it has been suggested that xenoliths may represent the deeper crust, but due to

* Corresponding author. Fax: +372 7 375 836; E-mail: ajoeleht@math.ut.ee

highly variable equilibration pressures and temperatures it is likely that both rock groups are derived from a wide range of crustal depths (Harley, 1989; Rudnick, 1992).

Investigations of granulite terrains around the world yielded a variety of heat production values (e.g. compilations in Iyer et al., 1984; Fountain et al., 1987; Rudnick and Fountain, 1995). For many areas the mean values are based on only a few samples. The aim of the present paper is to give new and statistically more representative data on the thermal properties of granulite facies rocks in the Baltic Shield and adjacent areas, and to find their relationships to conditions of formation as well as to other petrophysical parameters (P-wave velocity).

2. Granulite facies rocks in the Baltic Shield and adjacent areas

The Precambrian crust exposed in the Baltic Shield continues southeastward in the basement of the East European Platform, where it is covered by Neoproterozoic and Phanerozoic sedimentary rocks. Boundaries of the Fennoscandian segment of the East European Craton are related to a Proterozoic system of palaeorifts (Bogdanova, 1993; Gorbachev and Bogdanova, 1993a).

In the Fennoscandian crustal segment there are many high-grade metamorphic belts (Fig. 1) which are mainly Palaeoproterozoic in age. In the following an overview of the granulite belts studied in the present work is given.

2.1. Varpaisjärvi

The Varpaisjärvi granulite area is characterized by a block structure (Paavola, 1984). The Archaean crust was disrupted by Proterozoic faults and only some parts of the granulites outcrop. The larger existence of denser material along the Archaean–Proterozoic boundary in the upper crust is supported by gravity data (Elo, 1992). In the Varpaisjärvi area the gravity highs coincide with granulite rocks.

The rocks are presently amphibolite-banded tonalitic–trondhjemitic–granodioritic migmatites, which formed from partial melting of primarily basic–intermediate series of igneous rocks (Paavola, 1984). The granulite facies metamorphism conditions

reached 8–11 kbar and 800–900°C and the age of metamorphism is 2.6–2.7 Ga (Paavola, 1984; Hölttä, 1997).

2.2. Lapland

The Lapland granulite belt formed during the collision of the Archaean Inari–Kola and South Lapland–Karelia cratons, and represents a crustal sequence thrust from northeast to southwest (Barbey et al., 1984; Gaál et al., 1989). The belt has a continuation in the southeast on the coast of the White Sea (Barbey et al., 1984). Stratigraphically, the lower southwestern part of the belt consists of sheared granulites, which change gradually into anatectic granulites in the northeast. In the lower part of these mainly felsic metasedimentary rocks there are lenses of metaigneous rocks that are predominantly mafic to intermediate in composition (Barbey et al., 1984; Gaál et al., 1989). Syntectonic intrusive activity and metamorphism occurred 1.9–2.0 Ga ago (Bernard-Griffiths et al., 1984). Pressure and temperature of metamorphism decrease slightly from the southwest to the northeast. In the lower part of the granulite complex, metamorphism took place at about 820°C and 7 kbar, whereas in the upper part temperature and pressure were about 755°C and 6.2 kbar (Raith and Raase, 1986).

2.3. Pielavesi–Kiuruvesi

The Pielavesi–Kiuruvesi granulites formed on the eastern margin of the Archaean Karelian craton about 1.88–1.89 Ga ago (Salli, 1983; Hölttä, 1988). They occur as blocks bounded by shear zones. Mainly intermediate and felsic volcanic rocks were metamorphosed at a temperature of 800–880°C and a pressure of 5.5 ± 1 kbar (Hölttä, 1988).

2.4. Turku

The high-grade metasedimentary rocks in the Turku area are characterized by low pressure (4–6 kbar) and high temperature (750–800°C) metamorphic conditions (Hölttä, 1986; Väisänen et al., 1994). Pressures of 3–5 kbar are also typical in other granulite belts of southern Finland like the West Uusimaa (Schreurs and Westra, 1986) and Rantasalmi–Sulkava

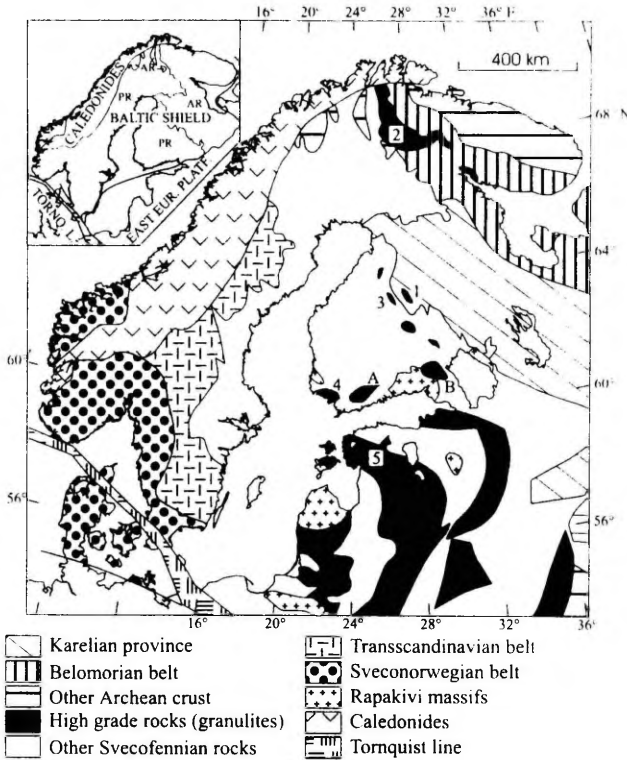


Fig. 1. Main structures of the Fennoscandian basement and location of granulite facies rocks in the eastern part of Fennoscandia (after Simonen, 1980 and Gorbachev and Bogdanova, 1993a, with additions). Areas of investigations: 1 = Varpaisjärvi, 2 = Lapland, 3 = Pielavesi–Kiuruvesi, 4 = Turku, and 5 = southern Estonia. A and B stand for the West Uusimaa and Rantasalmi–Sulkava granulite areas, respectively.

areas (Korsman, 1977; Korsman et al., 1984). Granulite facies metamorphism is 1.84–1.81 Ga in age (Korsman et al., 1984).

2.5. Southern Estonia

The southern Estonian granulites are a part of the Baltic–Belorussian granulite belt. Gorbachev and Bogdanova (1993a,b) suggest that the basement of the platform east of the Baltic Sea is a pattern of crustal belts younging westwards and stacking, marked by the beltform appearance of granulites (Fig. 1). Also the deep-seismic Sovetsk–Kohtla-

Järve profile (Sharov et al., 1989) shows a south-westward-dipping fault zone at the northeastern border of the Estonian granulite belt, which supports upthrusting.

The age of granulites is about 1.83 Ga (Petersell and Levchenkov, 1994). This correlates well with the 1.80 Ga determinations from the southern part of the belt (Bogdanova et al., 1994).

Granulites are represented by intermediate and mafic metavolcanic rocks with minor felsic parts (Koppelmaa et al., 1978). The high-grade is usually well preserved, but particularly in western Estonia strong retrograde metamorphism occurred (Koppel-

maa et al., 1978; Puura et al., 1983). The granulite facies metamorphism in Estonia took place at a temperature of about 800°C and a pressure of 6 kbar (Hölttä and Klein, 1991).

3. Analytical methods

Samples of southern Estonian granulite terrain were taken for heat production and thermal conductivity measurements from unweathered parts of nine drillcores, whereas samples from other areas belong to outcropping rocks, and therefore may be weathered to some extent. In the Estonian case, all samples represent areas which are not affected by retrograde metamorphism. Altogether, 252 rock samples were investigated.

For heat production purposes the U, Th and K concentrations were measured with gamma-ray spectrometry. Both the detection limit and the possible error of the equipment are about 1 ppm for U and Th and 0.1% for K. Sample sizes were usually from 30 to 80 g because of the small size of the well-type crystal. Heat production was calculated using the formula (Rybach, 1973):

$$A = \rho(9.52C_U + 2.56C_{Th} + 3.48C_K) \cdot 10^{-5} \quad (1)$$

where A is the heat production ($\mu\text{W m}^{-3}$), ρ is the density (kg m^{-3}) and C_U , C_{Th} and C_K are the concentrations of U (ppm), Th (ppm) and K (%), respectively. Rock densities were determined by weighing samples in air and water.

Thermal conductivity was measured with the divided bar method at room temperature on the apparatus described by Järvimäki and Puranen (1979). The error was estimated to be smaller than 5% (Kukkonen and Lindberg, 1995). P-wave velocity was measured from saturated samples at room tem-

perature and pressure using an ultrasonic instrument. All measurements were made at the Geological Survey of Finland.

4. Heat production and thermal conductivity data

Average heat production values, medians as well as (mean Th)/(mean U) and (mean K)/(mean U) ratios are given in Table 1. The median values of heat production are lower than the average values by 0.2–0.4 $\mu\text{W m}^{-3}$, due to the skewed nature of the distribution. The distribution diagrams of heat production values in each area are given in Fig. 2.

Based on heat production, these areas can be divided into three groups. The Varpaisjärvi area, which shows the lowest values, is the most mafic in composition and oldest, and the rocks were formed at the greatest depth. The highest heat production values are measured from low-pressure rocks of the Turku area. Moreover, the heat production values are of the same order as in the amphibolite facies rocks from the same area (Kukkonen and Jöeleht, unpubl. data). This indicates no depletion in heat producing elements. The other three areas (Lapland, Pielavesi–Kiuruvesi and southern Estonia) are characterized by heat production values that fall between the previous two groups. Except the Turku area, the heat production values are close to the average values of granulite facies rocks compiled by Rudnick and Fountain (1995).

Th/U ratios vary considerably (Table 1). In general, this seems to be characteristic of many granulite facies rock areas, but no satisfactory explanation was proposed yet (Mezger, 1992).

The thermal conductivity values of the granulite facies rocks in Pielavesi–Kiuruvesi, Turku and southern Estonia are close to each other and

Table 1
Average with standard deviation and median heat production values as well as Th/U and K/U ratios for granulite facies rocks from different areas

Area	Average (N)	Std. dev.	Median	mean Th/mean U	mean K/mean U ($\times 10^3$)
Varpaisjärvi	0.57 (34)	0.69	0.30	10.3	1.4
Lapland	1.00 (106)	1.10	0.76	17.9	5.3
Pielavesi–Kiuruvesi	0.96 (35)	0.84	0.68	7.1	2.4
Turku	2.24 (23)	0.81	2.08	5.5	1.4
Southern Estonia	1.35 (54)	1.39	0.94	2.5	1.5

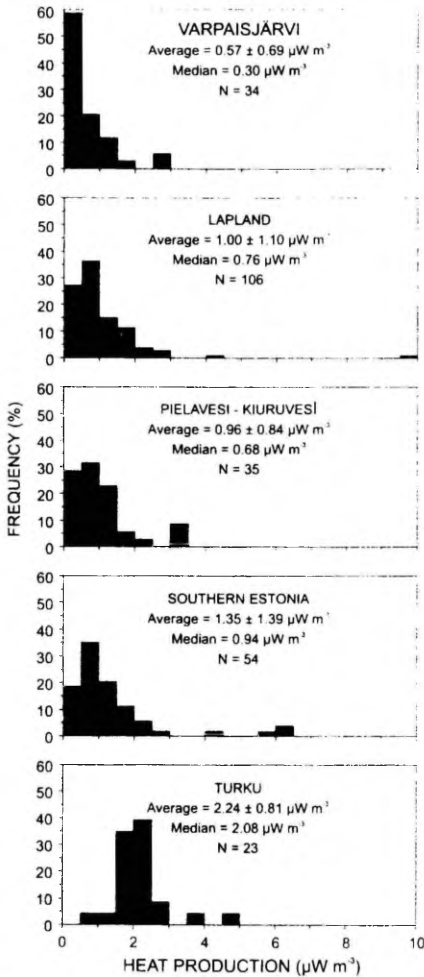


Fig. 2. Heat production histograms for granulite facies rocks from different areas.

mean values range from 3.01 to 3.06 $\text{W m}^{-1} \text{K}^{-1}$ (Table 2). The slightly higher thermal conductivity of the Varpaisjärvi rocks ($3.24 \text{ W m}^{-1} \text{K}^{-1}$) is related to the occurrence of sillimanite, whereas increased values of the Lapland granulites ($3.48 \text{ W m}^{-1} \text{K}^{-1}$)

Table 2

Thermal conductivities of granulite facies rocks from different areas

Area	N	Average	Std. dev.
Varpaisjärvi	34	3.24	0.87
Lapland	105	3.48	0.82
Pielavesi-Kiuruvesi	35	3.06	0.52
Turku	22	3.05	0.39
Southern Estonia	46	3.01	0.44

can be attributed to higher quartz contents of felsic rocks.

5. Mineralogy of heat-producing elements

In order to get more information about the mineralogy of heat-producing elements, three polished thin sections were studied with an electron probe microanalyser. Samples from the Varpaisjärvi, Lapland and southern Estonian areas were chosen to represent these areas on the basis of their Th and U concentrations and Th/U ratios. Thin sections were studied only for Th and U, because the microanalyser is not useful for mapping light elements.

At first the TURBO-SCAN rare-phase locating system (Walker, 1990) was used to find rapidly out locations of Th and U and later these areas were examined with a point logging system with $1 \mu\text{m}$ precision. The detailed description of the method is given in Johanson and Kojonen (1995).

Results of the microprobe analysis indicate that Th is concentrated in monazite, while U concentrations were mostly lower than the detection limit (0.2%). This agrees with zircon analyses by Petersell and Levchenkov (1994), where U concentrations varied from 0.02 to 0.2%. Microprobe measurements indicated monazites with homogeneous Th concentrations inside mineral grains, but with different concentration levels (0.2 to 1.8%) between grains. The lack of internal variations could be attributed to recrystallization of monazites during the metamorphic event or indicates that depletion is a process on a whole-rock scale and not at the mineral level. The first hypothesis is less probable since the monazite melting temperature in dry conditions is higher than the metamorphic peak temperatures in these areas. On the other hand, Th and U concentrations are

about one order of magnitude lower than those usually given for monazites and zircons (2–20% and 0.1–0.5%, respectively; e.g., Van Schmus, 1984).

6. Discussion

Seismic P-wave velocities were measured with the aim to study their relationship with heat production (e.g., Rybach and Buntebarth, 1984). Many of the samples investigated here are from outcrops and their P-wave velocities may be reduced due to weathering. In order to reduce this effect we also measured the porosity of samples. Typical porosity values for unweathered crystalline drillcore samples are less than 0.6% and this value was used to select data.

There seems to be no relationship between heat production and P-wave velocity in these granulite facies rocks (coefficient of correlation $r = -0.29$; Fig. 3). The lack of relationship applies to the whole data set as well as individual areas. Velocities range from 5400 to 7300 m s^{-1} and heat production values range almost over three orders of magnitude. Samples have $A-V_p$ values relatively close to the relationship line found by Rybach and Buntebarth (1984), but data points are scattered and do not show

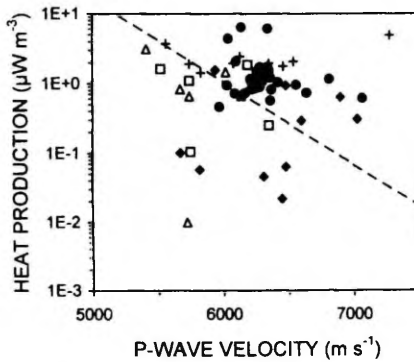


Fig. 3. Heat production versus P-wave velocity for samples with porosity < 0.6%, which is a typical value for unweathered crystalline rocks. Dashed line shows the relationship found by Rybach and Buntebarth (1984) at pressure 50 MPa: \blacklozenge = Varpaisjärvi; \square = Lapland; \triangle = Pielavesi–Kiuruvesi; $+$ = Turku; shaded circle = southern Estonia.

systematic variation. Moreover, the heat production values may deviate by up to two orders of magnitude from the relationship line.

Since the peak metamorphic temperature and pressure conditions are known in the studied areas, it is interesting to study whether they have any influence to heat production and thermal conductivity. Unfortunately metamorphic temperatures vary in a relatively small range (750–900°C) and do not allow any conclusions about systematic changes with temperature.

The metamorphic pressures vary in a relatively large range, but still thermal conductivities do not show systematic changes. Differences in thermal conductivity can be attributed mainly to differences in the composition of the original material, i.e. the silica content.

In addition to our five granulite areas, heat production and metamorphic pressure data from the Kapuskasing (Ashwal et al., 1987) and Pikwitonei (Fountain et al., 1987) areas in the Canadian Shield are included in Fig. 4. In general, heat production decreases with increasing metamorphic pressure. However, we do not propose any mathematical

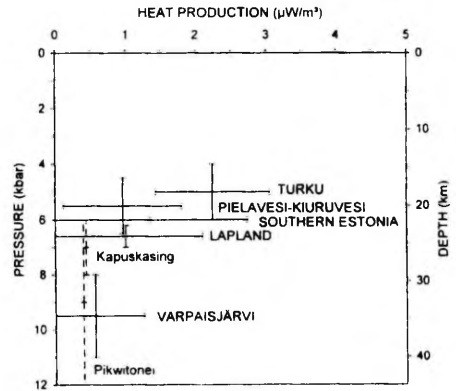


Fig. 4. Heat production versus metamorphic pressure peak conditions. Vertical bars show the range of maximum pressure and horizontal bars show standard deviations of heat production mean values. Additional data from Kapuskasing (Ashwal et al., 1987) and Pikwitonei (Fountain et al., 1987) are presented without heat production standard deviations. The depth scale was obtained assuming a mean density of 2800 kg m^{-3} for the crust.

relation between these two parameters because of the large variation in heat production. Fig. 4 shows that the ranges of heat production variation become smaller with the increase of the metamorphic pressure (depth), but still a wide range of heat production values can be expected at depths of 15–30 km.

Two different models for the formation of granulite facies rocks were principally suggested. In the case of isobaric cooling, granulites are products of magmatic underplating (Wells, 1980; Mezger, 1992) or extensional processes (Harley, 1989), and the uplift of granulites is not related to their formation. These rocks stayed for a long time in the lower crust and had enough time for equilibration under high-grade conditions. Another mechanism is isothermal decompression, which is considered as a result of double thickening of continental crust (Newton and Perkins, 1982; Harley, 1989), and the high pressures and temperatures are only a transient feature reached along the clockwise pressure–temperature path (England and Thompson, 1984). Granulites formed by the second model may not be truly representative for the lower crust (Rudnick and Fountain, 1995).

p–T history data are available for all studied areas. In the Pielavesi area the metamorphic peak was followed by isobaric cooling (Hölttä, 1988). Also in southern Estonia the cooling was nearly isobaric with no remarkable decompression (Hölttä and Klein, 1991). Isothermal decompression seems to be the formation process for the Varpaisjärvi (Hölttä and Paavola, 1989), Lapland (Barbey, 1982; Barbey et al., 1984) and Turku granulites (Väisänen et al., 1994). However, there is a lack of age determinations that might improve earlier conclusions. On the other hand, with the exception of Turku, the granulite areas have heat production values of about the same order, independently of their formation history. Probably the time during which these rocks experienced high-grade metamorphic conditions was long enough.

7. Conclusions

Heat production of granulite facies rocks varies widely. This is related to different lithological types and to variations in metamorphic pressure leading to different degrees of depletion in heat producing

elements. The decrease of heat production with the increase of the metamorphic pressure indicates that such a trend exists also with depth. However, considerable areal variations are expected, and a definite numerical expression cannot be presented for heat production, depth and pressure.

Current data do not suggest a heat production–P-wave velocity relationship in granulites. Changes in heat production are not systematic and values may differ for up to two orders of magnitude for a given P-wave velocity value. Thus the results are not encouraging for estimating heat production values from P-wave velocity data in thermal models of the Baltic Shield.

Acknowledgements

A. Jöeleht was financially supported by the Centre for International Mobility, Finland and Vilho, Yrjö and Kalle Väisälä Foundation, Finland. Samples were partly provided by H. Säävuori and P. Hölttä (Geological Survey of Finland, Espoo); the later also gave useful comments on the manuscript. M. Viljakainen (University of Oulu) helped with preparation of samples as a summer student. B. Johanson and L. Pakkanen (GSF, Espoo) carried out the microprobe studies. We are grateful to I.V. Golovanova and an anonymous referee for their comments on the manuscript. This is EUROPROBE publication number 207.

References

- Ashwal, L.D., Morgan, P., Kelley, S.A., Percival, J.A., 1987. Heat production in an Archean crustal profile and implications for heat flow and mobilization of heat-producing elements. *Earth Planet. Sci. Lett.* 85, 439–450.
- Barbey, P., 1982. Signification géodynamique des domaines granulitiques. La ceinture des Granulites de Laponie (Fennoscandie): Une suture de collision continentale d'âge protérozoïque inférieur (2.3–1.9 Ga). Reconstitution pétrologique et géochimique. Thèse d'Etat, Univ. de Nancy I, 346 pp.
- Barbey, P., Convert, J., Moreau, B., Capdevila, R., Hameurt, J., 1984. Petrogenesis and evolution of an early Proterozoic collisional orogenic belt: the granulite belt of Lapland and the Belomorides (Fennoscandia). *Bull. Geol. Soc. Finl.* 56, 161–188.
- Bernard-Griffiths, J., Peucat, J.J., Postaire, B., Vidal, Ph., Convert, J., Moreau, B., 1984. Isotopic data (U–Pb, Rb–Sr, Pb–Pb and Sm–Nd) on mafic granulites from Finnish Lapland. *Precambrian Res.* 23, 325–348.

- Bogdanova, S.V., 1993. The three-segments hypothesis for the East European Craton. *Terra Nova*, Abstr. 5, 313–314.
- Bogdanova, S.V., Bibikova, E.V., Gorbatshev, R., 1994. Paleoproterozoic U–Pb zircon ages from Belorussia: new geodynamic implications for the East European Craton. *Precambrian Res.* 68, 231–240.
- Čermák, V., Bodri, L., Rybach, L., Buntebarth, G., 1990. Relationship between seismic velocity and heat production: comparison between two sets of data and test of validity. *Earth Planet. Sci. Lett.* 99, 48–57.
- Elo, S., 1992. Gravity anomaly maps. In: Koljonen, T. (Ed.), *The Geochemical Atlas of Finland*, Part 2. *Till. Geological Survey of Finland*, pp. 71–75.
- England, P.C., Thompson, A.B., 1984. Pressure–temperature–time paths of regional metamorphism. I. Heat transfer during the evolution of regions of thickened continental crust. *J. Petrol.* 25, 894–928.
- Fountain, D.M., 1986. Is there a relationship between seismic velocity and heat production for crustal rocks? *Earth Planet. Sci. Lett.* 79, 145–150.
- Fountain, D.M., 1987. The relationship between seismic velocity and heat production — a reply. *Earth Planet. Sci. Lett.* 83, 178–180.
- Fountain, D.M., Salisbury, M.H., Furlong, K., 1987. Heat production and thermal conductivity of rocks from the Pikwitonei–Sachigo continental cross section, central Manitoba: implications for the thermal structure of the Archean crust. *Can. J. Earth Sci.* 24, 1583–1594.
- Gaal, G., Berthelsen, A., Gorbatshev, R., Kesola, R., Lehtonen, M.I., Marker, M., Raase, P., 1989. Structure and composition of the Precambrian crust along the POLAR Profile in the northern Baltic Shield. In: Freeman, R., von Knorring, M., Korhonen, H., Lund, C., Mueller, St. (Eds.), *The European Geotraverse, Part 5. The POLAR Profile*. *Tectonophysics* 162, 1–25.
- Gorbatshev, R., Bogdanova, S., 1993a. Frontiers in the Baltic Shield. *Precambrian Research* 64, 3–21.
- Gorbatshev, R., Bogdanova, S., 1993b. The Baltic Shield and the Precambrian basement along the Tornquist Zone. In: Gee, D.G., Beckholmen, M. (Eds.), *EUROPROBE in Jablonna 1991*. European Science Foundation–Polish Academy of Sciences, Publ. Inst. Geophys., Warsaw, A-20, 255, pp. 73–79.
- Harley, S.L., 1989. The origin of granulites: a metamorphic perspective. *Geol. Mag.* 126, 215–247.
- Hölttä, P., 1986. Observations on the metamorphic reactions and PT conditions in the Turku granulite area. *Geol. Surv. Finl., Bull.* 339, 43–58.
- Hölttä, P., 1988. Metamorphic zones and the evolution of granulite grade metamorphism in the early Proterozoic Pielavesi area, central Finland. *Geol. Surv. Finl., Bull.* 344, 50 pp.
- Hölttä, P., 1997. Geochemical characteristics of granulite facies rocks in the Archean Varpaisjärvi area, central Fennoscandian shield. *Lithos* (in press).
- Hölttä, P., Klein, V., 1991. PT-development of granulite facies rocks in southern Estonia. *Geol. Surv. Finl., Spec. Pap.* 12, 37–47.
- Hölttä, P., Paavola, J., 1989. Kornerupine-bearing granulites and evidence of uplift in the Archean Varpaisjärvi area, central Finland. *Geol. Surv. Finl., Spec. Pap.* 10, 11–18.
- Huenges, E., 1997. Factors controlling the variances of seismic velocity, density, thermal conductivity and heat production of cores from the KTB pilot hole. *Geophys. Res. Lett.* 24, 341–344.
- Iyer, S.S., Chonduri, A., Vasconcellos, M.B.A., Cordani, U.G., 1984. Radioactive element distribution in the Archean granulite terrane of Jequié–Bahia, Brazil. *Contrib. Mineral. Petrol.* 85, 95–101.
- Järvinmäki, P., Puranen, M., 1979. Heat flow measurements in Finland. In: Čermák, V., Rybach, L. (Eds.), *Terrestrial Heat Flow in Europe*. Springer, Berlin, pp. 172–178.
- Johanson, B., Kojonen, K., 1995. Improved electron probe microanalysis services at Geological Survey of Finland. *Geol. Surv. Finl., Spec. Pap.* 20, 181–184.
- Kern, H., Siegmund, S., 1989. A test of the relationship between seismic velocity and heat production for crustal rocks. *Earth Planet. Sci. Lett.* 92, 89–94.
- Koppelmaa, H., Klein, V., Puura, V., 1978. Metamorfitsheskije kompleksii kristallitsheskogo fundamenta Estonii. In: Dage-laiskii, V., Bondarenko, L. (Eds.), *Metamorfitsheskije kompleksii fundamenta russkoi plitii*. Nauka, Leningrad, pp. 43–76.
- Korsman, K., 1977. Progressive metamorphism of the metapelites in the Rantasalmi–Sulkava area, southeastern Finland. *Geol. Surv. Finl., Bull.* 290, 82 pp.
- Korsman, K., Hölttä, P., Hautala, T., Wasenius, P., 1984. Metamorphism as an indicator of evolution and structure of the crust in eastern Finland. *Geol. Surv. Finl., Bull.* 328, 40 pp.
- Kukkonen, I., Lindberg, A., 1995. Thermal conductivity of rocks at the TVO investigation sites Olkiluoto, Romuvaara and Kivetty. Report YJT-95-08, Geological Survey of Finland, 28 pp.
- Mezger, K., 1992. Temporal evolution of regional granulite terranes: implications for the formation of lowermost continental crust. In: Fountain, D.M., Arculus, R., Kay, R.W. (Eds.), *Continental Lower Crust*. Elsevier, Amsterdam, pp. 447–478.
- Newton, R.C., Perkins, D., 1982. Thermodynamic calibration of geobarometers based on the assemblages garnet–plagioclase–orthopyroxene (clinopyroxene)–quartz. *Am. Mineral.* 67, 203–222.
- Paavola, J., 1984. On the Archean high-grade metamorphic rocks in the Varpaisjärvi area, Central Finland. *Geol. Surv. Finl., Bull.* 327, 33 pp.
- Petersell, V., Levchenkov, O., 1994. On the geological structure of the crystalline basement of the southern slope of the Baltic Shield. *Acta Commentationes Univ. Tartuensis* 972, 16–39.
- Puura, V., Vaher, R., Klein, V., Koppelmaa, H., Niin, M., Vanamb, V., Kirs, J., 1983. *The Crystalline Basement of Estonian Territory*. Nauka, Moscow, 208 pp. (in Russian).
- Raith, M., Raase, P., 1986. High grade metamorphism in the granulite belt of Finnish Lapland. In: Dawson, J.B., Carswell, D.A., Hall, J., Wedepohl, K.H. (Eds.), *The Nature of the Lower Crust*. *Geol. Soc. Spec. Publ.* 24, 283–295.
- Rudnick, R.L., 1992. Xenoliths — samples of the lower conti-

- mental crust. In: Fountain, D.M., Arculus, R., Kay, R.W. (Eds.), *Continental Lower Crust*. Elsevier, Amsterdam, pp. 269–316.
- Rudnick, R.L., Fountain, D.M., 1995. Nature and composition of the continental crust: a lower crustal perspective. *Rev. Geophys.* 33, 267–309.
- Rudnick, R.L., Presper, T., 1990. Geochemistry of intermediate- to high-pressure granulites. In: Vielzeuf, D., Vidal, P. (Ed.), *Granulites and Crustal Evolution*. Kluwer, Dordrecht, pp. 523–550.
- Rybach, L., 1973. Wärmeproduktionsbestimmungen an Gesteinen der Schweizer Alpen. *Beitr. Geol. Schweiz, Geotech. Ser.*, 51, 43 pp.
- Rybach, L., Buntebarth, G., 1984. The variation of heat generation, density and seismic velocity with rock type in the continental lithosphere. In: Čermák, V., Rybach, L., Chapman, D.S. (Eds.), *Terrestrial Heat Flow Studies and the Structure of the Lithosphere*. *Tectonophysics* 103, 335–344.
- Rybach, L., Buntebarth, G., 1987. The relationship between seismic velocity and heat production — critical comments. *Earth Planet. Sci. Lett.* 83, 175–177.
- Salli, J., 1983. Pielaveden kartta-alueen kallioperä. Summary: Pre-Quaternary rocks of the Pielavesi map-sheet area. *Geological Map of Finland, explanation to the maps of Prequaternary rocks, Sheet 3314*.
- Schreurs, J., Westra, L., 1986. The thermotectonic evolution of a Proterozoic, low pressure, granulite dome, West Uusimaa, SW Finland. *Contrib. Mineral. Petrol.* 93, 236–250.
- Sharov, N.V., Zagorodny, V.G., Glaznev, V.N., Zhamaleidinov, A.A., 1989. Struktura litosfery i verkhney mantiy Baltiyskogo shchita. In: Sollogub, V.B. (Ed.), *Litosfera Tsentralnoy i Vostochnoy Evropy: Vostochno-Evropeyskaya Platforma*. Naukova Dumka, Kiev, pp. 52–77 (in Russian).
- Simonen, A., 1980. The Precambrian in Finland. *Geol. Surv. Finl., Bull.* 304, 58 pp.
- Väisänen, M., Hölttä, P., Rastas, J., Korja, A., Heikkinen, P., 1994. Deformation, metamorphism and the deep structure of the crust in the Turku area, southwestern Finland. *Geol. Surv. Finl., Guide* 37, 35–41.
- Van Schmus, W.R., 1984. Radioactivity properties of minerals and rocks. In: Carmichael, R.S. (Ed.), *CRC Handbook of Physical properties of Rocks*. CRC Press, Boca Raton, Vol. III, pp. 281–293.
- Walker, R.K., 1990. TURBO-SCAN, The Rare-Phase Locating System. Department of Mineral Resources Engineering, Royal School of Mines, Imperial College, London, 64 pp.
- Wells, P.R.A., 1980. Thermal models for the magmatic accretion and subsequent metamorphism of continental crust. *Earth Planet. Sci. Lett.* 46, 253–265.

Kukkonen, I. T. and Jöeleht, A., 1996.
Geothermal modelling of the lithosphere
in the central Baltic Shield and its southern slope.
Tectonophysics, 255: 25–45.



ELSEVIER

Tectonophysics 255 (1996) 25–45

TECTONOPHYSICS

Geothermal modelling of the lithosphere in the central Baltic Shield and its southern slope

Ilmo T. Kukkonen^{a,*}, Argo Jõelet^b

^a Geological Survey of Finland, Betonimiehenkuja 4, FIN-02150 Espoo, Finland

^b University of Tartu, Institute of Geology, Vanemuise 46, EE2400 Tartu, Estonia

Received 30 January 1995; accepted 22 September 1995

Abstract

Lithospheric temperature and heat flow density (HFD) were studied in the central Baltic (Fennoscandian) Shield and its subsurface continuation to the south, along a transect trending from eastern Finland to southern Estonia. The transect represents an example of a low HFD ($\leq 30 \text{ mW m}^{-2}$) Archaean craton on a thick (150–190 km) lithosphere surrounded by Early and Middle Proterozoic mobile belts on a thinner (110–150 km) lithosphere with slightly elevated HFD (35–55 mW m^{-2}). Numerical 2-D conductive models were constructed in which peridotite solidus temperatures were assigned to those depths which correspond to the seismically determined lithosphere/asthenosphere boundary. This technique was found to reduce the effect of uncertainties in heat production and thermal conductivity values on the simulation results. Upper crustal heat production values for the Finnish terrain were taken from published geochemical analyses of outcropping rocks. For the Estonian terrain new heat production values were measured from core samples representing nineteen deep boreholes. Middle and lower crustal lithologies were estimated with the aid of the deep seismic V_p/V_s data, and corresponding heat production values were adapted from global xenolith averages and from data for granulites cropping out in other Precambrian areas.

The results of the modelling suggest that the lithosphere and Moho depth variations are only weakly reflected in the measured surface heat flow data, which are mainly controlled by heat sources in the upper crust. The simulated heat flow densities at 50 km depth (approximately at the Moho) are relatively low and range from 12 mW m^{-2} at the Archaean northeastern end to 19 mW m^{-2} on the Proterozoic southwestern end of the transect. Simulated temperatures at 50 km depth increase from northeast to southwest, ranging from 450–550°C in eastern Finland to about 650°C in Estonia. Sensitivity of the simulations to parameter changes was studied by varying the heat production and thermal conductivity values. The extreme values for the Moho temperature estimates thus obtained may be about 50 K lower or 100 K higher than the values above. The corresponding sensitivity of the Moho HFD is about $\pm 6 \text{ mW m}^{-2}$ and of the surface HFD $\pm 5\text{--}20 \text{ mW m}^{-2}$, respectively.

1. Introduction

This paper uses numerical simulations in studying lithospheric temperatures and HFD's along a 700-km-long transect crossing eastern Finland, the Gulf

* Corresponding author. E-mail: ilmo.kukkonen@gsf.fi. Fax: +358-0-462205

of Finland and Estonia. The northeastern end of the transect is in eastern Finland near Nurmes at 30.06°E, 63.59°N and the southwestern end in southern Estonia near Vortsjärvi at 25.79°E, 57.81°N (Fig. 1a). The transect line coincides with the deep seismic sounding profiles BALTIC (Luosto et al., 1990) and the northern part of the Sovetsk–Kohtla–Järve profile (Sharov et al., 1989).

The transect crosses several Archaean and Proterozoic crustal units, including the late Archaean gneiss domain, the Early Proterozoic Outokumpu thrust system, the Middle Proterozoic Wiborg rapakivi intrusion and the Early Proterozoic granulite terrain in southern Estonia (Fig. 1b). To the north of the Gulf of Finland the shield is exposed but in Estonia it is covered by a thin layer (200–600 m) of Phanerozoic sediments (Cambrian to Devonian, and Quaternary). Moho depth varies from 40 to 62 km along the transect with the deepest parts near the northeastern end of the transect. The seismically determined lithosphere (Calcagnile, 1982; Babuska et al., 1988) is anomalously thick (160–190 km) in eastern Finland but thins quickly under southern Finland and the Gulf of Finland, reaching a value of about 110 km at the Estonian side of the Gulf of Finland. All these structural elements should be reflected in the thermal regime of the lithosphere.

The area represents a good example of an Archaean cratonic area surrounded by Early Proterozoic mobile belts and affected by Middle Proterozoic anorogenic magmatism. The geothermal systematics of such areas have been recently discussed by Nyblade and Pollack (1993a, b, c). Their results suggest that crustal heat production differences and lithospheric thickness variations can either independently or in combination produce the observed HFD pattern in shield areas. The central parts of the Baltic Shield are particularly well suited for a detailed study of these effects since seismic data on crustal and lithospheric structure (Sharov et al., 1989; Luosto et al., 1990) are available and the distribution of heat production at the bedrock surface is relatively well constrained (Kukkonen, 1989a; Kukkonen, 1993).

Measurements of HFD have been reported in Finland by Puranen et al. (1968), Järvimäki and Puranen (1979), Kukkonen (1988, 1989a, 1989b, 1993) and Kukkonen and Järvimäki (1992), in Esto-

nia by Urban et al. (1991) and in the adjacent Russian territory by Gordienko et al. (1985, Gordienko et al. (1987). Palaeoclimatic effects have been assessed by Kukkonen (1987) and they are mostly only a few mW m^{-2} . Modelling of lithospheric temperatures and HFD's in the area have been provided by Milanovsky (1984), Čermák et al. (1993), Kukkonen (1989b) and Pasquale et al. (1990, 1991). Rheological and thermal behaviour of the lithosphere have been investigated by Dragoni et al. (1993) and Bodri (1994). The effects of bedrock fluid circulation on the thermal regime have been discussed by Bodri (1994) and Kukkonen (1988, 1995).

The relationships between radiogenic heat production and seismic P-wave velocity (Rybach and Buntbarth, 1984) have been used for estimating heat production in many crustal studies (e.g. Čermák and Bodri, 1993), but the validity of the relationships has been criticized and strongly debated (Fountain, 1986, 1987; Rybach and Buntbarth, 1987; Čermák et al., 1990). In contrast to most previous studies of the geothermics of the central and eastern Baltic Shield we determine the upper crustal heat production values from published geochemical analyses of different rock units and from our own measurements. For the deeper crust we apply petrological models constructed from the DSS V_p/V_s data and compare these results with deep crustal heat production estimates based on xenolith data and outcropping deep crustal sections in other comparable areas. We also present new measurements of heat production and thermal conductivity of amphibolite and granulite facies rocks in the Estonian terrain.

Lithospheric thermal models are highly sensitive to input parameter variations (see, e.g., Baumann and Rybach, 1991). For instance, if lithospheric geotherms are calculated using the surface HFD and surface temperature values as boundary conditions (as is conventional in analytical layered half-space models), the resulting temperature estimates for the Moho level may differ by 100–200 K even where the surface HFD is changed by as little as 10 mW m^{-2} . The estimation error tends to increase cumulatively with depth, such that at the base of the lithosphere it may be several hundreds of degrees. Considering the various sources of uncertainty in HFD measurements (palaeoclimatic effects, fluid cir-

ulation, structural effects) and the detected vertical variation in HFD in the Kola super-deep hole (Kremenetsky and Ovchinnikov, 1986a, 1986b; Moiseyenko, 1986; Dragoni et al., 1993; Kukkonen and Clauser, 1994) biasing of $\pm 10 \text{ mW m}^{-2}$ could easily be incorporated within the data. Therefore, lithospheric thermal models, and particularly their parameter values and boundary conditions, should be based on the most reliable evidence obtainable for the thermal conditions of the lithosphere. The most reliable parameters are in fact the surface temperature and the thermal properties of the uppermost crust.

To constrain the deep lithospheric temperatures indirect information must be used. There are many temperature-dependent phenomena which could, in principle, be used for assigning temperatures to different depth levels. Such effects include mantle viscosities (Kirby, 1983), electrical conductivity of the asthenosphere (Adám, 1978, 1980; Shankland and Waff, 1977), seismic velocities at the lithosphere/asthenosphere (L/A) boundary (Murase et al., 1977; Murase and Kushiro, 1979; Murase and Fukuyama, 1980; Shankland et al., 1981), magnetic Curie depths (Wasilewski et al., 1979) and seismic reflectivity of the lower crust (Klemperer, 1987).

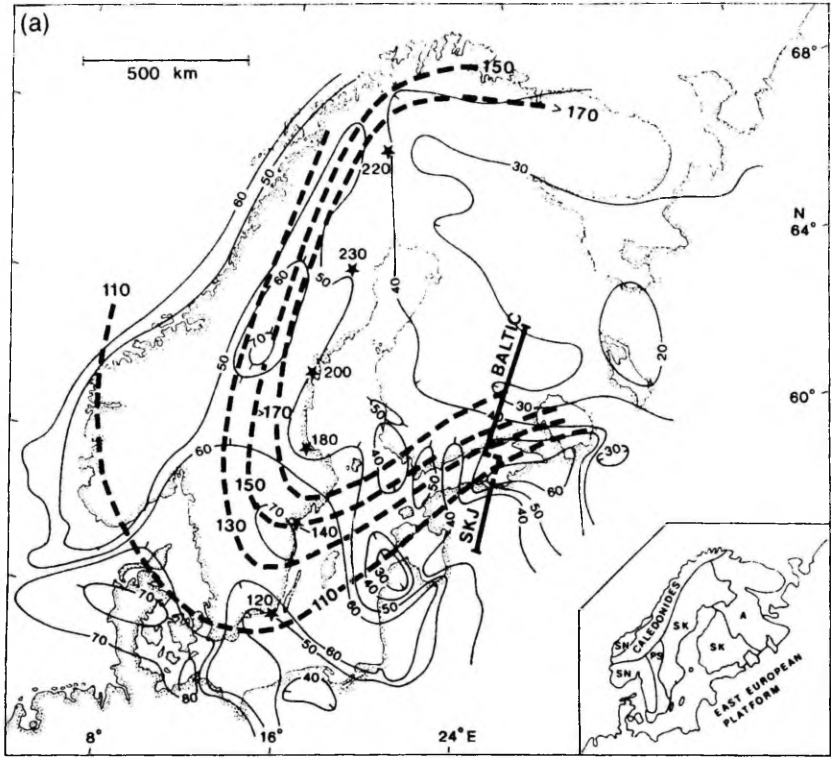
In this study we assume that the seismically determined L/A boundary (Calcagnile, 1982; Babuska et al., 1988) represents a true transition from solid to partially molten mantle rocks. We apply this hypothesis by assigning petrologically derived solidus temperatures to this boundary layer. The effects of both volatile-free "dry" and volatile-bearing "wet" solidi on the lithospheric thermal regime are studied and the sensitivity of the applied technique to parameter variations is discussed. For comparison we also apply a laterally variable basal heat flow density as a lower boundary condition.

2. Heat flow density data

There are about 38 HFD measurement sites located within 100 km of the transect. Within Finland data can be further supplemented using the heat flow density map estimated from a heat production survey and a linear heat flow-heat production relationship (Kukkonen, 1993). In the Finnish part of the transect

HFD increases from northeast towards southwest (Fig. 1a). For the Archaean part of the transect the measured HFD is about 30 mW m^{-2} or lower, while on the Proterozoic Svecokarelian–Svecofennian terrain it is about $30\text{--}45 \text{ mW m}^{-2}$, and on the Wiborg rapakivi batholith about 55 mW m^{-2} . There are no data from the Gulf of Finland. On the Estonian part of the transect HFD is $40\text{--}50 \text{ mW m}^{-2}$ with a southward decreasing trend. To the west of the transect in western Estonia there are three holes with very small HFD values ($< 10 \text{ mW m}^{-2}$; Fig. 1b; Urban et al., 1991), which, in our view can be attributed to disturbance of borehole temperatures by water flow in the holes.

Heat flow data are based on measurements in boreholes that vary in depth from 125–1100 m in Finland to 100–340 m in Estonia. The holes are shallow on a lithospheric scale, and therefore apt to hydrogeological disturbances. However, we assume here that they are generally representative of conductive heat flow values. This assumption is supported by the available data on the hydraulic permeability of bedrock obtained by drill hole measurements (Teollisuuden Voima Oy, 1992; Ahonen and Blomqvist, 1994; Niemi, 1994). At depths exceeding 200 m hydraulic permeability is usually smaller than $1 \times 10^{-15}\text{--}1 \times 10^{-14} \text{ m}^2$, which is the approximate threshold value between conductively and convectively dominated systems (see Bodri, 1994; Kukkonen, 1995). Interpretation of the seismic surface wave data on the DSS profile SVEKA, which is located about 250 km to the northwest of the BALTIC profile, suggested that fracture frequency decreases rapidly with depth in the uppermost 4 km (Grad and Luosto, 1987, 1992). This indicates that hydraulic permeability conceivably decreases downwards in the upper crust and is generally smaller than the values measured in boreholes. Further, topographic variation is quite small in Finland and Estonia, and is incapable of generating thermally significant regional flow systems. This, however, does not exclude the possibility of local deviations from conductive HFD values, as demonstrated by experimental data (Kukkonen, 1988; Urban et al., 1991). Local disturbances should, however, be masked in regional HFD trends providing that the heat flow density sites include equal proportions of discharge and recharge areas.



LEGEND

— 60 — HFD in mW m^{-2}

LITHOSPHERE THICKNESS (km):
 - - - from Rayleigh wave data
 * at FENNOLORA shot points
 (V_p data)

TECTONIC UNITS:

A Archaean > 2500 Ma
 SK Svecokarelian 2500–1750 Ma
 PS Post Svecokarelian 1750–1200 Ma
 SN Sveconorwegian 1800–900 Ma

Fig. 1. (a) Lithosphere thickness (Calcagnile, 1982; Guggisberg and Berthelsen, 1987) and generalized heat flow density (Čermák et al., 1993) in the Baltic Shield area and location of the modelled transect, the *BALTIC* and *Sovetsk-Kohtla-Järve (SKJ)* DSS profiles. (b) Simplified geological boundaries (Simonen, 1980; Koistinen, 1994) and surface heat flow densities (in mW m^{-2}) in the vicinity of the transect. Numbers 0–5 and letters A–G indicate DSS shot points. *WRB* = Wiborg rapakivi batholith; *CFGFC* = Central Finland granitoid complex; *TLN* = Tallinn; *HKI* = Helsinki.

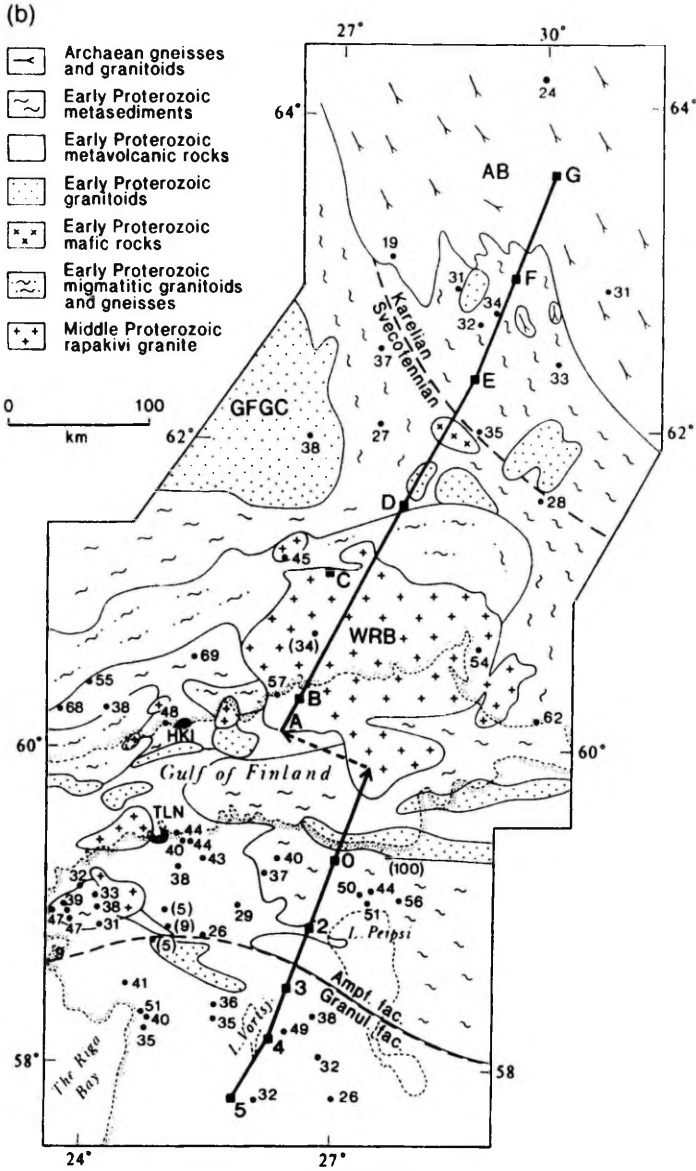


Fig. 1 (continued).

3. Radiogenic heat production at the bedrock surface

Heat production values based on geochemical surveys of U, Th and K have been presented for Finland by Kukkonen (1989a, 1993). There is a general increasing trend of heat production from the Archaean terrain towards younger formations in the southwest which can be correlated with the tectonic setting and origin of the respective lithological units. In southern Finland the highest values are related to the 1830 Ma migmatite belt ($2.0\text{--}3.5 \mu\text{W m}^{-3}$) and the Wiborg rapakivi granite batholith (up to $5 \mu\text{W m}^{-3}$).

We are not aware of any published heat production data for the Estonian Precambrian bedrock. The bedrock beneath the Phanerozoic sediments is, however, relatively well known as a result of extensive drilling (Koistinen, 1994). Core samples were collected from nineteen drill holes in northern and western Estonia at approximately 10 m depth intervals (Fig. 2). The holes penetrated 40–330 m into the Precambrian basement and are representative of different metamorphic areas in the Estonian bedrock: (1) the northern amphibolite facies area (mainly amphibolite, metasediments and some granitoids); (2) the southern granulite facies area (mainly gneisses and amphibolites); and (3) an area between the pre-

vious two and characterized by granulite facies with a retrograde overprint. Heat production data for the southern Estonian granulite facies rocks are particularly interesting since these rocks may also correspond to middle crustal rocks in the present situation. Southern Estonian granulites acquired their present metamorphic assemblages under 600 MPa pressures and 800°C temperatures (Hölttä and Klein, 1991).

U, Th and K concentrations of the samples were measured with gamma ray spectrometry at the Geological Survey of Finland assuming that the decay series have been in equilibrium. Heat production was calculated as follows (Rybach, 1973):

$$A = \rho(9.52C_U + 2.56C_{Th} + 3.48C_K)10^{-5} \quad (1)$$

where A is the heat production ($\mu\text{W m}^{-3}$), C_U and C_{Th} are the U and Th concentrations (ppm), respectively, C_K is the K concentration (%) and ρ is density (kg m^{-3}). The detection limit is about 1 ppm for U and Th and 0.1% for K. Density was measured by weighing in both air and water. In addition, thermal conductivity was also measured with the divided bar method on water-saturated samples at room pressure and temperature, and a summary of the results is given in Table 1. They indicate a general trend of decreasing heat production from amphibolite facies rocks ($3.23 \pm 1.89 \mu\text{W m}^{-3}$) to the granulite facies rocks ($1.26 \pm 0.71 \mu\text{W m}^{-3}$),

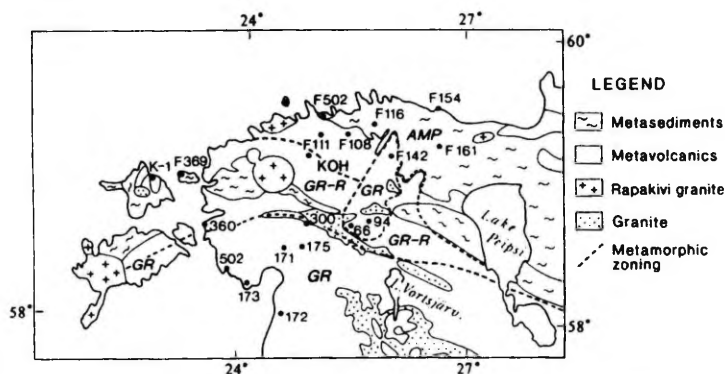


Fig. 2. Location of the drill core samples used for heat production measurements in Estonia (Table 1). Geological boundaries adapted from Koistinen (1994) and Hölttä and Klein (1991). The metamorphic zoning is divided into granulite facies (GR), amphibolite facies (AMP) and granulite facies with a retrograde overprint (GR-R) under amphibolite facies conditions.

Table 1
Thermal properties of rocks sampled in Estonian deep drill holes

Facies	Drill hole	A^a	k^a
AMPHIBOL	F111	5.88 ± 2.62 (11)	3.61 ± 0.16 (11)
AMPHIBOL	F108	1.17 ± 0.51 (7)	2.60 ± 0.24 (7)
AMPHIBOL	F116	2.07 ± 2.19 (33)	3.22 ± 0.40 (34)
AMPHIBOL	F161	2.37 ± 1.63 (9)	3.73 ± 0.22 (7)
AMPHIBOL	F154	2.62 ± 1.03 (11)	3.28 ± 0.19 (11)
AMPHIBOL	F502	5.25 ± 0.89 (6)	3.41 ± 0.10 (5)
GRANUL + RET	360	3.07 ± 1.92 (7)	2.91 ± 0.06 (6)
GRANUL + RET	KOH	1.25 ± 0.88 (36)	2.78 ± 0.49 (36)
GRANUL + RET	F369	2.08 ± 0.78 (5)	3.33 ± 0.52 (3)
GRANUL + RET	K-1	1.94 ± 0.89 (27)	2.95 ± 0.62 (26)
GRANUL	300	0.82 ± 0.38 (3)	–
GRANUL	66	2.67 ± 2.07 (9)	3.52 ± 0.17 (9)
GRANUL	94	0.88 ± 0.19 (8)	2.93 ± 0.18 (9)
GRANUL	502	1.19 ± 0.75 (2)	–
GRANUL	171	0.71 ± 0.14 (6)	3.26 ± 0.51 (6)
GRANUL	172	0.92 ± 0.50 (8)	2.86 ± 0.33 (8)
GRANUL	173	1.84 ± 1.74 (6)	2.57 ± 0.65 (4)
GRANUL	175	0.44 ± 0.41 (6)	2.45 ± 0.13 (4)
GRANUL	F142	1.83 ± 1.79 (9)	2.98 ± 0.33 (9)

Facies: GRANUL = granulite facies; AMPHIBOL = amphibolite facies; RET = retrograde overprint in amphibolite facies conditions. Drill hole: code refers to Fig. 2. A = radiogenic heat production ($\mu\text{W m}^{-3}$) \pm standard deviation. k = thermal conductivity ($\text{W m}^{-1} \text{K}^{-1}$) \pm standard deviation.

^a Number of samples in parentheses.

while granulites with a retrograde overprint fall between these two groups ($2.09 \pm 0.75 \mu\text{W m}^{-3}$). The results suggest either differences in original composition of the rocks or, alternatively, depletion during granulite facies metamorphism. The standard deviations of the mean values are large and suggest that the differences between groups may not necessarily be statistically representative. In any case the granulite facies rocks still show considerable heat production (Table 1).

4. Numerical model

4.1. Simulation techniques and boundary conditions

Conductive 2-D steady-state simulations were performed in which the heat conduction equation was solved using the finite difference code SHEMAT (Clauser, 1988; Clauser and Villinger, 1990). The 700-km-long and 200-km-deep transect was modelled with a constant discretization in the horizontal (10 km) and a variable discretization in the vertical dimension (0.5–10 km) (Fig. 3).

The following boundary conditions were applied in the model: (1) constant temperature (5°C) at the ground surface; (2) depth-dependent temperature at the L/A boundary, or alternatively, a prescribed lateral variation in the basal heat flow density; and (3) no flow of heat through the lateral boundaries.

Temperatures representative of the L/A boundary were taken from peridotite solidi. Two solidus variants were applied: one for a volatile-free ('dry') peridotite and another for a volatile-bearing ('wet') peridotite; these represent the extremes of the possible temperature ranges at the L/A boundary. We have used here the dry spinel lherzolite data of Takahashi and Kushiro (1983) and the wet peridotite data by Olafsson and Eggler (1983) and Kushiro et al. (1967). In the wet case the effects of volatile buffering with the mineral phases and the most plausible volatile composition of mantle rocks have been taken into account. Since the wet solidus is relatively uniform and varies by less than 100 K at depths of 70–200 km, we assumed a constant value of 1100°C . The dry solidus varies approximately linearly with depth between 1100°C (surface) and 1850°C (190 km).

Thermal conductivity ($\text{W m}^{-1} \text{K}^{-1}$) is assumed to be temperature dependent and to include the effects of lattice conductivity and radiative heat transfer according to the formula:

$$k = k_{\text{ref}} \left(\frac{1}{1 + bT} \right) + c(T + 273.15 \text{ K})^4 \quad (2)$$

where T is the temperature ($^{\circ}\text{C}$), k_{ref} is the conductivity at room temperature (20°C) and b (K^{-1}) and c ($\text{W m}^{-1} \text{K}^{-4}$) are experimental constants. For b we applied the value of 0.0015 which approximates the lattice conductivity data by Zoth and Haenel (1988) for common rock types at temperatures lower than about $1000\text{--}1200^{\circ}\text{C}$. Since the radiative heat transfer is important mainly in the lower crust and mantle at temperatures exceeding about 800°C , a value of $c = 1 \cdot 10^{-10}$ was applied, approximating the results of Schatz and Simmons (1972) for ultrabasic mantle materials. As a result of Eq. (2), thermal conductivity first decreases with increasing temperature until

about 800°C is reached, after which conductivity follows an increasing trend.

4.2. Compilation of the model parameters

4.2.1. Upper crust (0–10 km)

The outcropping lithology was assumed to be representative of the upper crust to a depth of 10 km. This is supported by the seismic data. There are usually no significant vertical variations in V_p in the uppermost crust, except for a small increase with depth which can be attributed to fracture and pore closure by pressure. In areas where more detailed gravity or magnetic modellings were available, these results were used as constraints for the model structures (for instance, the Wiborg rapakivi batholith, domains 4 and E in Fig. 3; Elo and Korja, 1993). The upper crustal low-velocity zone found on parts of the BALTIC profile (Luosto et al., 1990) is considered to be a tectonic feature (fracturing) and is assumed to be lithologically equivalent to the upper

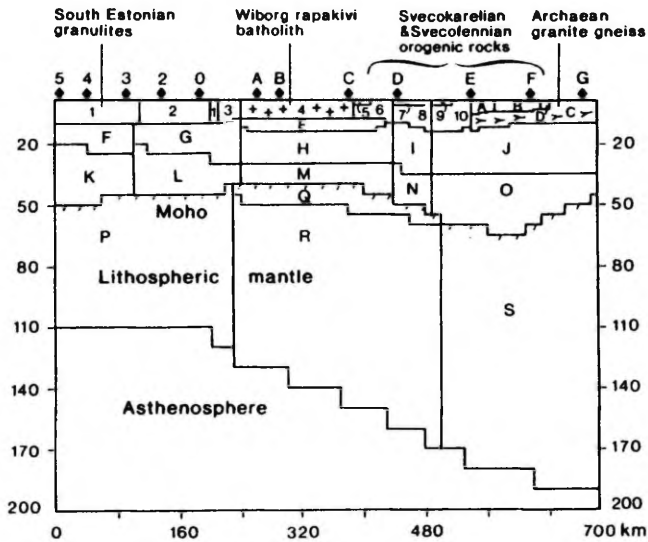


Fig. 3. The domain distribution used in the model. Diamonds indicate DSS shot points, shown also in Fig. 1b.

Table 2
Thermal, seismic and lithological parameters of the model

Domain	V_p	V_p/V_s	ν	Lithology	A^a	k^a	Reference
1	–	–	–	mafic and int. metavole (granulites)	1.0 (0.45–1.91)	3.0 (2.5–3.5)	This work
2	–	–	–	metasediments and amphibolites (amp.fac.)	1.9 (1.0–3.65)	3.2 (2.7–3.7)	This work
3	–	–	–	metasediments	1.7 (1.0–2.5)	3.2 (2.7–3.7)	Kukkonen (1989a)
4	–	–	–	Wiborg rapakivi granite	3.6 (1.2–6.0)	3.5 (3.0–4.0)	Rämö (1991)
5	–	–	–	Suomenniemä rapakivi batholite	4.0 (2.0–6.0)	3.5 (3.0–4.0)	Rämö (1991)
6	–	–	–	migmatite	1.7 (0.6–4.0)	3.2 (2.7–3.7)	Kukkonen (1989b) Nurmi (1984)
7	–	–	–	Sulkava high metam. area, migmatites	3.0 (2.0–4.0)	3.5 (3.0–4.0)	Nurmi (1984)
8	–	–	–	migmatite	1.7 (1.4–2.0)	3.2 (2.7–3.7)	Kukkonen (1989b)
9	–	–	–	Haukivesi mafic intrusions	0.2 (0.1–0.5)	2.5 (2.0–3.0)	assumed
10	–	–	–	migmatite + granitoid	1.4 (1.0–1.8)	3.2 (2.7–3.7)	Kukkonen (1989a)
A	–	–	–	Savo metasediments	1.0 (0.5–1.5)	3.2 (2.7–3.7)	Koistinen (1993)
B	–	–	–	Outokumpu assoc. mainly metasediments	1.7 (1.2–2.2)	3.0 (2.5–3.5)	Kukkonen (1989a)
C	–	–	–	Archaean granite gneiss	0.7 (0.4–1.0)	3.0 (2.5–3.5)	Koistinen (1993)
D	–	–	–	Jatulian quartzite	1.0 (0.1–2.4)	6.0 (5.0–7.0)	Koistinen (1993)
E	6.4–6.5	1.78–1.82	0.269–0.284	gabbro, anorthosite	0.50 (0.4–0.8)	2.5 (2.0–3.0)	this work
F	6.0–6.3 (6.2–6.5)	–	–	granodior., fels. amph. fac. gneiss, granite qt-mi schist, fels. granulite	0.8 (0.4–1.2)	3.0 (2.5–3.5)	this work
G	6.0–6.3 (6.2–6.5)	–	–	same as in domain F	0.8 (0.4–1.2)	3.0 (2.5–3.5)	this work
H	6.5–6.7	1.76–1.78	0.262–0.269	amphibolite, metapelitic granulite	0.8 (0.4–1.2)	3.0 (2.5–3.5)	this work
I	6.4–6.45	1.70–1.72	0.235–0.245	felsic amph. gneiss, felsic/int. granul.	0.4 (0.2–0.6)	3.0 (2.5–3.5)	this work
J	6.3–6.45	1.72–1.76	0.245–0.262	felsic. amph. gneiss, fels./int. granul.	0.4 (0.2–0.6)	3.0 (2.5–3.5)	this work
K	6.35–6.5 (6.8–6.9)	–	–	anorthosite, mafic granul., amphibol.	0.2 (0.1–0.3)	2.5 (2.0–3.0)	this work
L	6.35–6.5 (6.8–6.9)	–	–	Anorthosite, mafic granul., amphibol.	0.2 (0.1–0.3)	2.5 (2.0–3.0)	this work
M	7.0–7.2	1.78	0.269	amphibol., metapel. granulite	0.2 (0.1–0.3)	2.5 (2.0–3.0)	this work
N	7.0–7.2	1.74–1.78	0.253–0.269	amphibol., metapel. granulite	0.1 (0.05–0.15)	2.5 (2.0–3.0)	this work
O	7.0–7.3	1.78	0.269	metapel. granulite, amphibolite	0.1 (0.05–0.15)	2.5 (2.0–3.0)	this work
P	> 6.7–7.0	–	–	ultramafic	0.002	4.2	Jochum et al. (1983)

Table 2 (continued)

Domain	V_p	V_p/V_s	ν	Lithology	A^a	k^a	Reference
Q	8.0–8.2	> 1.78	> 0.269	ultramafic	(0.001–0.02)	(3.0–5.0)	Jochum et al. (1983)
					0.002	4.2	
R	> 8.2			ultramafic	(0.001–0.02)	(3.0–5.0)	Jochum et al. (1983)
					0.002	4.2	
S	> 8.5			ultramafic	(0.001–0.02)	(3.0–5.0)	Jochum et al. (1983)
					0.002	4.2	
					(0.001–0.02)	(3.0–5.0)	

Domain number refers to Fig. 3. V_p = P-wave velocity (km/s) from Luosto et al. (1990) or Sharov et al. (1989). V_p/V_s = ratio of P and S-wave velocities (Luosto et al., 1990). ν = Poisson ratio. Lithology: upper crust, domains 1–10 and A–D, outcropping lithology (Simonen, 1980; Koistinen, 1994); middle and lower crust, domains E–O, lithologies which correspond best with the V_p and Poisson ratio values (Holbrook et al., 1992). A = radiogenic heat production ($\mu\text{W m}^{-3}$). k = thermal conductivity ($\text{W m}^{-1} \text{K}^{-1}$). Reference = the reference for the used heat production values.^a In parentheses the range applied in simulations.

crustal rocks. The lithological boundaries were taken from Simonen (1980) and Koistinen (1994).

4.2.2. Middle and lower crust (> 10 km)

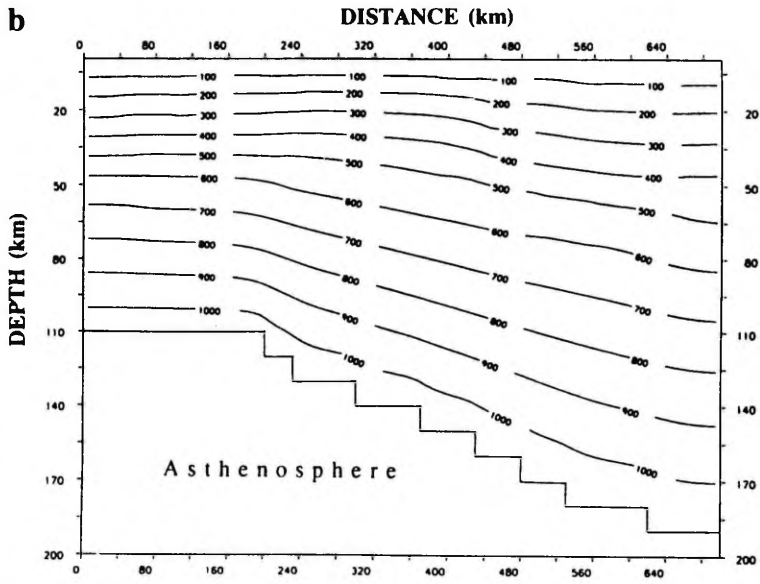
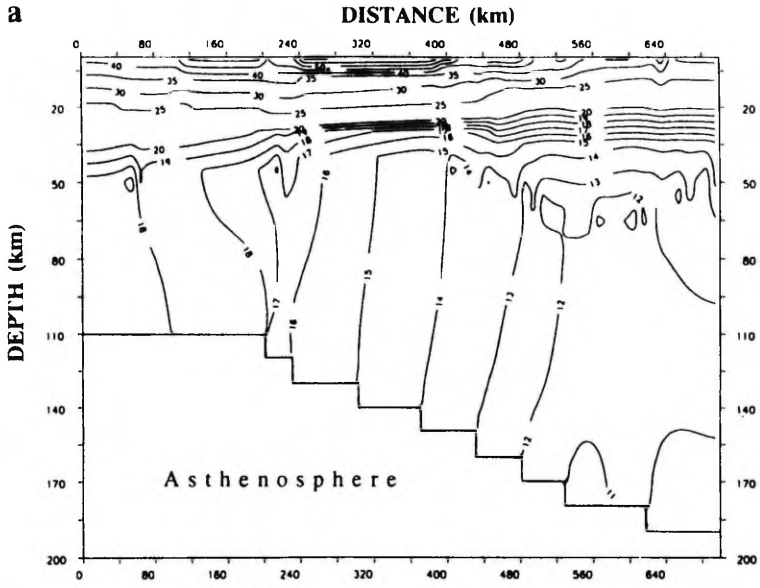
For these layers we have sought the most plausible lithological interpretations for the seismic V_p/V_s data and correlated the results with heat production data for similar lithologies in other areas. Holbrook et al. (1992) have compiled seismic P- and S-wave velocities and Poisson ratios of different rock types measured in laboratory under p - T conditions corresponding to those of middle and lower crust. On a V_p -Poisson ratio diagram, different lithological types can be identified, although considerable overlap usually remains between groups. Plotting the values from the BALTIC ray-tracing model (Luosto et al., 1990) yields estimates of rock composition (Table 2). For the Estonian area the DSS results given in Sharov et al. (1989) are average velocities, which are 0.2–0.5 km/s too low for layers beneath the upper crust. For this part of the transect we also present possible values of in situ V_p velocities based on a comparison of the ray tracing results and average velocities on the BALTIC data (domains F, G, K and L, Table 2), although these values may not be very reliable. The middle crust is most often interpreted as felsic amphibolite facies gneiss, felsic or intermediate granulite, amphibolite, granodiorite or quartz-mica schist. Beneath the Wiborg rapakivi batholite, gravity and magnetic studies (Elo and Korja, 1993)

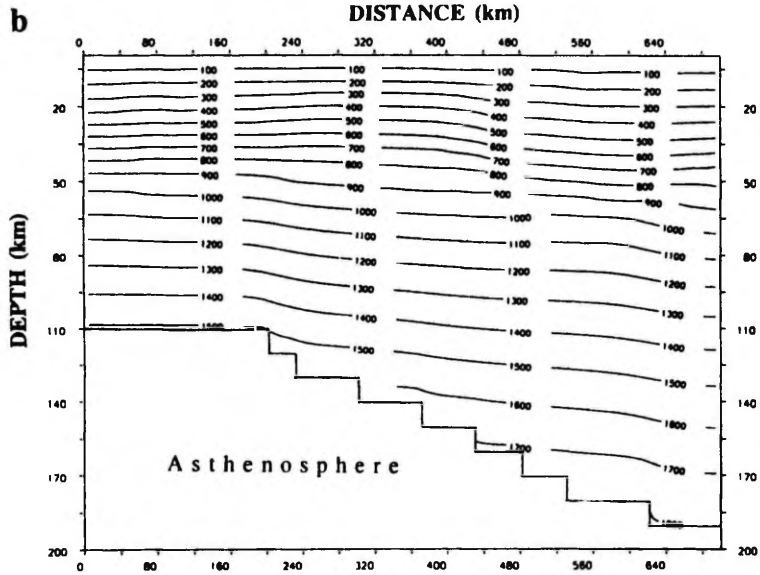
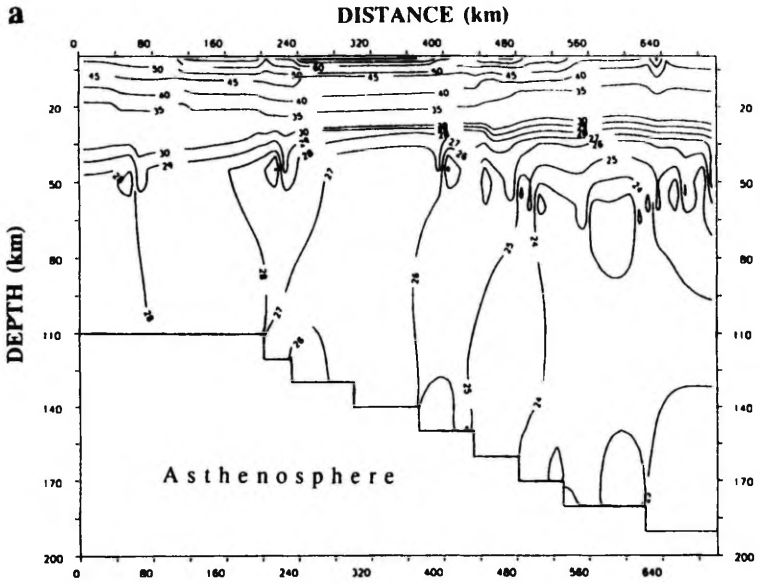
suggest a gabbroic/anorthositic body at the upper/middle crust boundary (domain Q, Fig. 3).

The seismic data for the lower crust are comparable with the presence of lithologies such as anorthosite, mafic granulite, amphibolite and metapelitic granulite. Beneath the Wiborg rapakivi intrusion the Moho is underlain by an eclogitic or ultramafic body (a magmatic "underplate").

Since the seismic data suggest a wide range of alternative lithologies for the middle and lower crust, it is not reasonable to present very detailed lateral or vertical variations in heat production. The current data available for middle and lower crustal xenoliths from the Baltic Shield (mainly from the Kola Peninsula) do not include analyses of heat producing elements (Downes, 1993). Therefore, we must use proxy data from other areas where middle and lower crustal rocks have been brought to the surface as xenoliths or in exhumed high-grade metamorphic units. In the Superior Province, Canadian Shield, an oblique natural cross-section has revealed a series of rocks representative of the middle and lower crust. The middle crustal amphibolite facies rocks (tonalite, granite, mafic gneiss and metasediments) have a mean heat production value of $1.37 \mu\text{W m}^{-3}$ and lower crustal granulite facies rocks (tonalite, anorthosite, mafic gneiss and metasediments) $0.44 \mu\text{W m}^{-3}$, respectively (Ashwal et al., 1987; Percival et al., 1992). Data from other Precambrian granulite areas in India, Australia, Greenland and Brazil sug-

Fig. 4. Simulated HFD (a) and temperature (b) in the lithosphere using the wet peridotite solidus at the L/A boundary.





gest that heat production in the lower crust typically ranges from 0.3 to 0.5 $\mu\text{W m}^{-3}$ but in certain cases it may attain to 1.6 and even to 2.8 $\mu\text{W m}^{-3}$ (Ashwal et al., 1987). The global average of heat production in lower crustal xenoliths is 0.28 $\mu\text{W m}^{-3}$ and the corresponding median value is 0.075 $\mu\text{W m}^{-3}$ (Rudnick, 1992). Generally granulite terranes yield higher values than xenoliths, which can be attributed to upper crustal contamination and a more felsic composition of the outcropping granulites. In this study we have adopted as first approximations values of 0.8 $\mu\text{W m}^{-3}$ for the middle crust (about 10–30 km) and 0.2 $\mu\text{W m}^{-3}$ for the lower crust (> 30 km).

4.2.3. Lithospheric mantle

The lithospheric mantle is assumed to be depleted in heat producing elements and accordingly a value of 0.002 $\mu\text{W m}^{-3}$ has been used (Jochum et al., 1983). The difference in heat production value between depleted and undepleted (0.017 $\mu\text{W m}^{-3}$; Jochum et al., 1983) mantle is trivial for the purposes of our modelling since mantle heat production is low in any case.

Thermal conductivity values were taken from measurements in Finland (Järvinmäki and Puranen, 1979; Kukkonen, 1988, 1993), or from data published for similar rock types (Zoth and Haenel, 1988), or calculated from the average mineralogical composition of the rocks.

4.3. Model variants

Several model variants were calculated, the main difference between them being the applied solidus temperature at the L/A boundary (wet vs. dry solidus) or the prescribed lateral variation in basal heat flow density. To find out the sensitivity of the results to parameter variations, conductivity and heat production values were varied within the extreme possible ranges in the original data (mostly about $\pm 0.5 \text{ W m}^{-1} \text{ K}^{-1}$ in conductivity and $\pm 50\%$ in heat production). Maximum lithospheric temperatures were calculated using the lower ends of the conductivity ranges and the upper ends of the heat

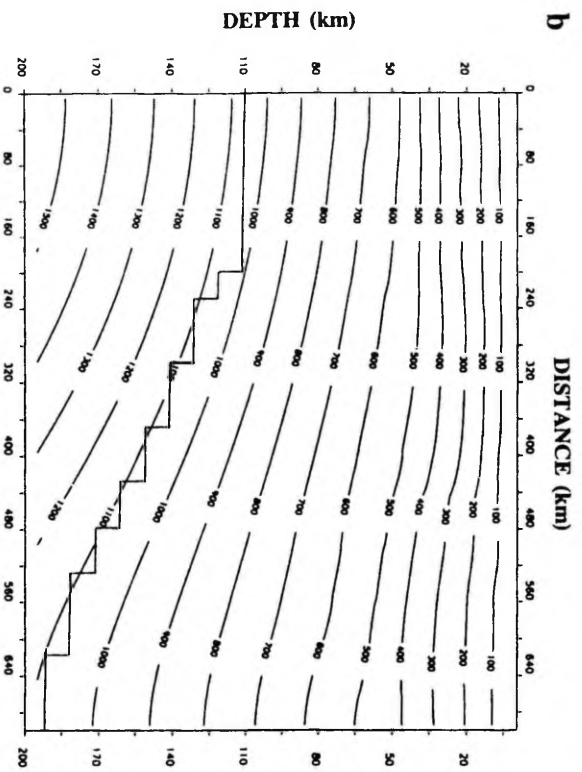
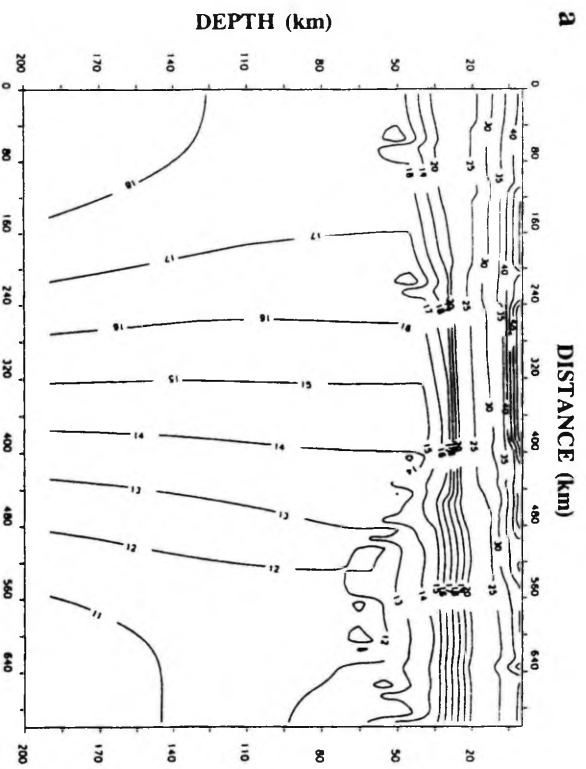
production ranges (Table 2) and, correspondingly, minimum temperatures using the upper ends of the conductivity ranges and the lower ends of the heat production ranges, respectively. Such a technique overestimates true variations, because in reality parameter variations may act in opposite directions, thus mitigating their individual effects.

4.4. Results

Lithospheric temperatures and HFD's are presented for the three main variants in Figs. 4–6. Selected lateral profiles of the results (surface HFD, HFD and temperature at 50 km) are given in Figs. 7–9. In the wet solidus case the surface HFD values range from about 30 to 60 mW m^{-2} , HFD at 50 km (approximately at the Moho) from 12 to 19 mW m^{-2} , and temperatures at 50 km from 450 to 650°C (Figs. 4 and 7). Surface HFD values are about 10 mW m^{-2} higher in the dry solidus case than in the wet case (Figs. 7 and 8). The wet case seems to yield a better fit with the measured HFD values. The dry solidus at the L/A boundary produces values about 10–12 mW m^{-2} higher for Moho HFD than the wet solidus (Figs. 7 and 8). The Moho temperatures, however, are very high in the dry case (800–1000°C), and the corresponding crustal temperatures would place the brittle–ductile transition (about 350°C) already at about 15–20 km depth (Fig. 5). This is in contradiction with data on the focal depths of earthquakes which extend to 30–40 km in the Baltic Shield (Ahjos and Uski, 1993). This and the poor fit of the measured and modelled surface HFD's suggest that the dry solidus temperatures are not appropriate for the L/A boundary.

For comparison a simulation with a prescribed basal heat flow density which decreased from 19 mW m^{-2} at the southwestern end of the transect to 10 mW m^{-2} at the northeastern end, was also used as a lower boundary condition at 200 km (Figs. 6 and 9). The lateral variation was assumed to be monotonous and sinusoidal in form. These basal heat flow values lead to results which are similar to those calculated with the wet solidus variant.

Fig. 5. Simulated HFD (a) and temperature (b) in the lithosphere using the dry peridotite solidus at the L/A boundary.



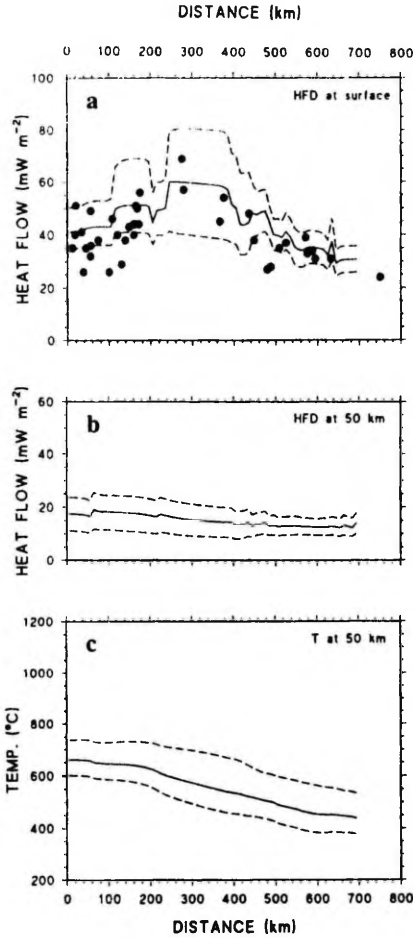


Fig. 7. Lateral profiles of HFD (in mW m^{-2}) at the surface (a), at 50 km depth (b) and temperature (in $^{\circ}\text{C}$) at 50 km depth (c) for the wet peridotite solidus at the L/A boundary (see Fig. 4). Solid lines present the results calculated with the heat production and conductivity values given in Table 2, whereas the broken lines present the minimum and maximum values calculated with the extreme ends of the thermal parameter values in Table 2. The solid symbols represent the measured HFD values (Fig. 1b). See text for details.

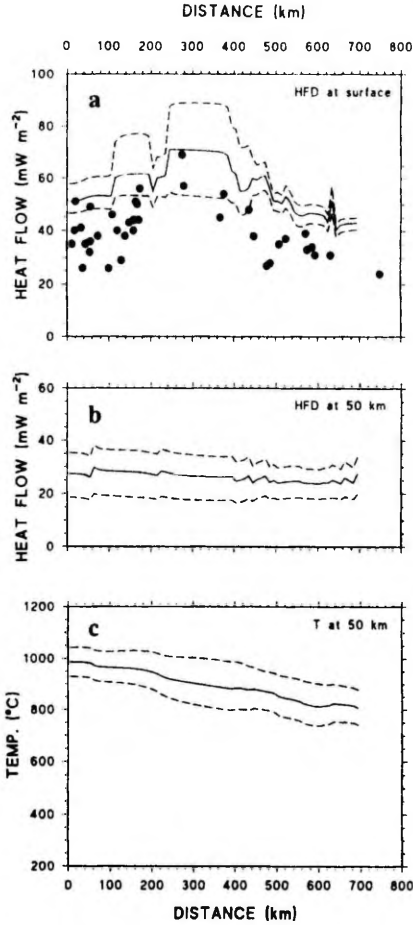


Fig. 8. Results as in Fig. 7, except that the dry peridotite solidus was used at the L/A boundary.

The sensitivity of the simulation results to parameter variations is about equal in the wet and dry solidus cases, being about $\pm 5\text{--}20 \text{ mW m}^{-2}$ for surface HFD, $\pm 5\text{--}8 \text{ mW m}^{-2}$ for Moho HFD and

Fig. 6. Simulated HFD (a) and temperature (b) in the lithosphere using a prescribed laterally variable basal HFD ($19\text{--}10 \text{ mW m}^{-2}$) as the lower boundary condition at 200 km. The seismic L/A boundary from Fig. 3 is included for comparison. See text for details.

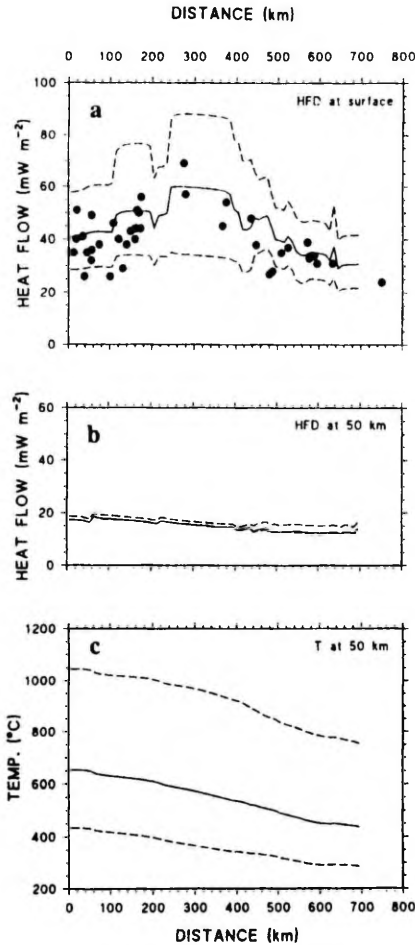


Fig. 9. Results as in Fig. 7, but with the prescribed HFD used as the lower boundary condition.

± 50 – 100°C for Moho temperatures. However, if the simulation is performed using the basal HFD as a boundary condition, the sensitivity is changed so that the minimum and maximum values of surface HFD deviate ± 10 – 30 mW m^{-2} from the best estimate. Moho HFD values are very narrowly constrained

($\pm 3 \text{ mW m}^{-2}$) due to the very low heat production and its small range in the mantle, but on the other hand, Moho temperatures are very sensitive to parameter variations and vary by several hundreds of degrees (Fig. 9).

If the simulations are performed with the radiative heat transfer effect being excluded from the temperature dependence of thermal conductivity (Eq. (2)), the results are not dramatically different in the wet case. This can be attributed to the low mantle temperatures, where radiative heat transfer has no significant role. As a result, the surface and Moho HFD values decrease about 3 mW m^{-2} and the Moho temperature about 50°C . In the dry case the effect is more pronounced and Moho and surface HFD's are decreased by 10 mW m^{-2} and Moho temperatures by 200°C .

The middle and lower crustal heat production values did not require much adjustment and the values of $0.8 \mu\text{W m}^{-3}$ for the middle and $0.2 \mu\text{W m}^{-3}$ for the lower crust were found to be appropriate for the Proterozoic parts of the model (domains F–H and K–M in Fig. 3 and Table 2). Only at the Archaean/Proterozoic boundary where the Moho is at about 60 km depth and in the Archaean part near the northeastern end of the transect, it was necessary to decrease these parameters to 0.4 and $0.1 \mu\text{W m}^{-3}$, respectively (domains I, J, N and O).

Otherwise, the resulting surface HFD would have been too high. Where the Moho is deepest this could be an indication of an increased mafic, low heat production component in the crust; this hypothesis is supported by the fact that the lower crust between 50 and 60 km has a high P-wave velocity (7.2–7.3 km/s; Luosto et al., 1990) and that the area coincides with a broad gravity maximum as well (Elo, 1992).

The simulated surface HFD values mainly follow the upper crustal heat production variations, and the lithospheric thickness variation has only a minor effect on the surface HFD values. This was checked with simulations using a laterally homogeneous crust of constant thickness, while the total lithosphere thickness was varied from 190 to 110 km over a distance of 700 km, and both dry and wet solidus temperatures were assigned to the L/A boundary. Surface HFD varied less than 5 mW m^{-2} in both simulations. Temperature isolines were practically

horizontal above 40 km depth, and most of the thermal effects of the lithospheric thickness variations were restricted to the subcrustal mantle. The result emphasizes the importance of (upper) crustal heat sources in understanding the measured HFD variations.

5. Discussion

Earlier investigations have suggested that the Moho HFD in eastern and southern Finland is 15–35 mW m^{-2} (Kukkonen, 1989b) or about 25 mW m^{-2} (Pasquale et al., 1991; Čermák et al., 1993). These results have been based on heat production estimates using $A-V_p$ relationships. The cited Moho HFD values are problematic because certain measured HFD values in the eastern Baltic Shield are very close to and in some cases smaller than these values (Hurtig et al., 1992). The present results, which are based on geochemical data on upper crustal rocks, petrological models of crustal cross sections and heat production values of middle and lower crustal rocks in other areas, suggest smaller Moho HFD values (wet solidus at L/A boundary, $Q_{50} = 12\text{--}19 \text{ mW m}^{-2}$). Guillou et al. (1994) have obtained similar Moho HFD values (10–14 mW m^{-2}) in the Abitibi greenstone belt, Superior Province, Canada, in a study which used thermal and gravity modelling combined with crustal heat production estimates.

Moho temperatures published previously for southern and eastern Finland include values such as 400–700°C (Kukkonen, 1989b), 400–500°C (Pasquale et al., 1991) and about 550°C (Čermák et al., 1993). The present simulations yielded values which are in the same range (the Finnish part of the transect, wet solidus at L/A boundary, 450–600°C). Practically all previous estimates are within our estimated range of Moho temperature (T at 50 km) variations.

The results of the main model variants (wet vs. dry solidi assigned to the L/A boundary) differ from each other. The measured surface HFD data fit better the results for the wet solidus case, and furthermore, the dry solidus case yields unreasonably high mid-crustal temperatures. These features support the hypothesis that temperatures at the L/A boundary

follow the solidus of volatile-bearing peridotite. Jordan (1978, 1981) and Pollack (1986) have proposed that the thick lithospheric roots under shields are due to volatile loss and geochemical evolution during continental growth, leading to a higher solidus temperature in the lithospheric mantle. The lithospheric mantle has consequently become more resistant to asthenospheric convection and thermal disturbances. The thickened lithospheric roots divert mantle heat flow to surrounding areas of thinner lithosphere, thus producing the typical low heat flow values recorded in shields (see also Ballard and Pollack, 1987). This reasoning suggests that the dry solidus would be a more correct assumption for L/A temperatures. However, the underlying asthenosphere is convecting and may have a different (volatile-bearing) composition than the lithospheric mantle.

When examined in detail, the simulation results of the wet solidus variant (Fig. 7) run about 3–5 mW m^{-2} above the mean of the measured heat flow density values in the thin lithosphere part of the transect in Estonia. Considering the high scatter of the measured data, the deviation is small and practically within noise. Anyway, it could be compensated by decreasing the mantle heat flow by 5 mW m^{-2} in this part of the model. This was done with the model using heat flow as the lower boundary condition. As a result, temperatures decrease in the whole lithosphere (for instance, 100 K colder at 50 km, in comparison to Fig. 6), but a colder lithosphere also implicates that temperatures at the seismic L/A boundary would be below solidus (about 900°C). Then the seismic L/A boundary could no more be interpreted as a thermal boundary layer with partial melting of ultramafic rocks. On the other hand, an appropriate decrease in the surface HFD could be produced by decreasing the crustal heat production values, which is a more plausible solution. A decrease of 0.25 $\mu\text{W m}^{-3}$ in the uppermost 20 km (domains 1, 2, F and G; Table 2) would be sufficient, and the values would still be within the uncertainties of the heat production values (Tables 1 and 2). Consequently, the upper and middle crust would be slightly colder (about 30 K at 25 km) in comparison to the values in Fig. 6. Mantle temperatures would be only about 20 K lower at 50 km, and the temperatures at the L/A boundary would be very close to the solidus.

The present modellings are affected by the applied temperature dependence of thermal conductivity. We have used here a function (Eq. (2)) that includes both the lattice conductivity and radiative heat transfer. However, if the radiation part is excluded from Eq. (2), temperatures and HFD's in the lower lithosphere would be reduced by increased insulation due to the lower conductivity values.

The sensitivity of the modelled temperatures to parameter variations is relatively small when temperatures are fixed at the L/A boundary. However, if HFD is used as a lower boundary condition, the same changes in thermal conductivity and heat production result in considerably higher variations in Moho temperatures. This result encourages the search for geologically and geophysically derivable temperatures for different depth levels and for their application in lithospheric geothermal modelling.

The relevance of the present results depends on the existence of a partially molten zone at the seismically determined L/A boundary. The boundary is characterized by a contrast of several per cent in P- and S-wave velocities. According to the FENNOLORA refraction experiment on the western Baltic Shield, P-wave velocity is 0.3 km/s lower in the seismic asthenosphere than in the lithosphere (Guggisberg and Berthelsen, 1987). Surface wave data have shown that the corresponding contrast is 0.1–0.2 km/s for S-waves (Calcagnile, 1982). These contrasts are compatible with about 0.5% of melt in peridotite if compared to laboratory experiments (Murase et al., 1977; Murase and Kushiro, 1979; Murase and Fukuyama, 1980) and theoretical models (Shankland et al., 1981). According to Calcagnile (1982) the thickness of the low-velocity asthenospheric layer under the Baltic Shield could not be exactly determined with the available surface wave data. In a more detailed study Calcagnile et al. (1990) gave a value of 100–200 km for the low-velocity asthenospheric layer thickness under the FENNOLORA profile.

Electromagnetic soundings have not detected a highly conductive electric asthenosphere beneath the central Baltic Shield. According to Korja (1990) any upper mantle conductor with a conductance above 1000 S would have been detected. Peridotite with less than 1% of melt has a conductivity of 0.1 S/m or less (Shankland and Waff, 1977). To produce a

conductance of 1000 S, the layer thickness should exceed 10 km. The above-mentioned seismic estimates for the thickness of the asthenospheric low-velocity layer should easily produce a detectable electric asthenosphere. A possible explanation is that the seismically indicated asthenosphere has much lower electric conductivity than the data by Shankland and Waff (1977) suggest, or that the crustal 2- and 3-D conductive structures prevent the detection of asthenospheric conductors. It should also be noted that relatively few long-period electromagnetic soundings have been carried out in the Shield area, so that it may be perhaps premature to draw definitive conclusions about the existence or absence of an electric asthenosphere.

6. Conclusions

Variation of HFD along the studied transect is mainly controlled by crustal heat sources that contribute 40–60% of the surface heat flow value. Variation in lithosphere thickness is only weakly reflected in the surface HFD variations, but does have an effect on the lower crustal and subcrustal thermal regime, particularly on temperature. The fact that the surface HFD values are lower in Estonia where the lithosphere is thinner than in southern Finland, can be attributed to the lower heat production of the Estonian upper crustal rocks. The present simulations and existing measured HFD data suggest that temperatures at the L/A boundary follow the solidus of volatile-bearing peridotite. The anomalously thick crust near the Archaean/Proterozoic boundary in eastern Finland conceivably contains significant amounts of mafic intrusions in the middle and lower crust, as evidenced by the low heat production values needed for these layers in the simulations. Furthermore, the Archaean middle and lower crust necessarily has a lower heat production than in the Proterozoic part of the transect. The Archaean lower crust is also 100–200 K colder than the Proterozoic. Simulated temperatures at 50 km depth (approximately at the Moho) increase from northeast to southwest and range from 450–550°C in eastern Finland to about 650°C in Estonia. The extreme values of the Moho temperatures may differ by ± 50 –100 K. Mantle HFD is relatively low and varies from 12 ± 5

mW m^{-2} at the Archaean northeastern end of the transect to $19 \pm 6 \text{ mW m}^{-2}$ at the Proterozoic southwestern end of the transect in Estonia.

Acknowledgements

We are grateful to K. Suuroja (Geological Survey of Estonia, Tallinn) for the opportunity to take drill core samples for heat production and thermal conductivity measurements, to C. Clauser (Niedersächsisches Landesamt für Bodenforschung, Hannover) for the possibility of using his computer code, to L. Eskola (Geological Survey of Finland, Espoo) and V. Klein (Geological Survey of Estonia, Tallinn) for reviews of an early version of the manuscript, to V. Pasquale (University of Genova, Genova) and an anonymous referee for their constructive comments on the manuscript, and to P. Sorjonen-Ward (Geological Survey of Finland, Espoo) for revising the English.

References

- Adám, A., 1978. Geothermal effects in the formation of electrically conducting zones and temperature distribution in the Earth. *Phys. Earth Planet. Inter.*, 17: P21–P28.
- Adám, A., 1980. Relation of mantle conductivity to physical conditions in the asthenosphere. *Geophys. Surv.*, 4: 43–55.
- Ahjos, T. and Uski, M., 1993. Earthquakes in northern Europe in 1375–1989. *Tectonophysics*, 207: 1–23.
- Ahonen, L. and Blomqvist, R., 1994. Mode of occurrence of deep saline groundwater in Finland based on hydraulic measurements. In: B. Olofsson (Editor), *Salt Groundwater in the Nordic Countries*. Res. Council. Nor. Rep., NHP 35: 49–59.
- Ashwal, L.D., Morgan, P., Kelley, S.A. and Percival, J.A., 1987. Heat production in an Archaean crustal profile and implications for heat flow and mobilization of heat producing elements. *Earth Planet. Sci. Lett.*, 85: 439–450.
- Babuska, V., Plomerova, J. and Padjusak, P., 1988. Seismologically determined deep lithosphere structure in Fennoscandia. *GFF*, 110: 380–382.
- Ballard, S. and Pollack, H.N., 1987. Diversion of heat by Archaean cratons: A model for southern Africa. *Earth Planet. Sci. Lett.*, 85: 253–264.
- Baumann, M. and Rybach, L., 1991. Temperature field modelling along the northern segment of the European Geotraverse and the Danish Transition Zone. In: V. Čermák and J.H. Sass (Editors), *Forward and Inverse Techniques in Geothermal Modelling*. *Tectonophysics*, 194: 387–407.
- Bodri, L., 1994. Hydrological disturbances of the conductive heat flow in stable continental crust. *Tectonophysics*, 234: 291–304.
- Calcagnile, G., 1982. The lithosphere-asthenosphere system in Fennoscandia. *Tectonophysics*, 90: 19–35.
- Calcagnile, G., Pierri, P., Del Gaudio, V. and Mueller, St., 1990. A two-dimensional velocity model for the upper mantle beneath FENNOLORA from seismic surface waves and body waves. In: R. Freeman, P. Giese and St. Mueller (Editors), *The European Geotraverse: Integrative studies. Results from the Fifth Study Centre, Rauischholzhausen 26 March–7 April, 1990*. European Science Foundation, Strasbourg, pp. 49–66.
- Čermák, V. and Bodri, L., 1993. Heat production in the continental crust, part I: data converted from seismic velocities and their attempted interpretation. *Tectonophysics*, 225: 15–28.
- Čermák, V., Bodri, L., Rybach, L. and Buntebarth, G., 1990. Relationship between seismic velocity and heat production: comparison between two sets of data and test of validity. *Earth Planet. Sci. Lett.*, 99: 48–57.
- Čermák, V., Balling, N., Kukkonen, I. and Zui, V.J., 1993. Heat flow in the Baltic Shield—results of the lithospheric geothermal modelling. *Precambrian Res.*, 64: 53–65.
- Clauser, C., 1988. Untersuchungen zur Trennung der konduktiven und konvektiven Anteile im Wärmetransport in einem Sedimentbecken am Beispiel des Oberrheingraben. *Fortschr. Ber. VDI, Reihe 19(28)*, 124 pp. (dissertation).
- Clauser, C. and Villingier, H., 1990. Analysis of conductive and convective heat transfer in a sedimentary basin, demonstrated for the Rheingraben. *Geophys. J. Int.*, 100: 393–414.
- Downes, H., 1993. The nature of the lower continental crust of Europe: petrological and geochemical evidence from xenoliths. *Phys. Earth Planet. Inter.*, 79: 195–218.
- Dragoni, M., Pasquale, V., Verdoya, M. and Chiozzi, P., 1993. Rheological consequences of the lithospheric thermal structure in the Fennoscandian Shield. *Global Planet. Change*, 8: 113–126.
- Elo, S., 1992. Gravity anomaly maps. In: T. Koljonen (Editor), *The Geochemical Atlas of Finland, Part 2: Till. Geol. Surv. Finl., Espoo*, pp. 70–75.
- Elo, S. and Korja, A., 1993. Geophysical interpretation of the crustal and upper mantle structure in the Wiborg rapakivi granite area, southeastern Finland. *Precambrian Res.*, 64: 273–288.
- Fountain, D.M., 1986. Is there a relationship between seismic velocity and heat production for crustal rocks? *Earth Planet. Sci. Lett.*, 79: 145–150.
- Fountain, D.M., 1987. The relationship between seismic velocity and heat production — a reply. *Earth Planet. Sci. Lett.*, 83: 178–180.
- Gordienko, V.V., Zavgorodnaya, O.V., Moiseenko, U.I. and Smyslov, A.A., 1985. Heat flow at the southern slope of the Baltic Shield. *Geophys. J.*, 6: 365–376.
- Gordienko, V.V., Zavgorodnaya, O.V., Moiseenko, U.I. and Smyslov, A.A., 1987. Karta teplovogo potoka evropeiskoi chasti SSSR. Mashtab 1:5 000 000. Vsegei. Leningrad, 35 pp. (in Russian).
- Grad, M. and Luosto, U., 1987. Seismic models of the Baltic Shield along the SVEKA profile in Finland. *Ann. Geophys.*, 5B: 639–650.
- Grad, M. and Luosto, U., 1992. Fracturing of the crystalline

- uppermost crust beneath the SVEKA profile in Central Finland. *Geophysica*, 28: 53–66.
- Guggisberg, B. and Berthelsen, A., 1987. A two-dimensional velocity-model for the lithosphere beneath the Baltic Shield and its possible tectonic significance. *Terra Cognita*, 7: 631–638.
- Gullou, L., Mareschal, J.-C., Jaupart, C., Garrépy, C., Bienfait, G. and Lapointe, R., 1994. Heat flow, gravity and structure of the Abitibi belt, Superior Province, Canada: Implications for mantle heat flow. *Earth Planet. Sci. Lett.*, 122: 103–123.
- Holbrook, W.S., Mooney, W.D. and Christensen, N.I., 1992. The seismic velocity structure of the deep continental crust. In: D.M. Fountain, R. Arculus and R.W. Kay (Editors), *Continental Lower Crust*. Elsevier, Amsterdam, pp. 1–43.
- Hölttä, P. and Klein, V., 1991. *PT*-development of granulite facies rocks in southern Estonia. *Geol. Surv. Finl., Spec. Pap.*, 12: 37–47.
- Hurtig, E., Čermák, V., Haenel, R. and Zui, V. (Editors), 1992. *Geothermal Atlas of Europe*. Hermann Haack, Gotha, 156 pp.
- Järvinmäki, P. and Puranen, M., 1979. Heat flow measurements in Finland. In: V. Čermák and L. Rybach (Editors), *Terrestrial Heat Flow in Europe*. Springer, Berlin, pp. 172–178.
- Jochum, K.P., Hofmann, A.W., Ito, E., Seufert, H.M. and White, W.M., 1983. K, U, and Th in mid-ocean ridge basalt glasses and heat production, K/U and K/Rb in the mantle. *Nature*, 306: 431–436.
- Jordan, T.H., 1978. Composition and development of the continental tectosphere. *Nature*, 274: 544–548.
- Jordan, T.H., 1981. Continents as a chemical boundary layer. *Philos. Trans. R. Soc. London, Ser. A*, 301: 359–373.
- Kirby, S.H., 1983. Rheology of the lithosphere. *Rev. Geophys. Space Phys.*, 21: 1458–1487.
- Klemperer, S.L., 1987. A relation between continental heat flow and the seismic reflectivity of the lower crust. *J. Geophys.*, 61: 1–11.
- Koistinen, T., 1993. Pre-Quaternary rocks of the Heinävesi map-sheet area. Geological map of Finland 1:100 000, explanation to the maps of Pre-Quaternary rocks. *Geol. Surv. Finl., Espoo*, 64 pp.
- Koistinen, T. (Editor), 1994. Precambrian basement of the Gulf of Finland and surrounding area, map 1:1 mill. *Geol. Surv. Finl., Espoo*.
- Korja, T., 1990. Electrical conductivity of the lithosphere. Magnetotelluric studies in the Fennoscandian Shield, Finland. Ph.D. Thesis, Univ. Oulu, 179 pp.
- Kremenetsky, A.A. and Ovchinnikov, L.N., 1986a. The Precambrian continental crust: Its structure, composition and evolution as revealed by deep drilling in the USSR. *Precambrian Res.*, 33: 11–43.
- Kremenetsky, A.A. and Ovchinnikov, L.N., 1986b. *Geohimiya glubinyh porod*. Nauka, Moscow, 262 pp. (in Russian).
- Kukkonen, I., 1987. Vertical variation of apparent and palaeoclimatically corrected heat flow densities in the central Baltic Shield. *J. Geodyn.*, 8: 33–53.
- Kukkonen, I., 1988. Terrestrial heat flow and groundwater circulation in the bedrock in the central Baltic Shield. *Tectonophysics*, 156: 59–74.
- Kukkonen, I., 1989a. Terrestrial heat flow and radiogenic heat production in Finland, the central Baltic Shield. In: V. Čermák, L. Rybach and E.R. Decker (Editors), *Heat Flow and Lithosphere Structure*. *Tectonophysics*, 164: 219–230.
- Kukkonen, I., 1989b. Terrestrial heat flow in Finland, the central Fennoscandian Shield. *Doct. Diss.*, Helsinki Univ. Technol., Geol. Surv. Finl., Nuclear Waste Disposal Res. Rep. YST-68, 99 pp.
- Kukkonen, I.T., 1993. Heat flow map of northern and central parts of the Fennoscandian Shield based on geochemical surveys of heat producing elements. *Tectonophysics*, 225: 3–13.
- Kukkonen, I.T., 1995. Thermal aspects of groundwater circulation in bedrock and its effect on crustal geothermal modelling in Finland, the central Fennoscandian Shield. In: N. Balling and E.R. Decker (Editors), *Heat Flow and Lithosphere Thermal Regime*. *Tectonophysics*, 244: 119–136.
- Kukkonen, I.T. and Clauser, C., 1994. Simulation of heat transfer at the Kola deep-hole site — implications for advection, heat refraction and paleoclimatic effects. *Geophys. J. Int.*, 116: 409–420.
- Kukkonen, I.T. and Järvinmäki, P., 1992. Finland. In: E. Hurtig, V. Čermák, R. Haenel and V. Zui (Editors), *Geothermal Atlas of Europe*. Hermann Haack, Gotha, p. 29.
- Kushiro, I., Syono, Y. and Akimoto, S., 1967. Stability of phlogopite at high pressures and possible presence of phlogopite in the Earth's upper mantle. *Earth Planet. Sci. Lett.*, 3: 197–203.
- Luosto, U., Tiira, T., Korhonen, H., Azbel, I., Burmin, V., Buyanov, A., Kosminskaya, I., Ionkis, V. and Sharov, N., 1990. Crust and upper mantle structure along the DSS Baltic profile in SE Finland. *Geophys. J. Int.*, 101: 89–110.
- Milanovsky, S.Yu., 1984. Deep geothermal structure and mantle heat flow along the Barents Sea–East Alps Geotraverse. *Tectonophysics*, 103: 175–192.
- Moiseyenko, F.S., 1986. The Kola superdeep drillhole and some problems of interpreting deep-level geophysical interpretations. *Int. Geol. Rev.*, 28: 1021–1030.
- Murase, T. and Fukuyama, H., 1980. Shear wave velocity in partially molten peridotite at high pressures. *Carnegie Inst. Washington, Geophys. Lab. Annu. Rep.*, 1979–1980: 307–310.
- Murase, T. and Kushiro, I., 1979. Compressional wave velocity in partially molten peridotite at high pressures. *Carnegie Inst. Washington, Geophys. Lab. Annu. Rep.*, 1978–1979: 559–562.
- Murase, T., Kushiro, I. and Fujii, T., 1977. Compressional wave velocity in partially molten peridotite. *Carnegie Inst. Washington, Geophys. Lab. Annu. Rep.*, 1976–1977: 414–419.
- Niemi, A., 1994. Modeling flow in fractured medium, uncertainty analysis with stochastic continuum approach. *Tech. Res. Cent. Finl., VTT Publ.* 184, 188 pp.
- Nurmi, P.A., 1984. Applications of lithochemistry in the search for Proterozoic porphyry-type molybdenum, copper and gold deposits, southern Finland. *Geol. Surv. Finl., Bull.*, 329, 40 pp.
- Nyblade, A.N. and Pollack, H.N., 1993a. A global analysis of heat flow from Precambrian terrains: Implications for the thermal structure of Archaean and Proterozoic lithosphere. *J. Geophys. Res.*, 98: 12,207–12,218.
- Nyblade, A.N. and Pollack, H.N., 1993b. Can differences in heat

- flow between east and southern Africa be easily interpreted? Implications for understanding regional variability in continental heat flow. *Tectonophysics*, 219: 257–272.
- Nyblade, A.N. and Pollack, H.N., 1993c. A comparative study of parametrized and full thermal-convection models in the interpretation of heat flow from cratons and mobile belts. *Geophys. J. Int.*, 113: 747–751.
- Olafsson, M. and Eggler, D.H., 1983. Phase relations of amphibole, amphibole-carbonate and phlogopite-carbonate peridotite: petrologic constraints on the asthenosphere. *Earth Plan. Sci. Lett.*, 64: 305–315.
- Pasquale, V., Cabella, C. and Verdoya, M., 1990. Deep temperatures and lithospheric thickness along the European Geotraverse. *Tectonophysics*, 176: 1–11.
- Pasquale, V., Verdoya, M. and Chiozzi, P., 1991. Lithospheric thermal structure of the Baltic Shield. *Geophys. J. Int.*, 106: 611–620.
- Percival, J.A., Fountain, D.M. and Salisbury, M.H., 1992. Exposed crustal cross sections as windows on the lower crust. In: D.M. Fountain, R. Arculus and R.W. Kay (Editors), *Continental Lower Crust*. Elsevier, Amsterdam, pp. 317–362.
- Pollack, H.N., 1986. Cratonization and thermal evolution of the mantle. *Earth Planet. Sci. Lett.*, 80: 175–182.
- Puranen, M., Järvinmäki, P., Hämäläinen, U. and Lehtinen, S., 1968. Terrestrial heat flow in Finland. *Geoexploration*, 6: 151–162.
- Rämö, O.T., 1991. Petrogenesis of Proterozoic rapakivi granites and related basic rocks of southeastern Fennoscandia: Nd and Pb isotopic and general geochemical constraints. *Geol. Surv. Finl. Bull.*, 335, 161 pp.
- Rudnick, R.L., 1992. Xenoliths-samples of the continental crust. In: D.M. Fountain, R. Arculus and R.W. Kay (Editors), *Continental Lower Crust*. Elsevier, Amsterdam, pp. 269–316.
- Rybach, L., 1973. Wärmeproduktionsbestimmungen an Gesteinen der Schweizer Alpen. *Beitr. Geol. Schweiz, Geotech. Ser.* 51, 43 pp.
- Rybach, L. and Buntebarth, G., 1984. The variation of heat generation, density and seismic velocity with rock type in the continental lithosphere. *Tectonophysics*, 103: 335–344.
- Rybach, L. and Buntebarth, G., 1987. The relationship between seismic velocity and heat production – critical comments. *Earth Planet. Sci. Lett.*, 83: 175–177.
- Schatz, J.F. and Simmons, G., 1972. Thermal conductivity of earth materials at high temperatures. *J. Geophys. Res.*, 77: 6966–6983.
- Shankland, T.J. and Waff, H.S., 1977. Partial melting and electrical conductivity anomalies in the upper mantle. *J. Geophys. Res.*, 82: 5409–5417.
- Shankland, T.J., O'Connell, R.J. and Waff, H.S., 1981. Geophysical constraints on partial melt in the upper mantle. *Rev. Geophys. Space Phys.*, 19: 394–406.
- Sharov, N.V., Zagorodny, V.G., Glaznev, V.N. and Zhamaletdinov, A.A., 1989. *Struktura litosfery i verkhney mantya Baltiyskogo shchita*. In: V.B. Sollogub (Editor), *Litosfera Tsentralnoy i Vostochnoy Evropy: Vostochno-Evropeyskaya Platforma*. Naukova Dumka, Kiev, pp. 52–77 (in Russian).
- Simonen, A., 1980. The Precambrian in Finland. *Geol. Surv. Finl. Bull.*, 304, 58 pp.
- Takahashi, E. and Kushiro, I., 1983. Melting of a dry peridotite at high pressures and basalt magma genesis. *Am. Mineral.*, 68: 859–879.
- Teollisuuden Voima Oy, 1992. Käytetyn polttoaineen loppusjoiutus Suomen kalliooperään, alustavat sijoituspaikkatutkimukset. (Final disposal of spent nuclear fuel in the Finnish bedrock, preliminary site investigations.) *Voimayhtiöiden Ydinjätetoimikunta, Rap. YJT-92-32*, 322 pp. (in Finnish with English abstract).
- Urban, G., Tsybulia, L., Cozel, V. and Schmidt, A., 1991. Geotermichesкая характеристика северной части Балтийской Синецисы. *Proc. Est. Acad. Sci.*, 40: 112–121 (in Russian).
- Wasilewski, P.J., Thomas, H.H. and Mayhew, M.A., 1979. The Moho as a magnetic boundary. *Geophys. Res. Lett.*, 6: 541–544.
- Zoth, G. and Haenel, R., 1988. Thermal conductivity. In: R. Haenel, L. Rybach and L. Stegena (Editors), *Handbook of Terrestrial Heat-Flow Density Determination*. Kluwer, Dordrecht, pp. 449–466.

CURRICULUM VITAE

ARGO JÕELEHT

Date and

place of birth: 12.10.1971, Tallinn

Nationality: Estonian

Address:

Institute of Geology, University of Tartu

Vanemuise 46, Tartu 51014, Estonia

e-mail argo.joeleht@ut.ee

Phone +372 7 375815

Fax +372 7 375836

Education

Graduated in 1993, University of Tartu, Institute of Geology

Msc. in 1995, University of Tartu, Institute of Geology

Employment

1993–1995 Geophysist, Geological Survey of Estonia

1993–1995 Laboratory assistant, Institute of Geology, University of Tartu, Estonia

1995–1997 Researcher, Institute of Geology, University of Tartu, Estonia

Research interests

* Temperature and heat flow density in Estonia

* Thermal effects of groundwater flow

* Influence of climate change to thermal field and inferring climate from temperature logs

* Thermal and other properties of sedimentary and crystalline rocks

CURRICULUM VITAE

ARGO JÕELEHT

Sünniaeg

ja koht: 12.10.1971 Tallinn

Rahvus: Eestlane

Address: Tartu Ülikooli geoloogia instituut
Vanemuise 46, Tartu 51014, Eesti

e-mail argo.joeleht@ut.ee

Tel. (27) 375815

Faks (27) 375836

Haridus: Tartu Ülikool, diplom geoloogia erialal, 1993

Tartu Ülikool, *Msc.* rakendusgeoloogia erialal, 1995

Teenistuskäik: 1993–1995 geofüüsik, Eesti Geoloogiakeskus

1993–1995 laborant, Tartu Ülikooli geoloogia instituut

1995–1997 teadur, Tartu Ülikooli geoloogia instituut

Peamised

uurimisteemad: * Eesti maasisene temperatuur ja soojusvoo tihedus

* Põhjavee voolamise termiline efekt

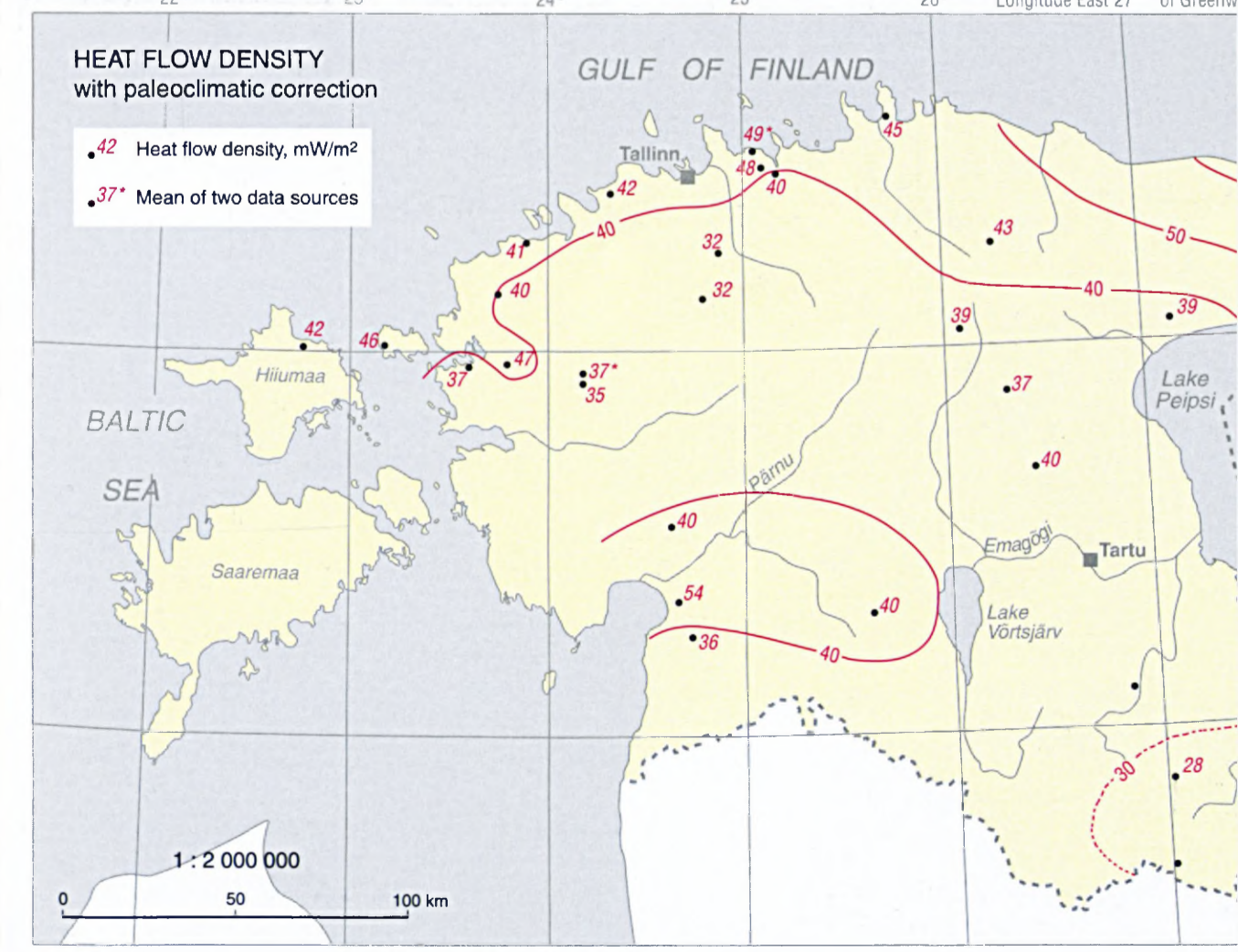
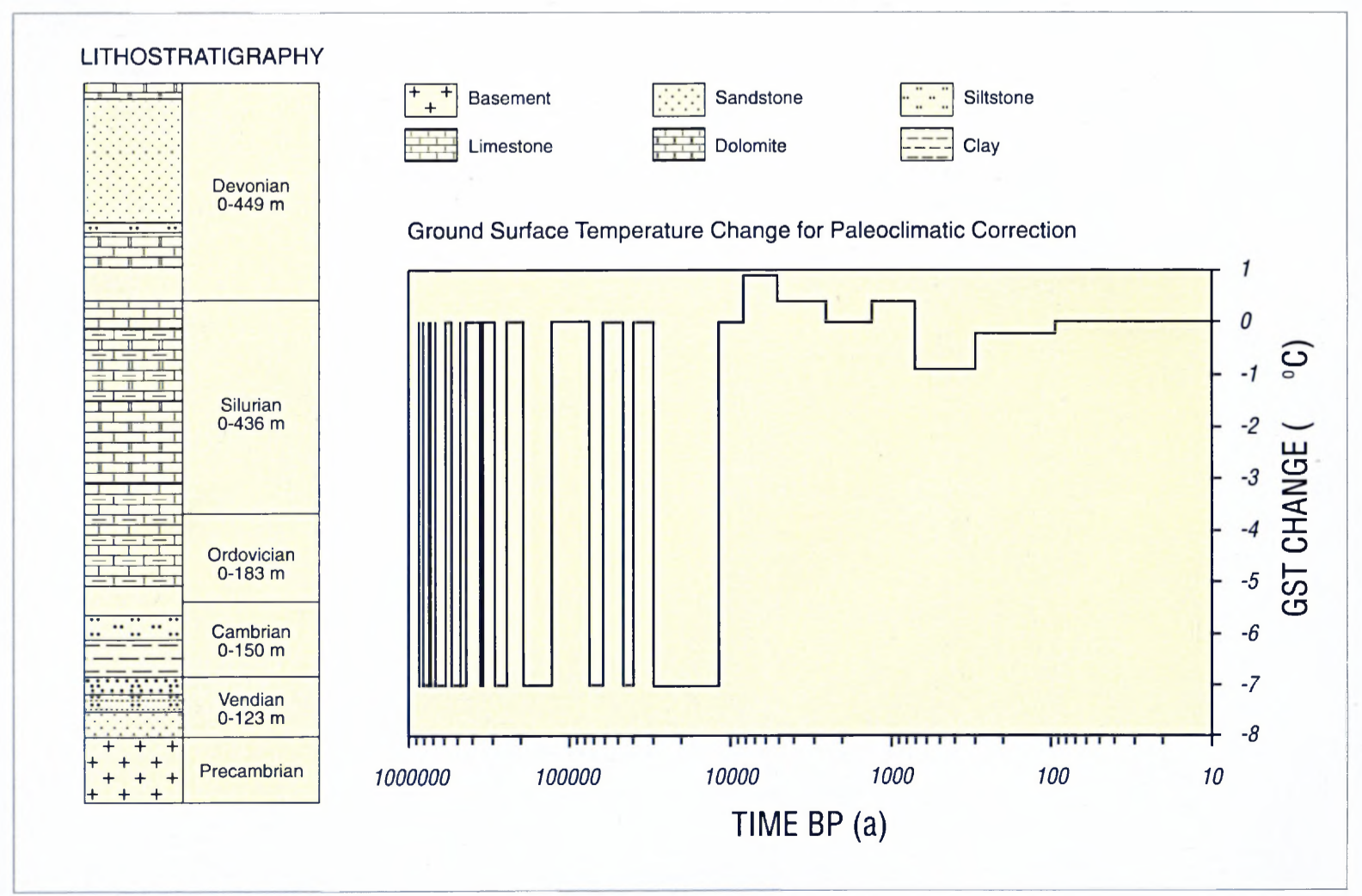
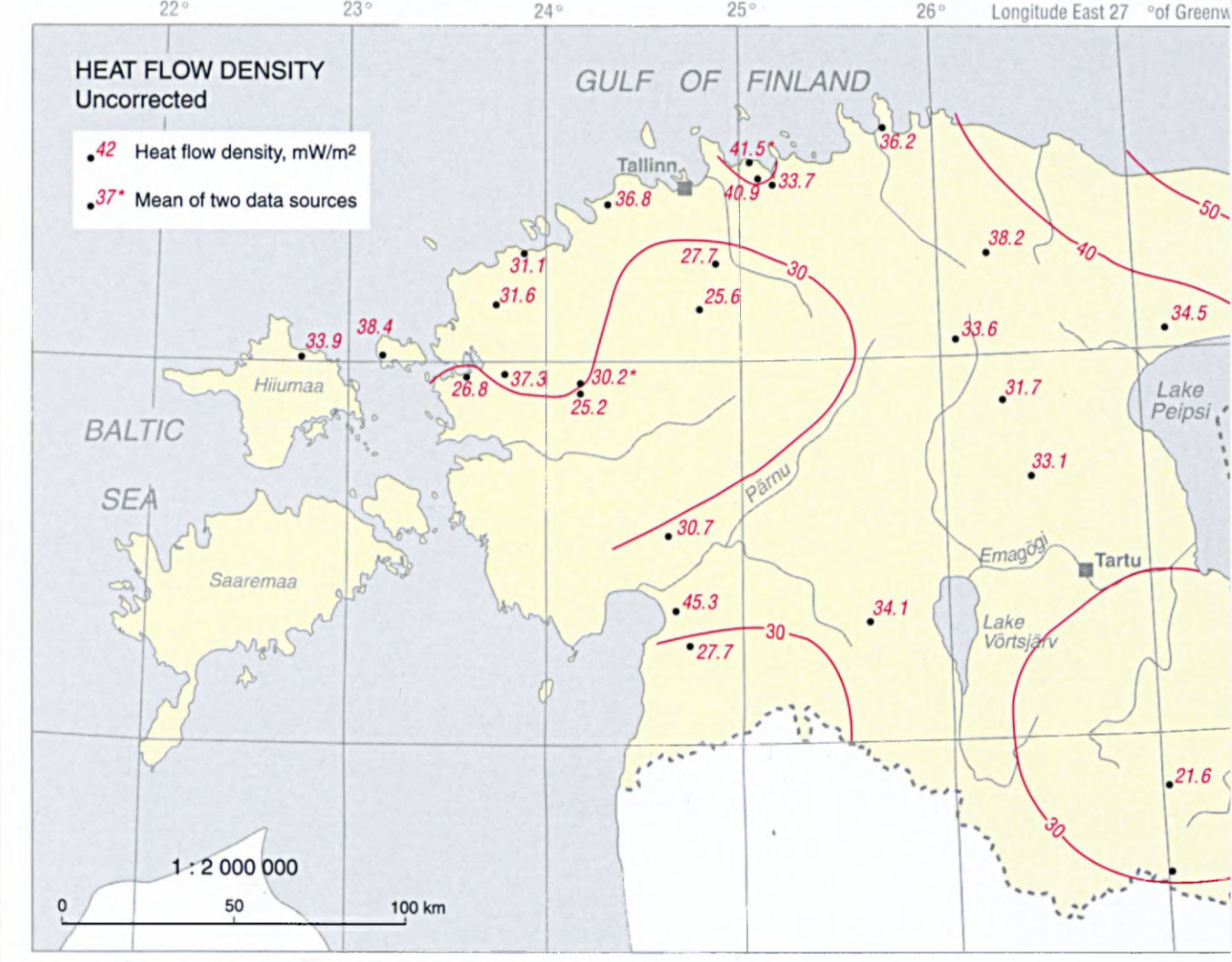
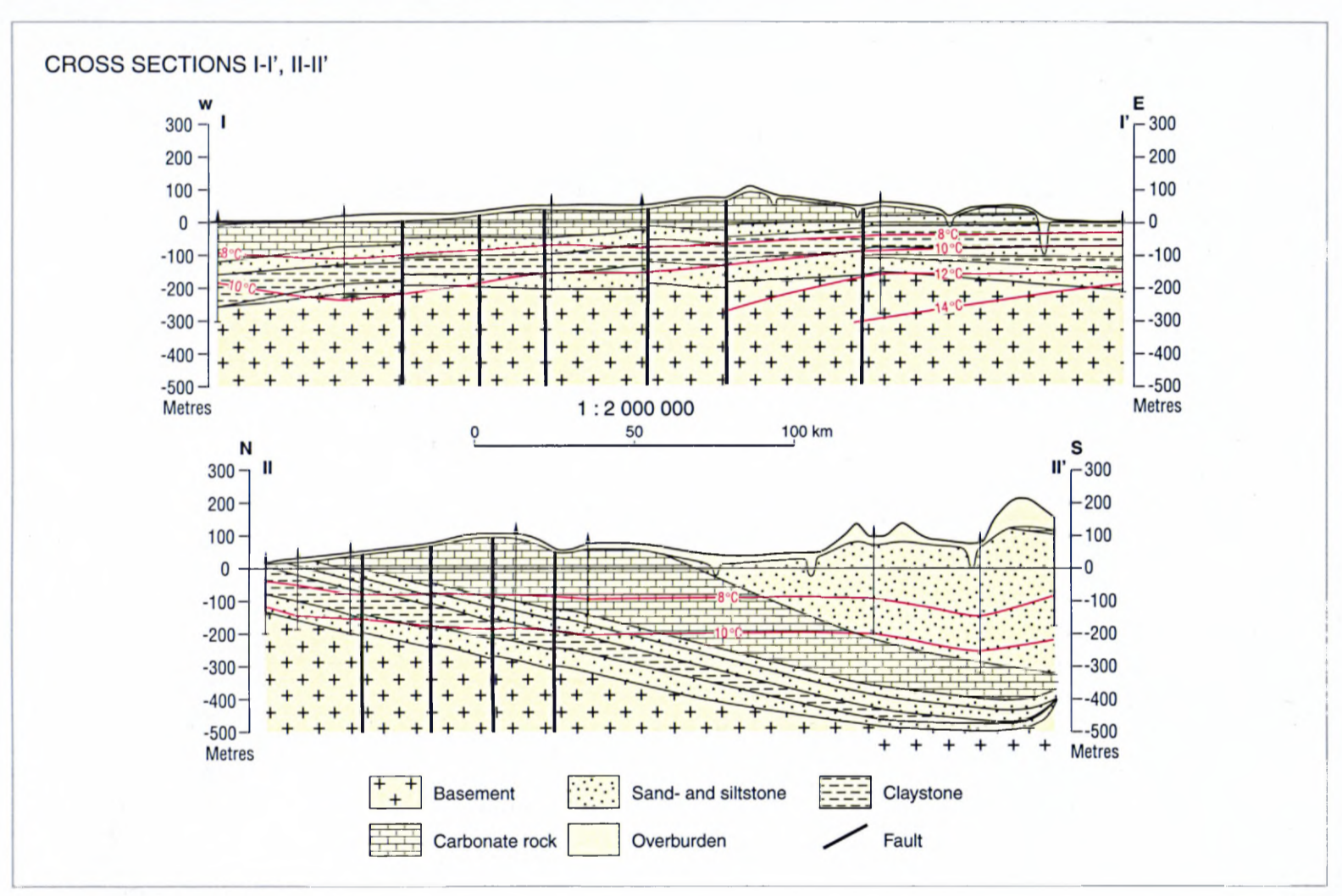
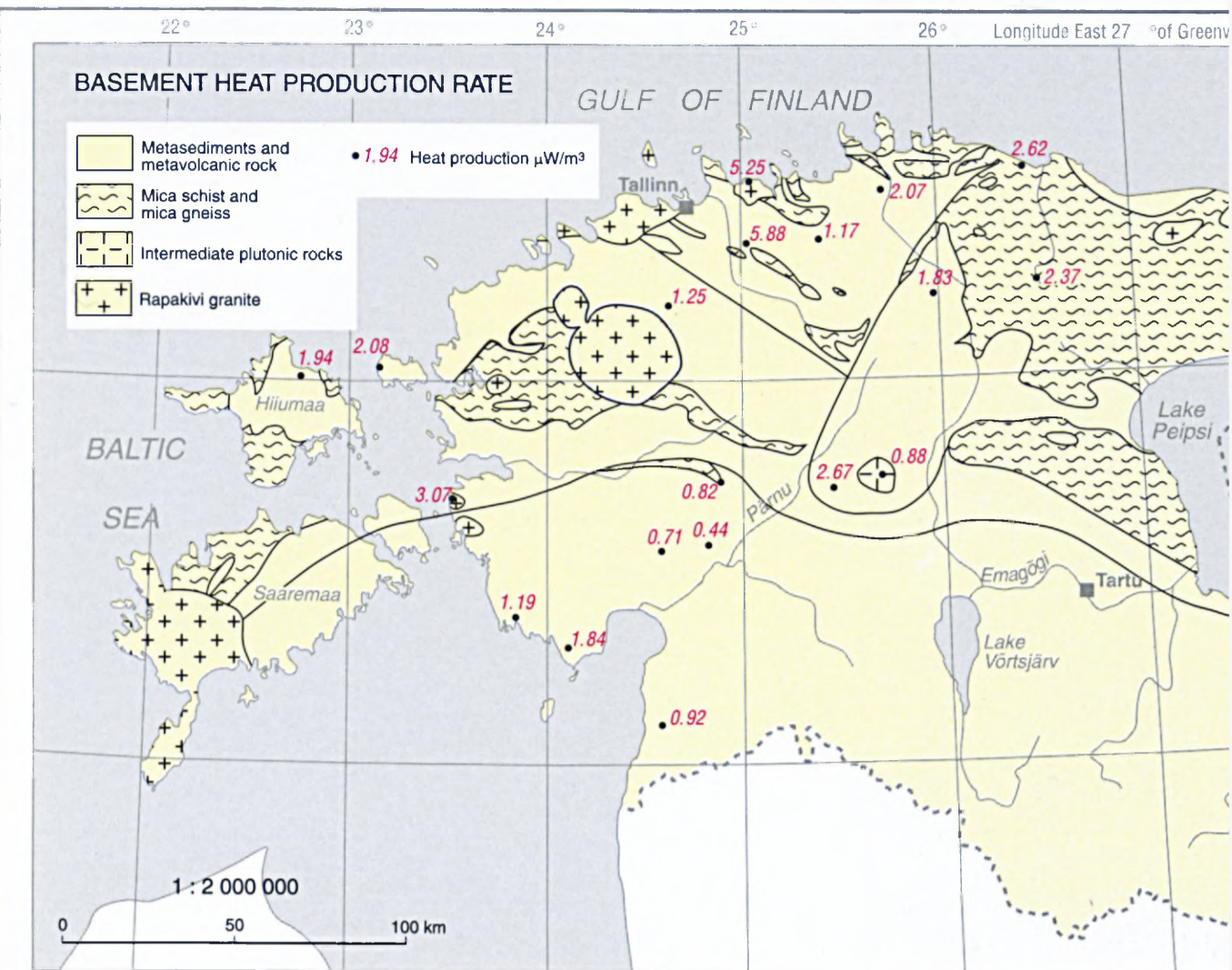
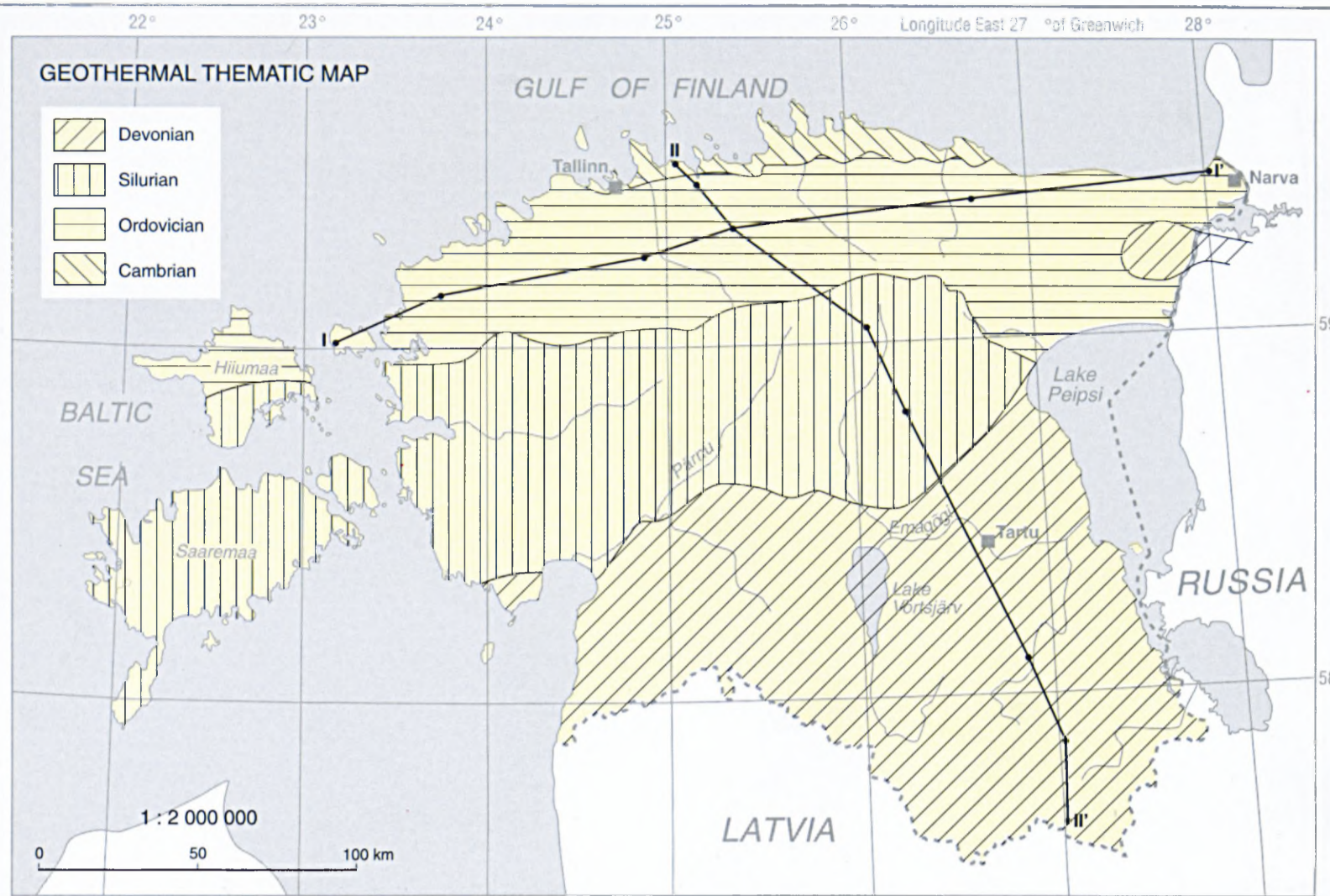
* Kliimamuutuste mõju soojusväljale ja mineviku kliima uurimine puuraugu andmestiku põhjal

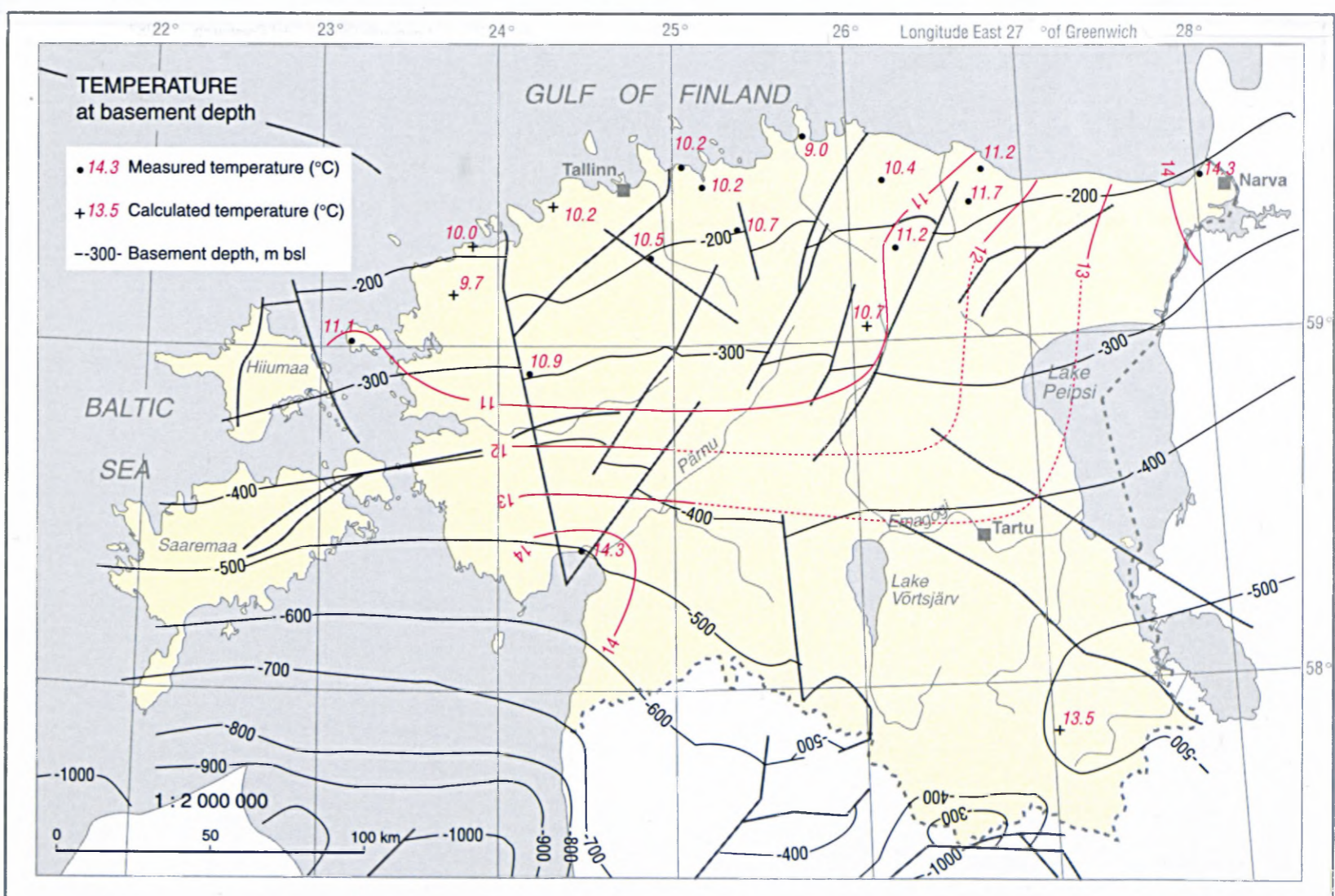
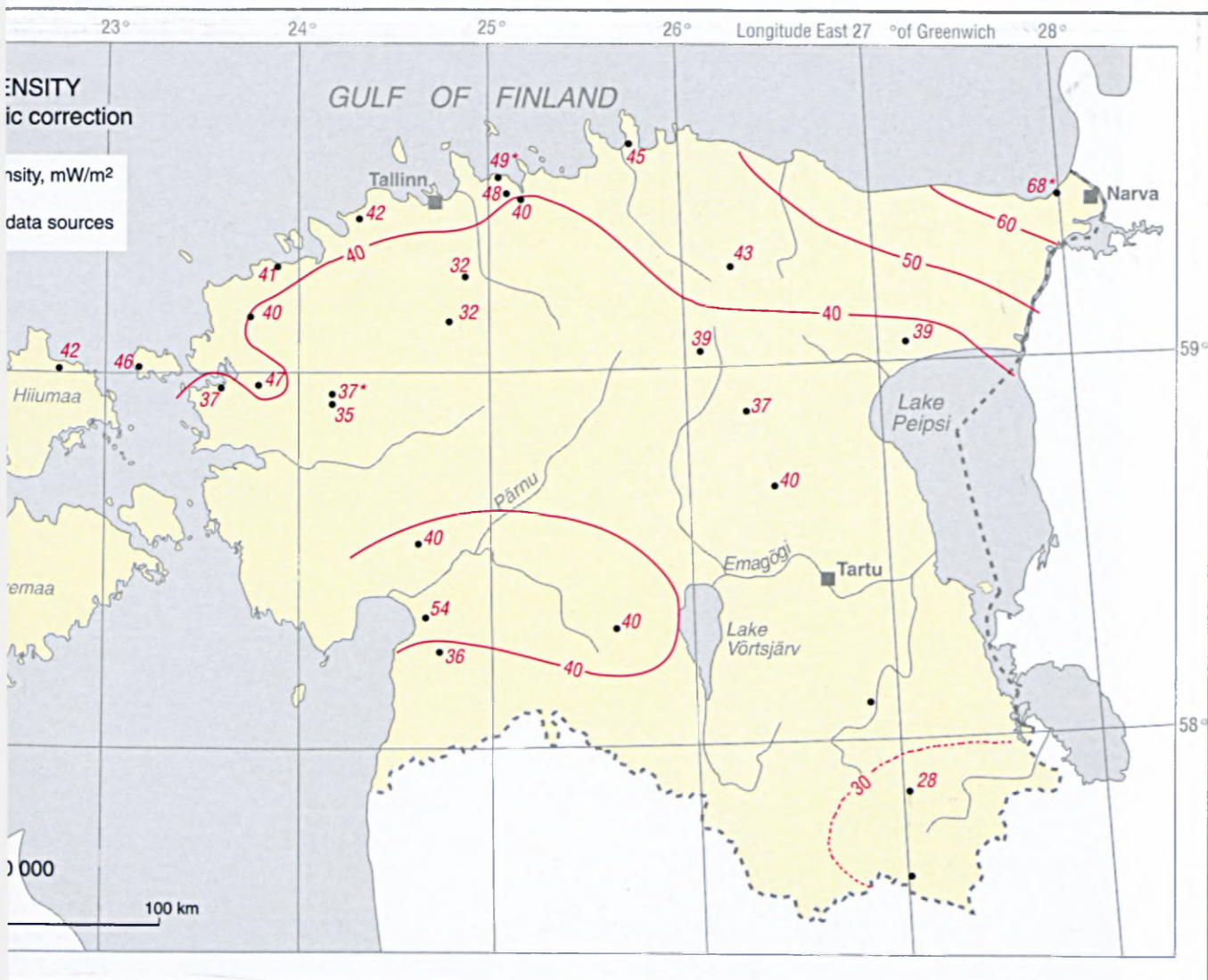
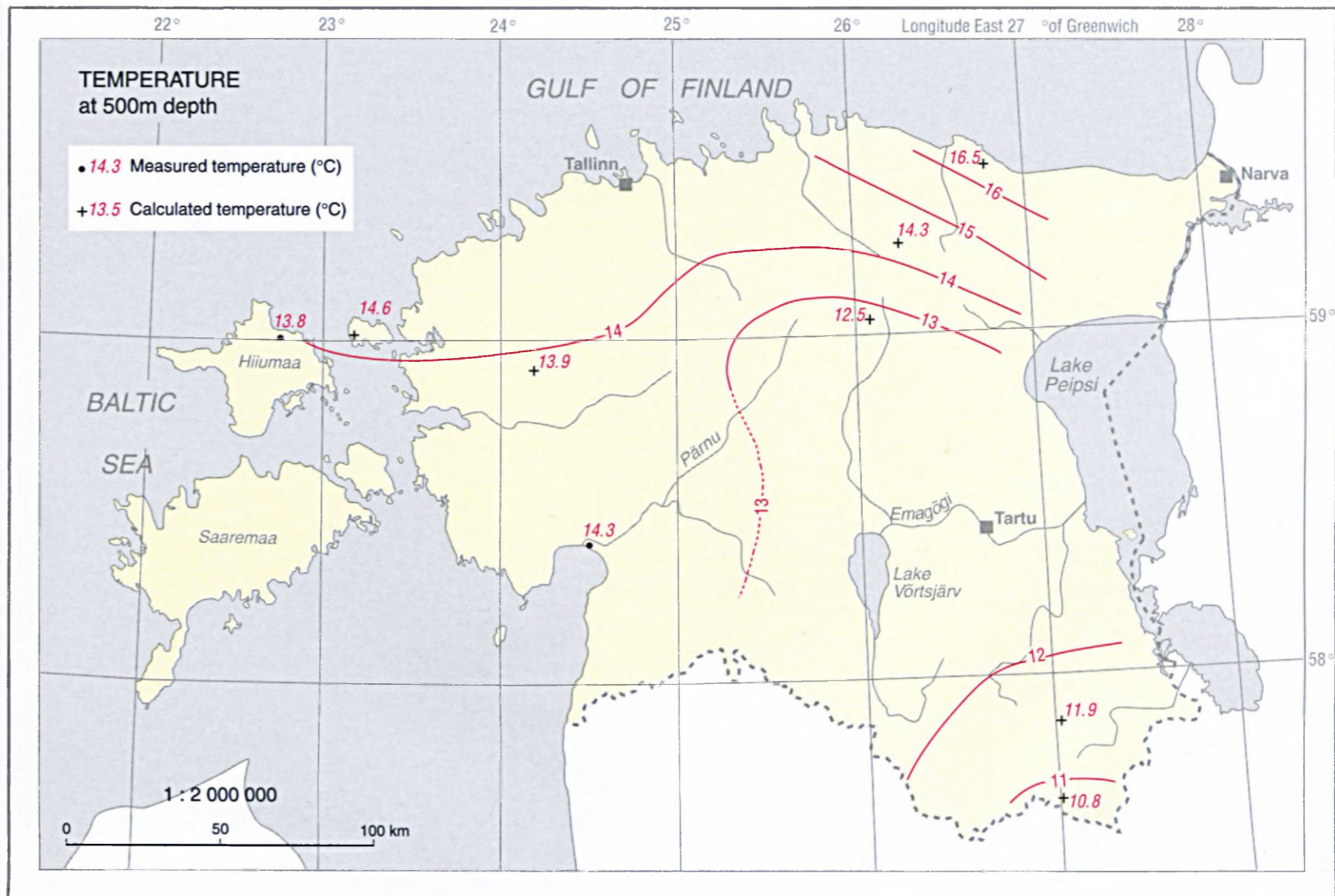
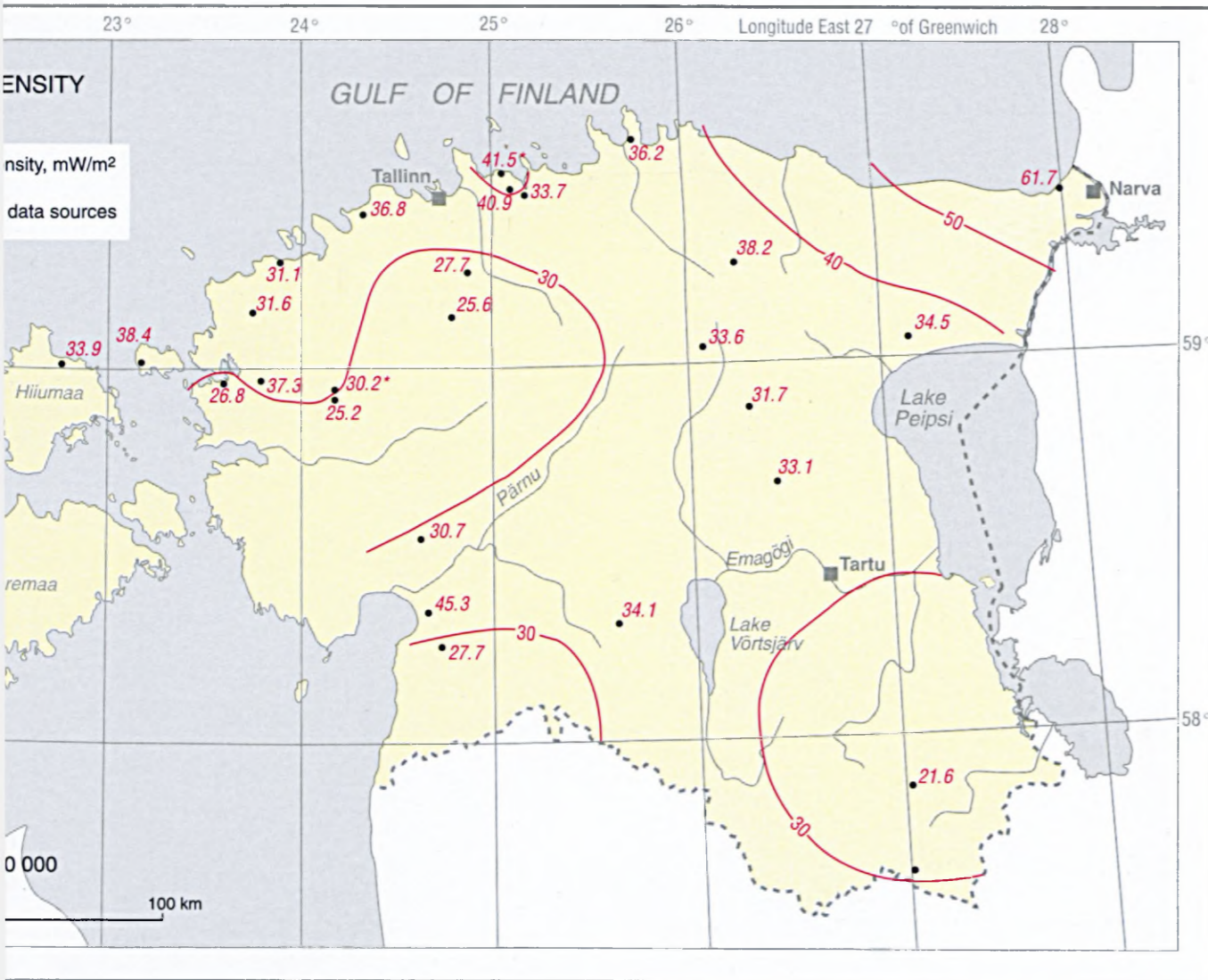
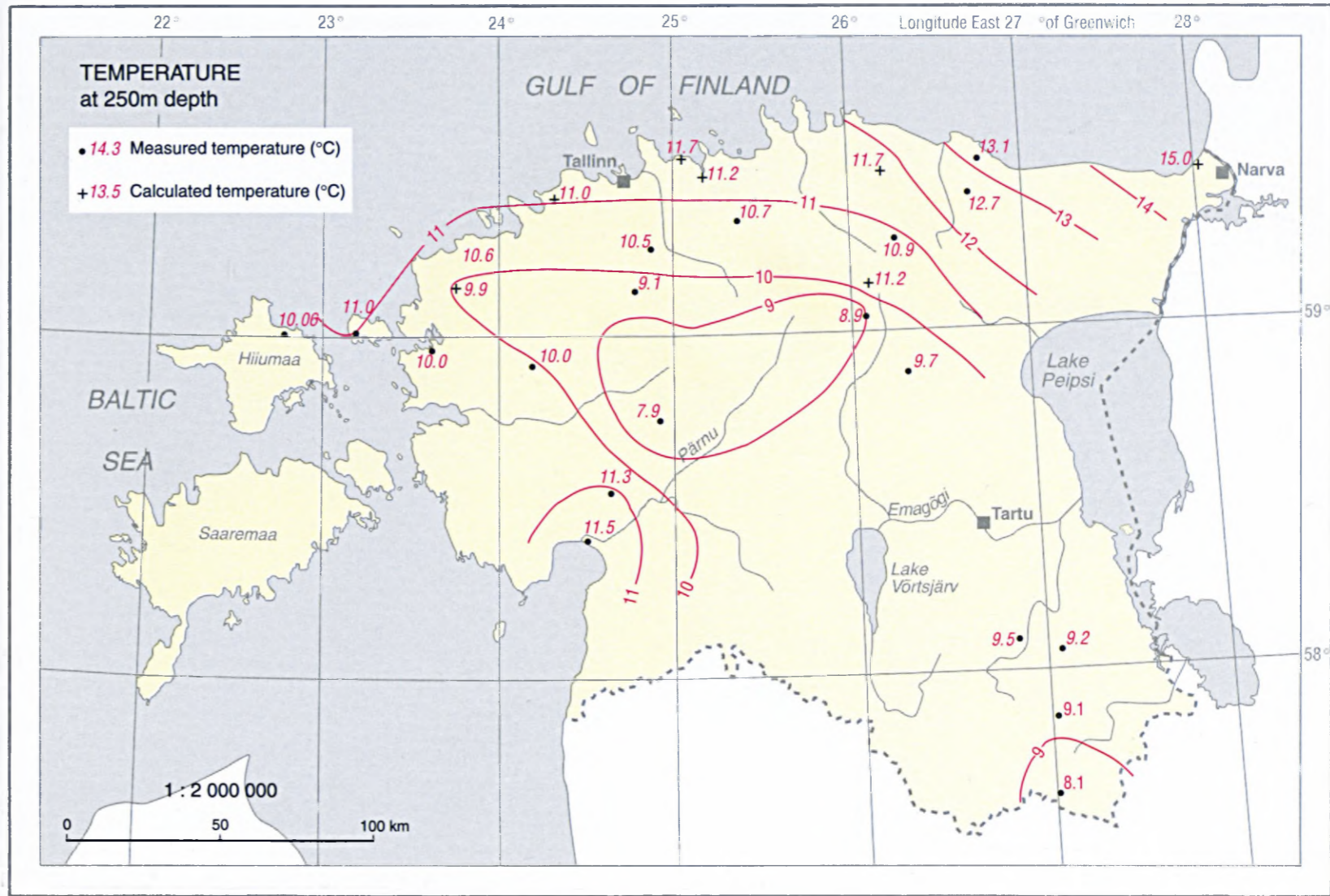
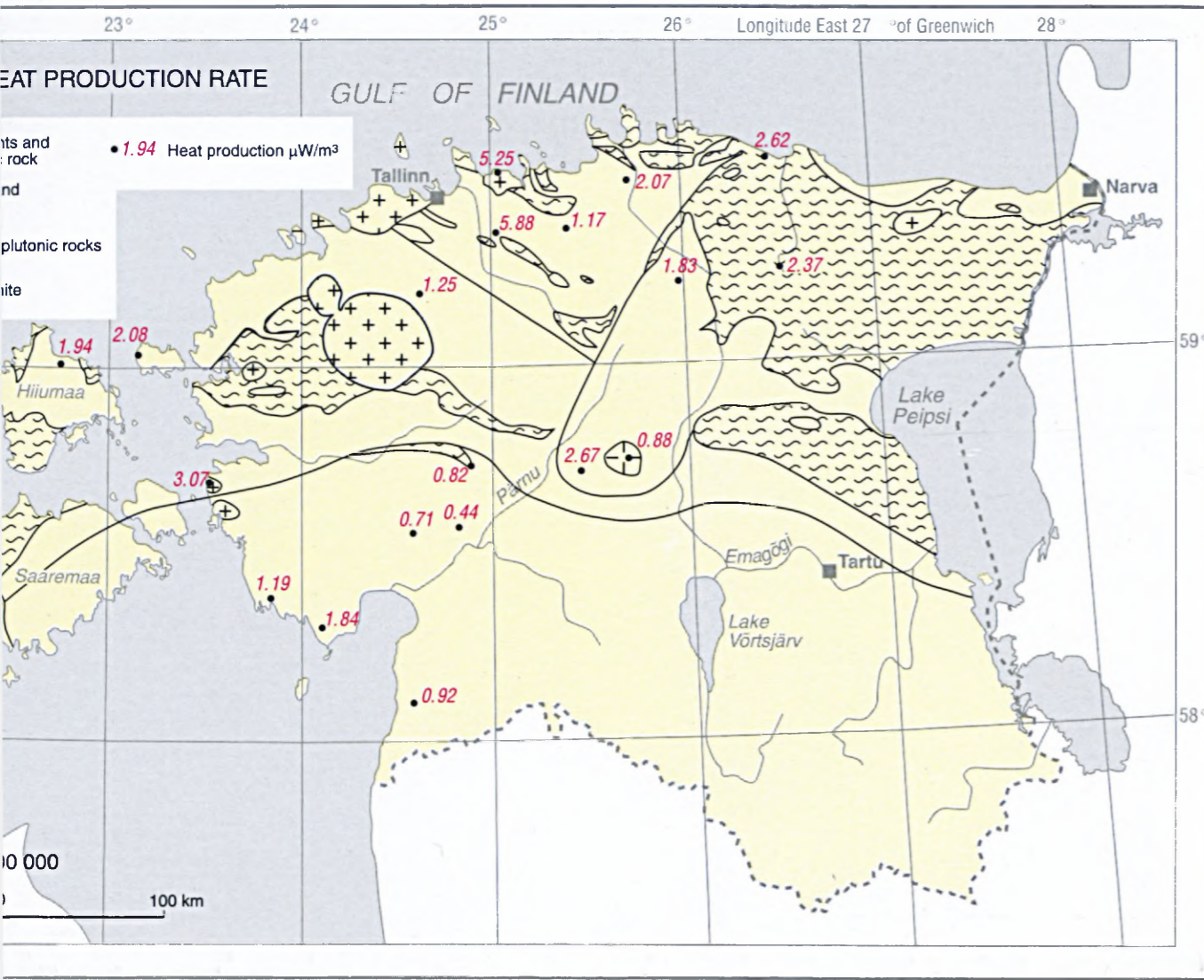
* Kristalsete ja settekivimite termilised ning muud petrofüüsikalised omadused

DISSERTATIONES GEOLOGICAE UNIVERSTATIS TARTUENSIS

1. Пээп Мянник. Конодонты в верхнеордовикских и нижнесилурийских отложениях Эстонии. Тарту, 1992. 355 с.
2. Elvi Tavast. Fennoskandia kilbi lõunanõlva ja sellega piirnevate alade aluspõhja reljeef. Tartu, 1992. 357 lk.
3. Kaarel Orviku. Characterisation and evolution of Estonian seashores. Tartu, 1992. 19 lk.
4. Анатолий Молодьков. ЭПР-анализ скелетного вещества моллюсков в хроностратиграфических исследованиях позднего кайнозоя. Тарту, 1992. 33 с.
5. Jaan Lutt. Late- and postglacial deposits on the Estonian shelf. Tartu, 1993. 31 lk.
6. Reet Karukäpp. Gotiglatsiaalne morfogenees skandinaavia mandriliustiku kagusektoris. Tartu, 1997. 181 lk.

ESTONIA







ISSN 1406-2658
ISBN 9985-56-358-1